Winter 1-31-2023

Terfezia Boudieri and Terfezia Claveryi Inhibit the LPS/IFN-γ-Mediated Inflammation in RAW 264.7 Macrophages Through an Nrf2-Independent Mechanism

Abdelhameed Dawood
abdelhameedsaeed@aucegypt.edu

THE AMERICAN UNIVERSITY IN CAIRO
الجامعة الأمريكية بالقاهرة

School of Sciences and Engineering

Terfezia boudieri and *Terfezia claveryi* inhibit the LPS/IFN-γ-mediated inflammation in RAW 264.7 macrophages through an Nrf2-independent mechanism

A thesis submitted to the Biotechnology Graduate Program

In partial fulfillment of the requirements for the degree of

Master of Science

By

Abdelhameed Saeed Dawood

Under the supervision of

Dr. Anwar Abd El Nasser

Assistant Professor, Institute of Global Health and Human Ecology (IGHHE)

The American University of Cairo

Declaration of Authorship

I, [Abdelhameed Saeed Dawood], declare that this thesis titled, **"[*Terfezia boudieri* and *Terfezia claveryi* inhibit the LPS/IFN-γ-mediated inflammation in RAW 264.7 macrophages through an Nrf2-independent mechanism]"** and the work presented in it are my own. I confirm that:

- This work was done wholly or mainly while in candidature for a research degree at thisUniversity.
- Where any part of this thesis has previously been submitted for a degree or any otherqualification at this University or any other institution, this has been clearly stated.
- Where I have consulted the published work of others, this is always clearly attributed.
- Where I have quoted from the work of others, the source is always given. With theexception of such quotations, this thesis is entirely my own work.
- I have acknowledged all main sources of help.
- Where the thesis is based on work done by myself jointly with others, I have made clear exactly what was done by others and what I have contributed myself.

Signed:

Date:
June 19, 2022

Acknowledgements

I would like to express my deepest gratitude to my supervisor **Dr. Anwar Abd Elnaser** for his dedicated support and academic guidance during my master's degree. Dr. Anwar continuously provided encouragement and was always willing and enthusiastic to assist in any way he could throughout my thesis project. His immense knowledge and plentiful experience have encouraged me in all the time of my academic research and daily life.

I am extremely grateful to the **Abdulla Al Ghurair Foundation for Education** for the funding opportunity to pursue my master's degree with a fully funded scholarship. I would also like to thank **Ms. Soha Khater**, Al Ghurair Scholarship coordinator, for her invaluable assistance and continuous support. I would like to recognize the financial support from The American University in Cairo to complete my thesis project.

I would like to thank all the faculty members in the Biotechnology Graduate Program and Institute of Global Health and Human Ecology for their help and support. This thesis was carried out at the Biotechnology and Institute of Global Health and Human Ecology labs. It was supported by a grant from The American University in Cairo and the Academy of Scientific Research and Technology (ASRT).

I would like to thank all my fellow graduate students, collaborators, and research technicians who contributed to this project. I am very grateful to all of you.

Finally, I would like to express my sincere gratitude to my parents, my wife, and my sisters for providing me with tremendous support and continuous encouragement throughout my study. This accomplishment would not have been possible without them.

Dedication

To

Dad, Mom, My wife (Marwa), and My sisters (Hana and Marwa)

Abstract

Terfezia boudieri and *Terfezia claveryi* inhibit the LPS/IFN-γ-mediated inflammation in RAW 264.7 macrophages through an Nrf2-independent mechanism

Desert truffles have been used as traditional treatments for a variety of inflammatory disorders. However, the molecular mechanisms underlying their anti-inflammatory effects in RAW 264.7 macrophages have remained to be fully elucidated. Therefore, the present study investigated the anti-inflammatory activities of two main desert truffles, *Terfezia boudieri* and *Terfezia claveryi* and the underlying mechanisms associated with their anti-inflammatory activities in RAW 264.7 macrophages stimulated with lipopolysaccharide/interferon-gamma (LPS/IFN-γ) in order to develop innovative therapeutics for the treatment of inflammation.

To address this objective, RAW 264.7 cells were treated with increasing concentrations of *T. boudieri* and *T. claveryi* extracts in the presence or absence of LPS/IFN-γ to determine the non-cytotoxic concentrations to be used in the study using MTT assay. RAW 264.7 cells were then stimulated with 100 ng/mL of LPS plus 10 U/mL of IFN-γ and co-incubated with *T. boudieri* and *T. claveryi* extracts at concentrations of 5, 10, and 20 µg/mL. Thereafter, the nitric oxide (NO) was measured using Griess assay. Quantitative real-time polymerase chain reaction (qPCR) was used to measure the mRNA expression levels of inducible nitric oxide synthase (iNOS), cyclooxygenase-2 (COX-2), tumor necrosis factor-α (TNF-α), interleukin-6 (IL-6), heme oxygenase-1 (HO-1), oxidative stress-induced growth inhibitor-1 (OSGIN1), and the microRNA expression levels of miR-21, miR-146a, and miR-155. On the protein level, enzyme-linked immunosorbent assay (ELISA) was used to determine the concentration of TNF-α and IL-6 proteins secreted into the cell

culture supernatant, while western blotting was used to determine the protein expression of iNOS and COX-2.

Our results demonstrated that LPS/IFN-γ significantly upregulated the mRNA expression of iNOS, COX-2, TNF-α, and IL-6. The production of NO, TNF-α, and IL-6 was remarkably increased in the medium of LPS/IFN-γ-treated RAW 264.7 cells. Moreover, the expression levels of miR-21, miR-146a, and miR-155 was induced in response to LPS/IFN-γ stimulation. The protein expression levels of iNOS and COX-2 were also increased in LPS/IFN-γ-activated RAW 264.7 cells. However, treatment with *T. boudieri* and *T. claveryi* extracts suppressed NO production in a concentration-dependent manner that coincided with downregulation of iNOS expression at the mRNA and protein levels in LPS/IFN-γ-stimulated RAW 264.7 cells. Both extracts also downregulated the mRNA expression of COX-2, but only *T. boudieri* which reduced the expression of COX-2 protein. On the level of pro-inflammatory cytokines, *T. boudieri* extract downregulated the expression of TNF-α and IL-6, as evidenced by dose-dependent reductions in their mRNA and protein levels. On the other hand, *T. claveryi* exhibited a significant inhibitory effect on the mRNA expression of TNF-α and IL-6 as well as the inhibition of TNF-α protein secretion. However, this effect failed to extend to the protein level of IL-6. Moreover, both studied extracts significantly downregulated the miRNA expression levels of miR-21, miR-146a, and miR-155, which implies that *T. boudieri* and *T. claveryi* suppress the inflammatory response in LPS/IFN-γ-stimulated RAW 264.7 cells through an epigenetic mechanism. To determine whether the anti-inflammatory effects of both *Terfezia* extracts in LPS/IFN-γ-induced RAW 264.7 cells were related to modulation of the nuclear factor erythroid 2-related factor 2 (Nrf2) signaling pathway, we examined the

potential effect of *T. boudieri* and *T. claveryi* on the Nrf2 target genes, HO-1 and OSGIN1. Our findings revealed that both extracts did not activate the Nrf2 target genes, suggesting that *Terfezia*-mediated anti-inflammatory properties are independent of Nrf2 pathway. Therefore, these results indicate that *T. boudieri* and *T. claveryi* exhibit anti-inflammatory activities through suppressing multiple inflammatory mediators and cytokines and may be potential anti-inflammatory agents.

Graphical Abstract

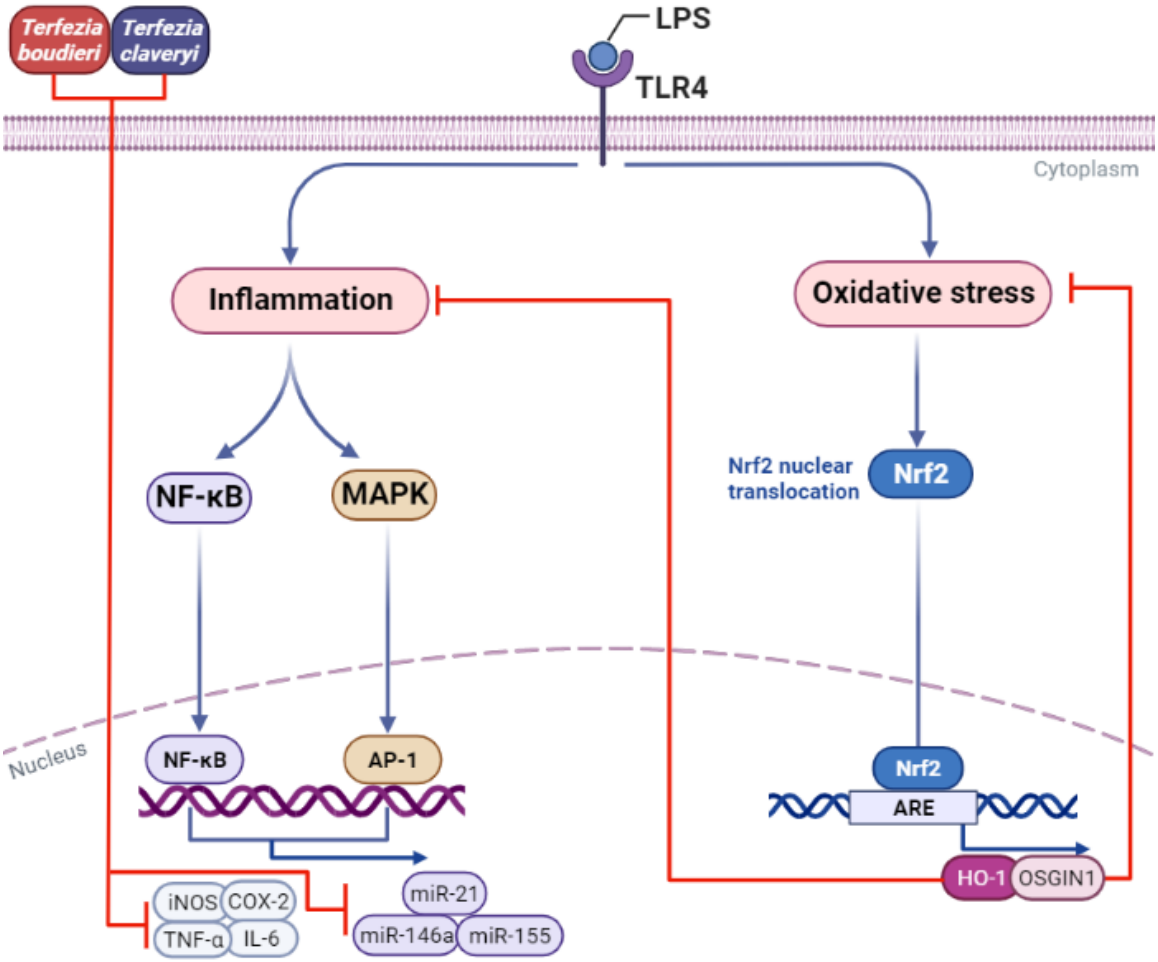

Table of Contents

List of Tables

List of Figures

List of Abbreviations

AP-1	Activator protein 1
APCs	Antigen-presenting cells
ARE	Antioxidant response elements
BMMCs	Mouse bone marrow-derived mast cells
COX	Cyclooxygenase
COX-1	Cyclooxygenase
COX-2	Cyclooxygenase
HO-1	Heme oxygenase 1
IBD	Inflammatory bowel disease
IFN- γ	Interferon-gamma
IKKγ	IkappaB kinase-gamma
IL-1	Interleukin-1
IL-6	Interleukin-6
iNOS	Inducible nitric oxide synthase
IRAK	Interleukin-1 receptor-associated kinases
IRF3	Interferon regulatory factor 3
IκB	Inhibitory-κB
LPS	Lipopolysaccharides
LRP	Leucine-rich repeats
MAPKs	Mitogen-activated protein kinases
MD-2	Myeloid differentiation factor 2
MHC	Major histocompatibility complex
miRNAs	MicroRNAs
mRNAs	messenger RNAs
MyD88	Myeloid differentiation primary response gene 88
NF-κB	Nuclear factor-kappa B
NK cells	Natural killer cells
NKT	Natural killer T cells
NO	Nitric oxide

Nrf2	Nuclear factor erythroid 2–related factor 2
NSAIDs	Non-steroidal anti-inflammatory drugs
OMC	Oyster mushroom concentrate
OSGIN1	Oxidative stress induced growth inhibitor 1
PAMPs	Pathogen-associated molecular patterns
PGE2	Prostaglandin E2
PRRs	Pattern recognition receptors
PUFAs	Polyunsaturated fatty acids
RNS	Reactive nitrogen species
ROS	Reactive oxygen species
SFN	Sulforaphane
TBK1	TANK-binding kinase 1
TCR	T-cell receptor
TGF-β	Transforming growth factor beta
THP-1	Human monocytic leukemia cells THP-1
TIR	Toll/interleukin-1 receptor
TIRAP	TIR-domain-containing adaptor protein
TLR	Toll-like receptor
TLR 4	Toll-Like Receptor 4
TNF-α	Tumor necrosis factor alpha
TRAF6	TNF receptor associated factor 6
TRAM	TRIF-related adaptor molecule
TRIF	TIR-domain-containing adapter-inducing interferon-β

Chapter 1: Introduction

1.1 Immune System

The immune system is a collection of cells and molecules that are designed to perform rapid, specific, and efficient immune responses against invading pathogens, such as bacteria, viruses, parasites, and fungi (Delves & Roitt, 2009; Marshall et al., 2018; Medina, 2016). It also supports the host in the elimination of toxins or allergens that enter across the mucosal surfaces. Central to its ability to identify any intruding microbe, toxic or allergenic substances, the immune system can discriminate between self and non-self-antigens, a feature known as self-tolerance (Chaplin, 2010). The immune system is fundamentally divided into two lines of defense determined by the speed and specificity of the immune response: innate immune system and adaptive immune system (**Figure 1.1**) (Parkin & Cohen, 2001). The host utilizes both innate and adaptive immune mechanisms to detect and eliminate pathogens, with defects in either system, leading to diseases, such as autoimmune diseases, immunodeficiency disorders, inflammation, and hypersensitivity reactions (Chaplin, 2010; Marshall et al., 2018).

1.1.1 Innate Immune System

Innate immune system is the first immunological line of defense, playing a critical role in eliminating pathogens, maintaining normal immune homeostasis, and participating in the activation of the adaptive immunity (Iwasaki & Medzhitov, 2015; Zimmerman et al., 2010). It is a non-specific (antigen-independent) defense mechanism that is rapidly initiated after encountering an antigen. The components of the innate immune system

include physical barriers (skin, mucous membranes, and mucous secretions), physiologic barriers (low pH and temperature), humoral elements (acute phase proteins, antimicrobial peptides, lysozyme, cytokines, complement, and natural antibodies), and cellular elements, including: phagocytic cells (macrophages, monocytes, and neutrophils), cells that release the inflammatory mediators (basophils, eosinophils, and mast cells), dendritic cells, natural killer cells (NK cells), and natural killer T (NKT) cells (Delves & Roitt, 2009; Marshall et al., 2018; Riera Romo et al., 2016; Turvey & Broide, 2010). Among innate immunity cells, dendritic cells act as antigen-presenting cells (APCs), initiating the activation of the T and B cells of the adaptive immune system, and thus acting as key mediators between innate and adaptive immunity (Chaplin, 2010). In addition to their phagocytic properties, macrophages contribute to the antigen presentation to T cells (Martinez-Pomares & Gordon, 2007). NK cells and NKT represent the main sources of the interferon-gamma (IFN- γ), a cytokine produced as a part of the innate immune response to promote antigen presentation and induce the development of anti-viral immunity (Marshall et al., 2018; Schoenborn & Wilson, 2007).

The innate immune system depends on the pattern recognition receptors (PRRs), which are the host receptors that recognize a wide range of microbes sharing common structural features, known as pathogen-associated molecular patterns (PAMPs), such as lipopolysaccharides (LPS), a component of the gram-negative bacterial cell wall. The recognition of PAMPs by cells with PRRs indicates the presence of infection (Marshall et al., 2018; Taguchi & Mukai, 2019). The innate immune system is characterized by its ability to recruit immune cells to the site of inflammation or infection rapidly via the release of signaling proteins, known as chemokines which recruit inflammatory leukocytes,

reactive free radical species, lipid mediators of inflammation, bioactive amines, and enzymes that participate in tissue inflammation, and cytokines which are involved in the regulation of cell-cell communication. During innate immunity, cytokines induce multiple defense mechanisms across the body along with activating local cellular responses to injury or infection. (Chaplin, 2010; Turner et al., 2014). Tumor necrosis factor alpha (TNF-α), interleukin-1 (IL-1), and interleukin-6 (IL-6) are three important inflammatory cytokines produced during the early immune response to bacterial infection. These cytokines are essential for cell recruitment and local inflammation which is required for the elimination of many infections (Beutler, 2001; Chaplin, 2010; Marshall et al., 2018). Therefore, the dysregulation in the inflammatory cytokines production is commonly related to inflammatory diseases, making them potential therapeutic targets (Marshall et al., 2018).

1.1.2 Adaptive Immune System

Adaptive immune system, on the other hand, is an antigen-dependent, and it has evolved to execute broader and more finely tuned antigen-specific reactions. Adaptive immune system applies a tightly regulated interplay between the T lymphocytes (T cells), which are antigen-specific cells that mature in the thymus, and induced to proliferate via the effect of APCs, and the B lymphocytes (B cells) which can be developed into plasma cells to produce antibodies. Adaptive immunity enables the host to produce a more rapid and vigorous immune response upon subsequent exposure to the antigen through the generation of immunologic memory (Bonilla & Oettgen, 2010; Chaplin, 2010; Delves & Roitt, 2009; Takahama, 2006). Lymphocytes are distinguished by their high mobility. Flowing maturation in the primary lymphoid organs, including bone marrow and thymus, they migrate to the secondary lymphoid organs, such as spleen and lymph nodes, where

they capture the circulating antigens from blood and lymph, respectively (Bonilla & Oettgen, 2010). Adaptive immune responses in the secondary lymphoid organs are generally triggered by innate immune system signals, which are transmitted either directly by circulating pathogens or indirectly by APCs moving to these areas. Therefore, lymphocytes immigrating from the lymph nodes and spleen can subsequently move to many sites throughout the body to execute the cellular immune responses (Bonilla & Oettgen, 2010; Delves & Roitt, 2009).

T cells are characterized by their unique cell-surface expression of the T-cell receptor (TCR), which is a transmembrane protein recognizes the fragments of antigens (peptides) displayed by the APCs. On the other hand, the APCs express both class I and class II of the major histocompatibility complex (MHC) proteins, which allow the TCR on T cells to detect antigens (Chaplin, 2010). The MHC-antigen complex activates the TCR, and the T cells subsequently produce cytokines which regulate the immune response. Furthermore, T cells are stimulated to differentiate into either T-helper (T_h) cells (CD4+ cells) or cytotoxic T cells (CD8+ cells) due to the antigen presentation process. Cytotoxic T cells are mainly responsible for the destruction of cells infected with any pathogen, such as bacteria or virus (Bonilla & Oettgen, 2010; Marshall et al., 2018). Unlike T cell, B cells have unique antibodies on their cell surface that allow them to recognize antigens directly without the need for APCs. When induced by foreign antigens, B cells differentiate into plasma cells producing antibodies (Bonilla & Oettgen, 2010; Marshall et al., 2018).

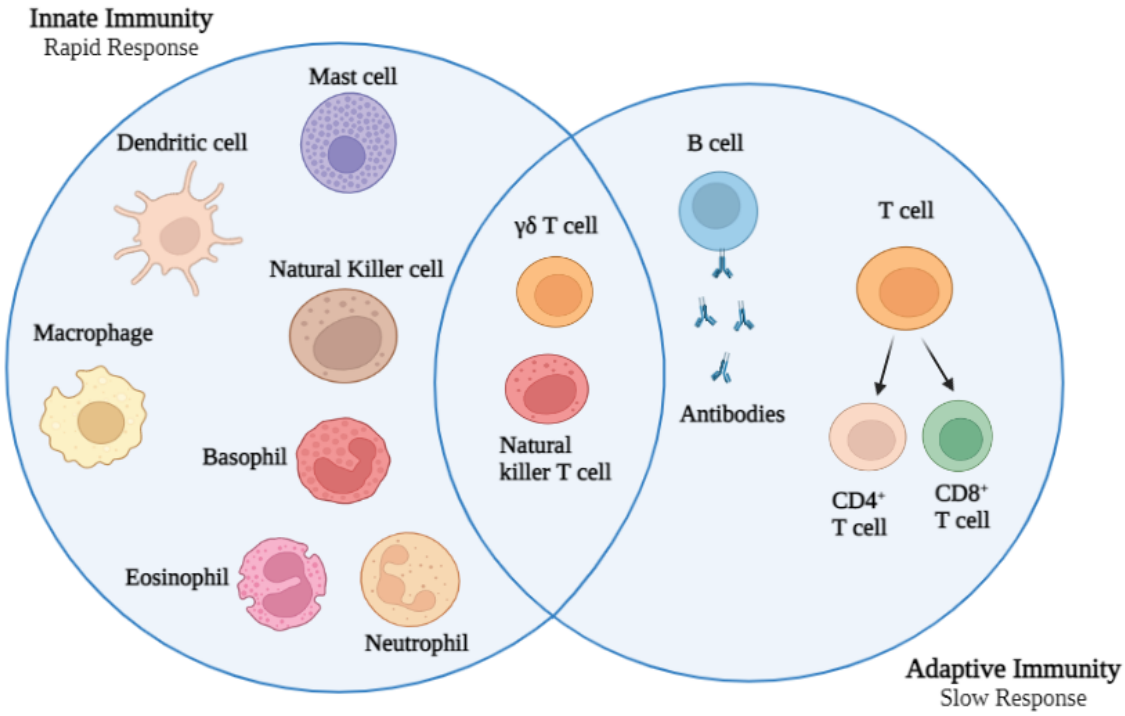

Figure 1.1 A schematic diagram of the innate and adaptive immune systems

1.1.3 Inflammation

Inflammation is a highly regulated process that can be triggered by biological, chemical, and/or physical stimuli, such as infection and tissue injury (Tasneem et al., 2019). It is the primary response of the immune system through which the body can remove infection and repair tissue damage (K. Newton & Dixit, 2012). The acute inflammatory response is characterized by coordinated delivery of leukocytes to the site of infection or injury, which appears in the form of redness, swelling, heat, and pain (Medzhitov, 2010). This response is promoted by the innate immune cells that can produce a variety of inflammatory mediators, which in turn elicit a local inflammatory exudate (Medzhitov, 2008). For example, inflammatory mediators, including histamine, prostaglandins, and nitric oxide (NO) enhance vasodilation, which subsequently leads to apparent increase in blood flow and recruitment of leukocytes to the region of inflammation. Moreover, cytokines, such as TNF-α and IL-1 stimulate leukocytes extravasation through elevating the levels of leukocyte adhesion molecules on endothelial cells (K. Newton & Dixit, 2012).

The inflammation process is generally divided into acute and chronic phases. Acute inflammation is characterized by the exudation of plasma proteins and leukocytes to the extravascular tissues at the site of infection, or injury. It lasts for a few minutes to several hours or days, depending on the degree of injury. Chronic inflammation, on the other hand, lasts for prolonged periods of several months to years, and is associated with tissue damage and fibrosis (Abdulkhaleq et al., 2018; Germolec et al., 2018). A successful and well-controlled acute inflammatory response is a beneficial process that results in the elimination of the noxious stimuli and restoring the body homeostasis, as if the inflammatory trigger is not removed or persists, the inflammation can become chronic

(Medzhitov, 2008, 2010). Chronic inflammation can contribute to several diseases, such as asthma, arthritis, autoimmune diseases, atherosclerosis, cancer, and diabetes (Germolec et al., 2018)

1.1.4 Inflammatory Mediators and Major Signaling Pathways

The inflammatory response is mediated by a wide range of mediators forming complex regulatory networks that prevent further tissue damage and restore the normal physiology of the inflamed tissues. The secreted inflammatory mediators, including cytokines (e.g., TNF-α, IL-1, and IL-6), chemokines (e.g., IL-8), vasoactive amines (e.g., histamine and serotonin), eicosanoids (e.g., prostaglandins, thromboxanes, and leukotrienes), peptides (e.g., bradykinin), and reactive nitrogen species (e.g., NO) are commonly associated with several inflammatory diseases (Medzhitov, 2010).

Cytokines are key signaling proteins, regulating the interactions between different cell types involved in the immune and inflammatory response (Abdulkhaleq et al., 2018). Cytokines are mainly produced by phagocytic cells and NK cells during innate immune responses, while they are mostly secreted by lymphocytes and APCs during adaptive immune responses. Therefore, cytokines coordinate the crosstalk between the innate and adaptive immune systems (Turner et al., 2014). They are classified into pro-inflammatory cytokines (TNF-α, IL-1, IL-6, IL-15, IL-17, and IL-23), and anti-inflammatory cytokines (IFN-γ, IL-4, IL-10, IL-13, and transforming growth factor β (TGFβ)) (Berczi & Szentivanyi, 2003).

Among cytokines, TNF-α is the major mediator of inflammation with several effects, including stimulating other cytokines production, activation of cell adhesion molecules,

and promoting cell growth and proliferation. TNF-α has also been reported to induce the expression of the MHC (Class I and II) molecules, leading to the activation of immune cells and ultimately cytokine production (Turner et al., 2014; Zelová & Hošek, 2013). It is also essential to the process of eliminating dead and injured cells through inducing apoptosis (S. Gupta, 2002; *TNF*, 2008). IL-6 is another important cytokine released during inflammation, and its dysregulation causes a variety of inflammatory disorders (Balkwill & Mantovani, 2010). IL-6 is primarily produced by monocytes, macrophages, and T cells at the site of inflammation (Heinrich et al., 2003). It has also been recognized as the B-cell differentiation factor that facilitate the differentiation of B cells into antibody-producing cells. Moreover, IL-6 aids in the activation and differentiation of T cells (Akdis et al., 2016; Germolec et al., 2018). Chemokines or chemoattractant cytokines are a group of small cytokines produced by immune cells to attract leukocytes to the site of infection or injury (Raman et al., 2011). IL-8 is the major pro-inflammatory chemokine whose secretion is regulated by TNFα, IL-1β, hypoxia and steroidal hormones (estrogens, androgens). IL-8 enhances the chemotaxis and modulates the cell proliferation and apoptosis (A. Li et al., 2003).

Eicosanoids are another major class of inflammatory mediators, which regulate the inflammatory response. Eicosanoids are bioactive signaling molecules that are produced when arachidonic acid or other polyunsaturated fatty acids (PUFAs) are metabolized by cyclooxygenases to produce prostaglandins and thromboxanes, or lipoxygenases to produce leukotrienes and lipoxins (Khanapure et al., 2007). Eicosanoids play a significant role in modulating numerous physiological processes, particularly during immune responses. This can be seen by the extensive use of the non-steroidal anti-inflammatory

drugs (NSAIDs) during inflammatory conditions, which are potent inhibitors of cyclooxygenases (Khanapure et al., 2007; Tasneem et al., 2019).

Reactive nitrogen species (RNS), such as NO are another key signaling molecules that play an important role in the inflammatory response. NO is released as a cellular signaling molecule to increase the vasodilation in blood vessels by the activation of nitric oxide synthase (NOS), which is found in three isoforms: endothelial nitric oxide synthase (eNOS), neuronal nitric oxide synthase (nNOS), and inducible nitric oxide synthase (iNOS). The iNOS isoform is mainly associated with the inflammatory immune cells, where it is activated during the inflammatory process (Alderton et al., 2001; Tasneem et al., 2019).

Several transcription factors, including nuclear factor-kappa B (NF-κB), and nuclear factor erythroid 2-related factor 2 (Nrf2) play a key role in modulating the expression of the pro-inflammatory mediators during inflammation (Saha et al., 2020; Tornatore et al., 2012). NF-κB is an evolutionarily conserved transcription factor, consisting mainly of two subunits p50 and p65. It has been identified to play an active role in chronic inflammatory disorders, such as Crohn's disease and inflammatory bowel disease (IBD) (Kaser et al., 2008). NF-κB is found in the cytoplasm associated with the inhibitory-κB (IκB) as an inactive complex form (Gilmore, 2006; Hayden & Ghosh, 2008). Oxidative and pro-inflammatory stimuli, such as cytokines and LPS, activate NF-κB via phosphorylation-dependent proteasomal degradation of IkBα, leading to the nuclear translocation and binding of NF-κB to kB elements found in the proximal promoter region of genes encoding pro-inflammatory mediators, such as cytokines, iNOS, and COX-2 (S. C. Gupta et al., 2011; R. Newton et al., 1997; Y. Wu et al., 2014; Xie et al., 1994).

Nrf2 is another key transcription factor, playing a central role in the inflammation signaling pathways and oxidative stress responses. Inflammatory cells, including macrophages, mast cells, monocytes, and lymphocytes produce numerous inflammatory mediators, which subsequently attract more inflammatory cells to the site of injury, leading to increase in the level of intracellular reactive oxygen species (ROS) and oxidative stress (Saha et al., 2020). Meanwhile, persistent oxidative stress has been found to be associated with chronic inflammation (Tu et al., 2019). Nrf2 contributes to the maintenance of intracellular redox homeostasis and protection against oxidative stress through binding to the antioxidant response element (ARE) located in the promoter region of genes encoding phase II detoxifying enzymes or antioxidant enzymes (e.g., heme oxygenase-1 (HO-1)), and oxidative stress response proteins (e.g., oxidative stress induced growth inhibitor 1 (OSGIN1)) (Ahmed et al., 2017; Brennan et al., 2017; Chen et al., 2006; R. Li et al., 2007; Martín-de-Saavedra et al., 2013; Sukkar & Harris, 2017). Nrf2/ARE signaling pathway is also important in reducing inflammation-related disorders, including atherosclerosis, asthma, autoimmune diseases, and rheumatoid arthritis (Lee & Johnson, 2004). Several studies have reported that the activation of Nrf2 signaling pathway suppressed cytokines, chemokine, iNOS, COX-2 secretion, which in turn modulate the NF-kB and other inflammatory cascades that regulate the transcription and activity of downstream target proteins during the inflammation process (Ahmed et al., 2017; Kobayashi et al., 2016).

1.1.5 Toll-Like Receptor 4 (TLR4) Signaling Pathway in Inflammation

Toll-like receptors (TLRs) are a class of conserved PRRs that are triggered by a broad range of PAMPs, eliciting an innate immune response and inflammation through the production of pro-inflammatory cytokines (Kawai & Akira, 2010; O'Neill et al., 2013).

Each class of PAMP has a unique TLR that can be used to fine-tune the inflammatory response so that the pathogen can be removed more effectively (Swanson et al., 2020).

TLR4 is a member of the TLR family that can be stimulated by LPS, which is the major component of the gram-negative bacterial cell wall (Beutler, 2002; Beutler et al., 2001; Swanson et al., 2020). TLR4 is transmembrane protein containing an extracellular region with leucine-rich repeats (LRR) that recognizes PAMPs, coupled to an intracellular Toll/interleukin-1 receptor (TIR) domain which is responsible for the signal transduction **(Figure 1.1) (**Kuzmich et al., 2017; K. Newton & Dixit, 2012). Firstly, LPS is recognized by the TLR4 in the presence of myeloid differentiation factor 2 (MD-2), which is an adaptor protein required for binding of LPS to TLR4 (Shimazu et al., 1999). The receptors are then dimerized on the cell membrane, initiating the intracellular signal, which can proceed into two distinct pathways, myeloid differentiation primary response gene 88 (MyD88)-dependent pathway and TIR-domain-containing adapter-inducing interferon-β (TRIF)-dependent pathway (O'Neill & Bowie, 2007).

In the MyD88-dependent pathway, the TIR-domain-containing adaptor protein (TIRAP), which is an intracellular protein is attached to the intracellular TLR4-TIR domains, constituting an interface for MyD88 attachment (Z. Lin et al., 2012; Valkov et al., 2011). Then, the MyD88 adaptor molecules aggregate and interact with Interleukin-1 receptor-associated kinases 2 and 4 (IRAK2 and IRAK4), forming a complex known as the myddosome, which induces the autophosphorylation of IRAK4. Phosphorylation of IRAK1 can also occur through binding to the MyD88-IRAK4 complex, with further interaction with the TNF receptor associated factor 6 (TRAF6) to form IRAK1-TRAF6 complex (Ferrao et al., 2014; S.-C. Lin et al., 2010). The recognition of TRAF6

polyubiquitin chains by the adaptor proteins TAB2/TAB3 along with the IkappaB kinase-gamma (IKKγ) subunit of the IKK-complex results in the activation of TAK1 and phosphorylation of IκB complex, releasing the NF-κB with further translocation to the nucleus. TAK1 can also induce the Activator protein 1 (AP-1) through the activation of mitogen-activated protein kinases (MAPKs). NF-κB and AP-1 eventually promote the production of the pro-inflammatory cytokines that can modulate the immune response in the cells (Akira & Takeda, 2004; Ferrao et al., 2014; Kawai & Akira, 2010).

In the TRIF-dependent pathway, the TRIF-related adaptor molecule (TRAM) is selectively recruited to the TIR-domains of the TLR4 to conduct the signal from TLR4 to TRIF. Then, TRAF3 induces the phosphorylation of the interferon regulatory factor 3 (IRF3) through recruiting the TANK-binding kinase 1 (TBK1) and IKKi. Phosphorylated IRF3 subsequently dimerizes and translocate to the nucleus to induce the expression of type I IFN genes (Kawasaki & Kawai, 2014).

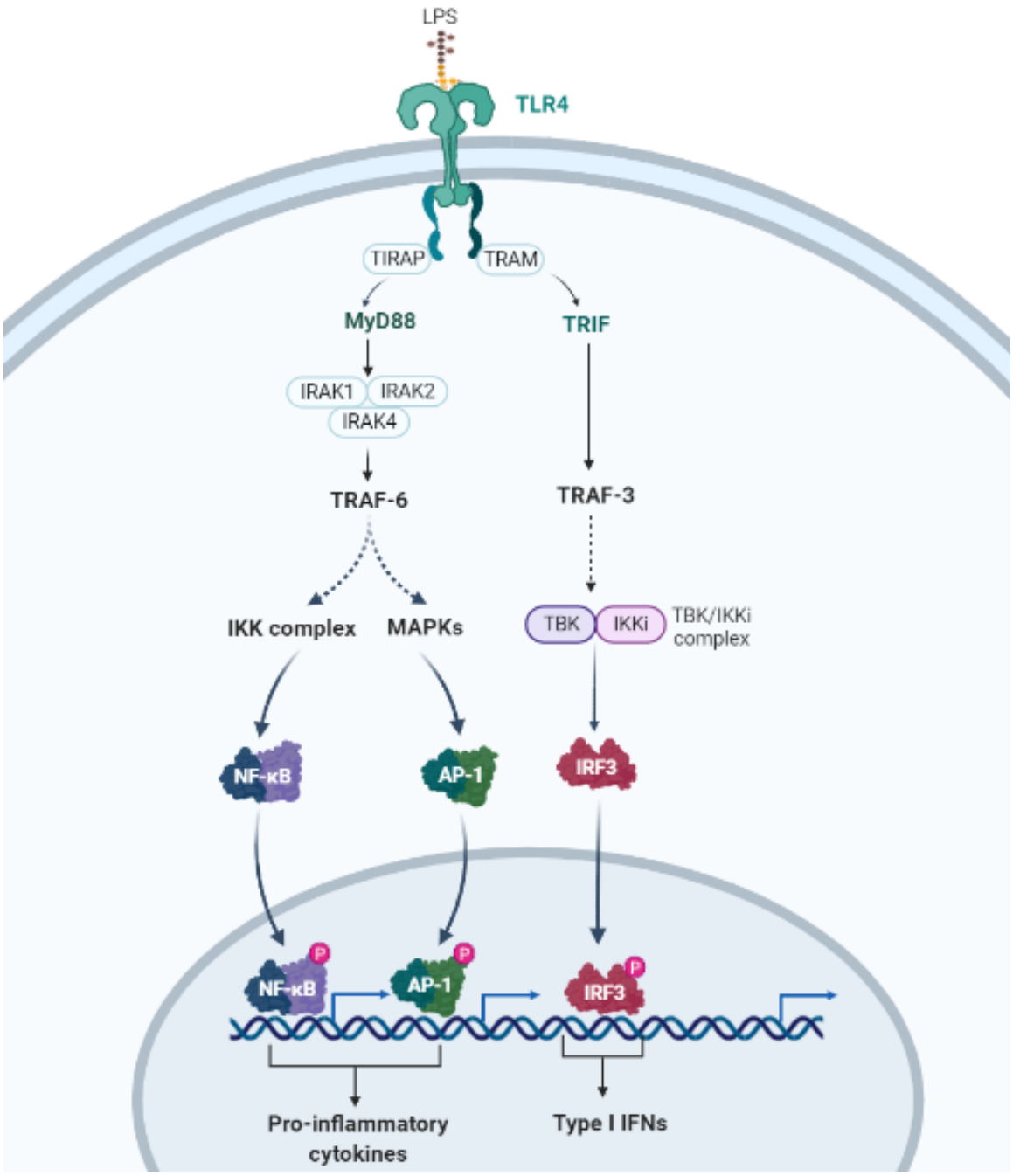

Figure 1.2 TLR4 Signaling Pathway

1.1.6 Role of Macrophages in Inflammation

Macrophages are innate immune cells derived from bone marrow monocytes which can be differentiated into macrophages in the tissues after exposure to pro-inflammatory cytokines, local growth factors and microbial products (Epelman et al., 2014; Wynn et al., 2013). They have several functions during the inflammation process, including phagocytosis of microbes, antigen presentation, and secretion of inflammatory mediators (Shapouri-Moghaddam et al., 2018). Furthermore, macrophages are essential for maintaining homeostasis and tissue regeneration after injury (Watanabe et al., 2019; Wynn et al., 2013).

Macrophages are extraordinary flexible cells that can change their phenotype and function in response to microenvironmental stimuli and signals in each tissue. This process is known as macrophage polarization (Sica & Mantovani, 2012). Macrophages are typically classified into two subtypes M1 or M2 macrophages based on their cell surface markers, secreted cytokines, and functions (Shapouri-Moghaddam et al., 2018). M1 or classically activated macrophages are pro-inflammatory cells that can be induced by LPS or IFN-γ, leading to secretion of several pro-inflammatory cytokines, such as TNF-α, IL-1β, IL-6, IL-12, and IL-23 (Cassetta et al., 2011; Shapouri-Moghaddam et al., 2018; Sica et al., 2015). On the other hand, M2 or alternatively activated macrophages are anti-inflammatory cells that can be stimulated in response to IL-4 and IL-13, producing anti-inflammatory cytokines, such as IL-10 and TGF-β (Porta et al., 2015; N. Wang et al., 2014). It is recognized that the balance between M1 and M2 macrophage polarization determines the status of an organ during the inflammation or injury. Macrophages initially adopt M1 phenotype in response to infection or inflammation, releasing TNF-α, IL-1β, IL-

12, and IL-23. However, if M1 macrophages continue to work, they can induce tissue damage. As a result, M2 macrophages produce IL-10 and TGF-β to reduce the inflammation and restore tissue homeostasis (Shapouri-Moghaddam et al., 2018).

1.1.7 Role of MicroRNAs (miRNAs) in TLR4 Signaling Pathway During Inflammation

MicroRNAs (miRNAs) are small single-stranded non-coding RNAs, containing approximately 22 nucleotides in length that can post-transcriptionally regulate gene expression via binding to the 3′-untranslated region (UTR) of target messenger RNAs (mRNAs) to repress translation or degradation of the mRNAs (Bartel, 2018; O'Brien et al., 2018). Each miRNA can control the expression of several target genes, indicating that a large part of the human genome can be regulated by miRNAs (Quinn & O'Neill, 2011; H. Wang et al., 2019). miRNAs are now recognized to play major roles in the regulation of immune cell functions of both the innate and adaptive systems through targeting of the inflammation-related genes, including TLRs. Moreover, miRNAs can function as physiological ligands for TLRs, and thus triggering the immune response (Fabbri et al., 2013; Mehta & Baltimore, 2016). Among miRNAs involved in the immune and inflammatory pathways, miR-21, miR-146a, and miR-155 have been predominant in most of miRNA research because of their significant relevance to TLR signaling pathway and their ubiquitous expression (Quinn & O'Neill, 2011).

1.1.7.1 miR-21

The miR-21 is a multifunctional miRNA that play a central role in several tumors due to its abnormal expression as well as multiple inflammatory pathways, including TLR signaling pathway (Quinn & O'Neill, 2011; Sheedy et al., 2010). In a study conducted by Sheedy et al., they indicated that miR-21 negatively regulated the inflammatory response to LPS through targeting of the programmed cell death protein 4 (PDCD4), which is a pro-inflammatory protein contributing to the activation of the pro-inflammatory mediator (NF-κB) and suppression of the anti-inflammatory cytokine (IL-10). The induction of miR-21 by LPS resulted in downregulation of PDCD4 expression. This process inhibited NF-κB activity and promoted IL-10 production to decrease the lethality of LPS (Sheedy et al., 2010).

1.1.7.2 miR-146a

The miR-146a belongs to the miR-146 family which contain miR-146a and miR-146b that are found on the chromosomes 5 and 10, respectively (Quinn & O'Neill, 2011). miR-146a has been identified as a major mediator in tumorigenesis and inflammatory response, with overexpression in a variety of inflammatory disorders, including osteoarthritis and rheumatoid arthritis (Bhaumik et al., 2008; Nakasa et al., 2008; Sonkoly et al., 2008).

The role of miR-146a in TLR signaling was revealed in a study by Baltimore et al. They demonstrated that LPS, TNFα, and IL-1β induce miR146a transcription in an NF-κB -dependent manner, and thus miR-146a potentially mediated IRAK1 and TRAF6, suggesting it as a negative regulator of the innate immune response (Baltimore et al., 2006).

1.1.7.3 miR-155

The miR-155 is another cancer-associated miRNA that has a well-characterized role in inflammation through targeting multiple signaling proteins involved in the TLR and NF-κB signaling pathways (Ferrajoli et al., 2013; X. He et al., 2014). According to Baltimore et al., the macrophage inflammatory response is characterized by the presence of upregulated miR-155 (O'Connell et al., 2007). Another study by Ceppi et al. reported that miR-155 was induced in response to LPS in monocyte-derived dendritic cells and in turn negatively regulated the inflammatory cytokine production, and hence acting as anti-inflammatory agent. This negative regulation by miR-155 was related to its ability to target TAB2 in the TLR/IL-1 inflammatory pathway, suppressing its activation of TAK1, and thus the NF-κB and MAPK (Ceppi et al., 2009). Therefore, miR-155 represent a key modulator in the downstream inflammatory pathways (Quinn & O'Neill, 2011).

1.1.8 *In vitro* Models of Macrophages for the Screening of Anti-inflammatory Drugs

In vitro models are important tools in testing the anti-inflammatory drugs and biomaterials through assessing the inflammatory response, cytotoxicity, and biocompatibility. Cells of the mononuclear phagocytic system, including monocytes and macrophages, such as RAW 264.7 macrophages and human monocytic leukemia cells (THP-1) are extensively used as *in vitro* models of inflammation (Chamberlain et al., 2009; Patil et al., 2019). The activation of such cell with LPS and/or IFN-γ produces several inflammatory mediators, such as prostaglandin, NO, TNF-α, IL-1, and IL-6 (Gunawardena et al., 2014; Tian et al., 2021).

1.2 Anti-inflammatory Drugs

Currently, nonsteroidal anti-inflammatory drugs (NSAIDs) are the most widely prescribed drugs to treat both acute and chronic inflammatory disorders. However, their long-term use is associated with serious adverse effects, such as peptic ulcers, cardiovascular toxicity, hypertension, acute renal failure, and nephrotic syndrome (Sinha et al., 2013; Vonkeman & van de Laar, 2010). Therefore, there is an imperative need for research on the development of new natural-based anti-inflammatory compounds without side effects as alternatives to the current NSAIDs (Jung et al., 2019; C. Park et al., 2021). The natural products have been demonstrated to be a valuable source of biologically active compounds, many of which have been the basis for the development of novel drugs (Palombo, 2011). In this regard, truffles have a long history of use as traditional remedies to treat many human diseases, especially eye and skin diseases (Khalifa et al., 2019).

1.3 Truffles

Truffles have traditionally been used as functional foods and therapeutic agents (H. El Enshasy et al., 2013). This is mainly attributed to their high nutritional value as potential sources of amino acids, proteins, carbohydrates, fats, lipids, and minerals (S. Wang & Marcone, 2011; Yan et al., 2017). Moreover, they contain abundant bioactive compounds, such as phenolics, phytosterols, polysaccharides, flavonoids, and terpenoids, which are related to their anti-inflammatory, immunomodulatory, antioxidant, anticancer, antibacterial, antiviral, and antidiabetic properties (AlAhmed & Khalil, 2019; Beara et al., 2014; Dahham et al., 2018; Elkhateeb et al., 2019; Janakat et al., 2004; Lee et al., 2020; Patel et al., 2017). Therefore, there has been an increasing interest in truffles as a source of biologically active substances which provide to humans medicinal and health benefits, such as the prevention and treatment of diseases (Lee et al., 2020).

1.3.1 Classification and Types

Truffles are hypogeous fruiting bodies of the ascomycetes fungi that grow between 5 and 10 centimeters underground. There are over a hundred different species of truffles identified around the world, and new species are being discovered on a regular basis (Lee et al., 2020). Truffles are taxonomically classified as members of the Tuberaceae and Terfeziaceae families, and the order Pezizales (Jamali, 2014). Truffle species within the genus *Tuber*, family Tuberaceae are also known as true truffles, such as *Tuber magnatum* (white truffle) and *Tuber melanosporum* (black truffle) growing naturally in Europe (Berch & Bonito, 2016). On the other hand, desert truffle species growing in the semi-arid and arid of the Mediterranean region such as Egypt belong to the genus *Terfezia* and *Tirmania*, family Terfeziaceae (Bradai et al., 2015). The genus *Terfezia* is composed of more than 20

species. Among these species, *Terfezia boudieri* and *Terfezia claveryi* are the most popular desert truffle species (Khalifa et al., 2019). More details about the phylogeny of truffle species are illustrated in **Figure 1.3**. In general, truffles are characterized by their distinguished structure of firm, dense, and woody feature (Lee et al., 2020). Truffles are ecologically symbiotic microorganisms that form an ectomycorrhizal symbiotic relationship with the roots of different trees (Elsayed et al., 2014; Mello et al., 2006). In this mutualistic interaction, fungi facilitate mineral and water uptake and plants produce sugar through photosynthesis (Khalifa et al., 2019). Due to this ectomycorrhizal relationship, truffles distribution is limited not only by the environmental conditions but also by the availability of the host plant (H. El Enshasy et al., 2013).

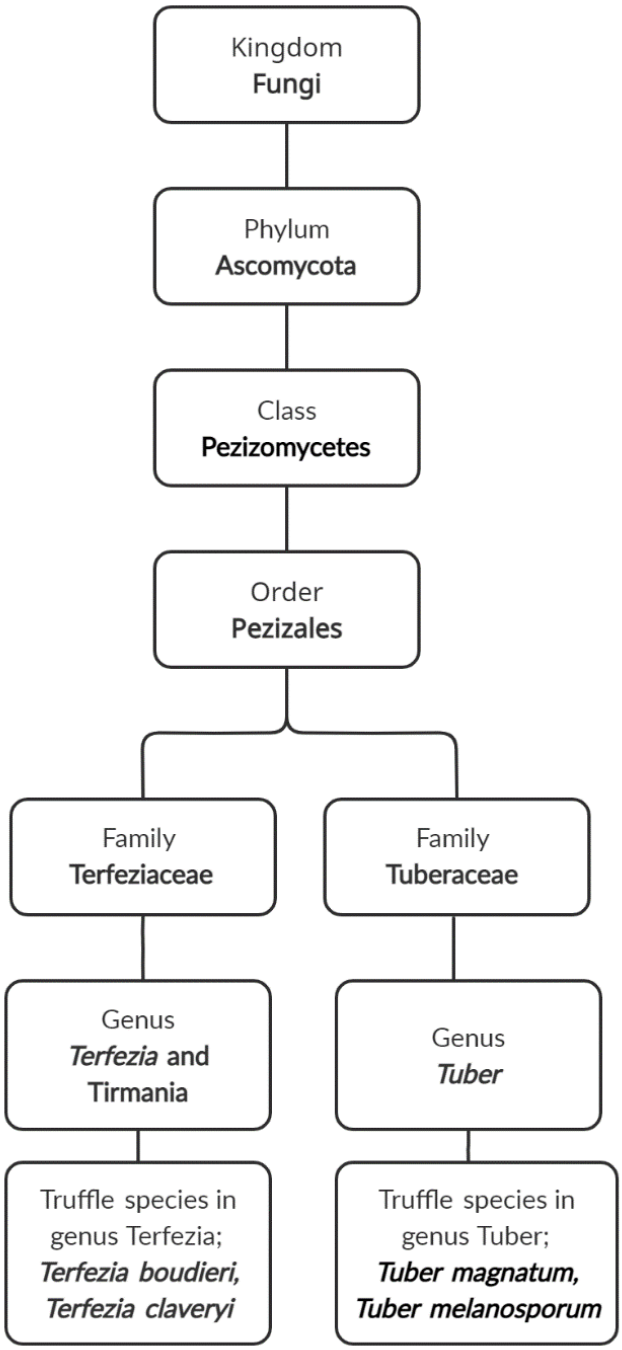

Figure 1.3 A schematic overview of the two major families identified in the order Pezizales

1.3.2 Chemical Properties of *T. boudieri* and *T. claveryi*

1.3.2.1 The Nutritional Profile of *T. boudieri* and *T. claveryi*

T. boudieri and *T. claveryi* contain high amounts of nutritionally beneficial compounds, and thus their chemical profile and nutritional value were well explored (Veeraraghavan et al., 2021). The nutritional composition results expressed on a truffle dry mass of *T. boudieri* and *T. claveryi* were presented in **Table 1.1** (Bokhary & Parvez, 1993; Hamza et al., 2016). Carbohydrates and proteins were the most abundant nutrients in both species, but the contents of *T. boudieri* were found to be higher than the values reported for *T. claveryi*. The chemical analysis of *T. boudieri* showed that the dry mass contained (26 g/100 g) carbohydrates, (26 g/100 g) proteins, (8 g/100 g) fats, (4.49 g/100 g) ash. The results of anthocyanins, ascorbic acid, carotenoids of *T. boudieri* were 3.5 g/100 g, 1.2 g/100 g, and 0.1 g/100 g, respectively (Hamza et al., 2016). On the other hand, *T. claveryi* exhibited lower contents with (28 g/100 g) carbohydrates, (16 g/100 g) proteins, (2 g/100 g) fats, and (4 g/100 g) ash (Bokhary & Parvez, 1993). The primary metabolome of *T. boudieri* was characterized by the abundance of fatty acids, such as linoleic acid, oleic acid, and palmitic acid, accounting for more than 95% of its total fat content. On the other hand, fatty acids in *T. claveryi* represented by linoleic acid, oleic acid, margaric acid, lauric acid, and stearic acid (Darwish et al., 2021a; Hamza et al., 2016). Amino acids constituted a major class of primary metabolites in *T. boudieri* and *T. claveryi*, indicating that these desert truffles represent a valuable source of essential amino acids. Alanine and glutamic acid were the predominant amino acids in *T. boudieri*, while proline and glycine were the main amino acids in *T. claveryi* accounting for 16 and 19 µg/mL, respectively (Kıvrak, 2015; Owaid, 2018).

Minerals are important dietary elements that are essential for various metabolic processes, transmission of nerve impulses, rigid bone formation, and the maintenance of water and salts (Gençcelep et al., 2009). Several studies have demonstrated that *T. boudieri* and *T. claveryi* provide a wide range of essential minerals, such as potassium, calcium, magnesium, sodium, phosphorus, iron, cupper, and manganese **(**

Table 1.2**)** (Akyüz, 2013; Dundar et al., 2012; Kıvrak, 2015; Şahin et al., 2020). Therefore, truffles intake could be expected to contribute a large proportion of the essential mineral requirements in the body.

Table 1.1 Nutritional contents (% of dry weight) of *T. boudieri* and *T. claveryi*

Nutritional contents	***T. boudieri***	***T. claveryi***
Carbohydrates	62%	28%
Proteins	26%	16%
Fats	8%	2%
Ash	4.49%	4%
Anthocyanins	3.5%	-
Ascorbic acid	1.2%	-
Carotenoids	0.1%	-

Table 1.2 Mineral concentrations (mg/100 g dry weight) in *T. boudieri* and *T. claveryi*

Minerals	***T. boudieri***	***T. claveryi***
K	1513	1130
Ca	474	50
Mg	126	100
Na	27	130

P	323	430
Fe	170	110
Cu	0.92	3
Mn	3	15

1.3.2.2 Functional Anti-inflammatory Compounds in the Chemical Profile of *T. boudieri* and *T. claveryi*

The metabolomic analysis of *T. boudieri* and *T. claveryi* revealed that their extracts contained several bioactive compounds, such as polysaccharides, phenolics, terpenoids, proteins, and fatty acids, which may be responsible for their anti-inflammatory potential (Elsayed et al., 2014; Farag et al., 2021). However, the mechanisms underlying their anti-inflammatory properties still require further investigations. To our knowledge, so far, there were no available studies about the anti-inflammatory properties of *T. boudieri* or *T. claveryi* in RAW 264.7 macrophages.

1.3.2.2.1 Polysaccharides

The primary metabolome of *T. boudieri* was characterized by the abundance of sugars at 92.70 µg/mL compared to 58.71 µg/mL in *T. claveryi*. Meanwhile, trehalose and turanose are the predominant disaccharides in both *T. boudieri* and *T. claveryi* (Farag et al., 2021). In general, the majority of polysaccharides found in fungi are β-glucan polymers, with the main chain containing β-(1, 3) linkage and some β-(1-6) branches (Friedman, 2016; Hou et al., 2020). Recently, polysaccharides have attracted increasing interest due to their accessibility, safety, and potent anti-inflammatory properties (Guo et al., 2018).

It has been reported from previous studies that natural polysaccharides exhibited anti-inflammatory activities through various targets and cell signaling pathways. In a study of subarachnoid hemorrhage conducted to elucidate the anti-inflammatory effects of trehalose on blood-induced inflammation in RAW264.7 macrophages, Echigo et al. revealed that trehalose decreased the levels of cytokines (TNF-α, IL-1α, IL-1β, and IL-6) in hemolysate-induced RAW264.7 macrophages. The expression of iNOS and COX-2 was also reduced in trehalose-treated cells (Echigo et al., 2012). Another study conducted on *Agaricus blazei* mushroom extract, which is particularly rich in *β*(1,3)-, *β*(1,4)-, and *β*(1,6)-D-glucans. The chloroform-soluble extract of *A. blazei* suppressed the secretion of IL-6 and downregulated the phosphorylation of the protein kinase (B) AKT in mouse bone marrow-derived mast cells (BMMCs). Moreover, the extract inhibited β-hexosaminidase degranulation as well as the secretion of IL-6, leukotriene C4, and prostaglandin D2 in BMMCs (Song et al., 2012). Jedinak et al. demonstrated that oyster mushroom concentrate (OMC), containing α- and β-glucans inhibited LPS-dependent induction of TNF-α, IL-6, and IL-12 in RAW 264.7 macrophages. In addition, OMC suppressed LPS-induced production of NO and prostaglandin E2 (PGE2) through downregulation the expression of iNOS and COX-2 expression, respectively. They also reported that OMC reduced LPS-dependent induction of NF-κB in RAW 264.7 macrophages (Jedinak et al., 2011). According to Li et al. the natural polysaccharides derived from *Pleurotus eryngii* significantly decreased the cytokine production ratios (TNF-α/IL-10, IL-1β/IL-10,and IL-6/IL-10) in RAW 264.7 macrophages (S. Li & Shah, 2016).

The anti-inflammatory activities of polysaccharide are correlated with their chemical structures, including their molecular weights, sulfate contents, chain conformations,

monosaccharide compositions, and glycosidic bond types and positions (Cheng et al., 2016; Cho et al., 2010; Du et al., 2015). For instance, Wu et al, reported that the polysaccharides isolated from brown alga *Sargassum cristaefolium*, with molecular weight of 386.1 kDa and 9.42% sulfate content showed higher NO inhibitory effect in LPS-stimulated RAW264.7 macrophages. They suggested that the sulfate content of *Sargassum cristaefolium* might impact its binding to the cell receptor, and thus affect NO secretion in the cells (G.-J. Wu et al., 2016). Chain conformation is another critical aspect affecting the anti-inflammatory activities of polysaccharides. Generally, polymers can adopt different chain conformations, such as duplex, or triplex, random coil, rod-like, and sphere-like shapes (Y. Meng et al., 2020). Polysaccharides were shown to be more active in the triple-helix configuration (H. A. El Enshasy & Hatti-Kaul, 2013; Palleschi et al., 2005). For example, β-glucans that found in a triple-helix state frequently displayed higher immunomodulatory effects. Studies indicated that the triple-helix configuration of β-glucans might be better identified by immune cell receptors due to its higher stiffness (Y. Meng et al., 2020; Mueller et al., 2000). The bioactivities of polysaccharides are also regulated by monosaccharide compositions (Ji et al., 2018). Further research identified that dendritic cells and macrophages express abundant carbohydrate receptors, such as Dectin-1, Mannose receptors (MR), macrophage galactose-type lectin (MGL), which can identify saccharides rich β-glucan, mannose, and galactose, respectively. These recognitions induce downstream signals, resulting in a dynamic change in cellular functions (L.-Z. Meng et al., 2014; B. S. Park & Lee, 2013; Zhang et al., 2016). Previous studies reported that the types and positions of glycosidic linkages markedly affect the anti-inflammatory activities of

polysaccharides. Z. Wang et al. demonstrated that the β-(1, 3), (1-6) glycosidic bonds have an important role in enhancing the immunomodulatory properties (Z. Wang et al., 2004).

While there were several studies about the anti-inflammatory properties of natural polysaccharides, most of them have been performed on polysaccharides extracted from other species, such as mushroom and algae species. There were no available studies about the anti-inflammatory properties of polysaccharides isolated from desert truffles in RAW 264.7 macrophages. Most of the studies conducted on desert truffle polysaccharides so far, investigated the antioxidant or anti-cancer activities. Therefore, further investigations are required to examine the anti-inflammatory potential of polysaccharides derived from diverse desert truffle species.

1.3.2.2.2 Phenolics

Phenolic compounds are among the most important classes of secondary metabolites, present in the fungal fruiting bodies with proven anti-inflammatory activities (Badalyan, 2012; Sánchez, 2017). The chemical profile of *T. boudieri* and *T. claveryi* was characterized by the abundance of phenolic compounds. The concentrations of total phenolic content in both *Terfezia* species are presented in **Table 1.3.** Among phenolic compounds, catechin was the most abundant one at 20 mg/g, followed by ferulic acid at 15 mg/g, p-coumaric acid at 10 mg/g, and cinnamic acid at 6 mg/g in *T. boudieri*, whereas protocatechuic acid, gentisic acid, and 4-hydroxybenzoic acid were the predominant phenolics in *T. claveryi*, at 0.016, 0.015, and 0.017 mg/g, respectively (Doğan & Aydın, 2013; İbrahim Kıvrak, 2015; Özyürek et al., 2014; Sevindik et al., 2018).

In a study conducted by Stanikunaite et al., the anti-inflammatory properties of phenolic compounds, including syringic acid derived from *Elaphomyces granulatus* truffle was evaluated. They revealed that the extract of *E. granulatus* significantly inhibited COX-2 activity in LPS-stimulated RAW 264.7 macrophages (Stanikunaite et al., 2009). In another study, Taofiq et al. examined the anti-inflammatory activities of fourteen edible mushrooms by measuring NO production in LPS-induced RAW 264.7 macrophages. Moreover, chemical characterization was performed to identify the phenolic composition of the extracts. The identified individual compounds (cinnamic acid, *p*-coumaric acid, and *p*-hydroxybenzoic) were also assessed for the same bioactivity. Among studied mushroom species, the extracts of *Agaricus bisporus, Boletus impolitus, Macrolepiota procera*, and *Pleurotus ostreatus* demonstrated the highest anti-inflammatory activities. These mushroom species also showed the highest cinnamic acid concentration, which was the individual phenolic compound that produced the highest anti-inflammatory effect, presenting the strongest inhibition of NO production (Taofiq et al., 2015)

Table 1.3 Phenolic concentrations (mg/g dry weight) in *T. boudieri* and *T. claveryi*

Phenolic compounds	***T. boudieri***	***T. claveryi***
Catechin	20	-
Ferulic acid	15	0.003
p-coumaric acid	10	0.008
Cinnamic acid	6	0.003
Vanillic acid	0.007	0.011
Gallic acid	0.030	-
Syringic acid	0.55	0.002
p -hydroxybenzoic acid	0.006	0.017

Gentisic acid	-	0.015
Homogentisic acid	-	0.010
Protocatechuic acid	0.0010	0.016

1.3.2.2.3 Terpenoids

Terpenoids represent a large group of fungal bioactive compounds with anti-inflammatory properties (Elsayed et al., 2014). Monoterpenes were reported to be more abundant in *T. claveryi* (18.04 ng/g) than *T. boudieri* (2.20 ng/g). Moreover, α-Pinene was the dominant monoterpene in *T. claveryi* at 7.49 ng/g, while *α*-terpinene was the prevalent monoterpene in *T. boudieri* at 0.85 ng/g. Sesquiterpenes also found at trace levels <1 ng/g in *T. boudieri* and *T. claveryi*, and represented by γ-muurolene, β-caryophyllene, β-copaene, β-cubebene, γ-cadinene, calamenene, and β-bourbonene (Farag et al., 2021). The chemical profile of *T. claveryi* also revealed the presence of the squalene triterpene (Dahham et al., 2018). The concentrations of terpenoids in both *Terfezia* species are presented in **Table 1.4 and Table 1.5.**

Recently, several studies revealed the anti-inflammatory potential of terpenoids (De Cássia da Silveira e Sá et al., 2013; Ma et al., 2013; Y. K. Rao et al., 2007). Kim et al. revealed that α-pinene monoterpene suppressed the production of NO, IL-6, and TNF-α in mouse peritoneal macrophages. α-Pinene also downregulated the expression of iNOS and COX-2 along with inhibition of the NF-κB and MAPKs signaling pathways (D.-S. Kim et al., 2015). In an *in vivo* study to evaluate the anti-inflammatory activities of α-humulene and (−)-trans-caryophyllene sesquiterpenes extracted from the essential oil of *Cordia verbenacea*, it was revealed that both compounds showed anti-inflammatory characteristics

through decreasing bradykinin, platelet activating factor, and ovoalbumin-induced mouse paw oedema. Systemic treatment with both compounds inhibited PGE2 production, iNOS, and COX-2 expression in carrageenan-treated rats. α-Humulene also suppressed TNFα and IL-1β production, while –(-)trans-caryophyllene reduced only TNFα secretion (Fernandes et al., 2007). In study conducted by Jiang et al., the anti-inflammatory properties of triterpene extracts from *Ganoderma lucidum* was investigated in LPS-stimulated RAW 264.7 macrophages. The triterpene extract of *G. lucidum* significantly reduced NO and PGE2 secretion along with downregulation of iNOS and COX-2 expression. The level of cytokines (TNF-α and IL-6) was also decreased. They suggested that the extract exhibited its anti-inflammatory effects via inhibition of NF-κB and AP-1 signaling pathways (Jiang et al., 2008). In another study, Fernando et al. reported that squalene isolated from *Caulerpa racemosa* macroalgae inhibited LPS-dependent induction of TNF-α, IL-1β, and IL-6 in RAW 264.7 macrophages. Furthermore, squalene suppressed LPS-induced production of NO and PGE2 through downregulation the expression of iNOS and COX-2, respectively (Fernando et al., 2018).

Table 1.4 Monoterpene concentrations (ng/g dry weight) in *T. boudieri* and *T. claveryi*

Monoterpene compounds	***T. boudieri***	***T. claveryi***
α-Pinene	0.03	7.49
β-Pinene	0.11	0.04
α-Terpinene	0.85	1.64
γ-Terpinene	0.65	2.64
α-Thujene	0.08	0.43
β-Thujene	0.04	0.81
β-Myrcene	0.08	0.41

3-Carene	-	1.53
Sabinene	0.12	1.90
Camphene	-	0.28
Limonene	0.24	0.88
Total monoterpene concentrations	**2.20**	**18.04**

Table 1.5 Sesquiterpene concentrations (ng/g dry weight) in *T. boudieri* and *T. claveryi*

Sesquiterpene compounds	***T. boudieri***	***T. claveryi***
α-Humulene	0.01	0.06
γ-Muurolene	0.10	0.10
β-Caryophyllene	-	0.06
β-Copaene	-	0.09
β-Cubebene	-	0.05
γ-Cadinene	-	0.09
Calamenene	-	0.08
β-Bourbonene	-	0.07
Total sesquiterpene concentrations	**0.12**	**0.60**

1.3.2.2.4 Proteins

The anti-inflammatory activities of *T. boudieri* and *T. claveryi* can be attributed to their amino acid contents, which have been associated with the metabolism of prostaglandin (Saxena et al., 1984). As previously mentioned, amino acids constituted a major class of primary metabolites in both *Terfezia* species. Alanine and glutamic acid were the predominant amino acids in *T. boudieri*, while proline and glycine were the main amino acids in *T. claveryi* (Kıvrak, 2015; Owaid, 2018). In studying *Pleurotus ostreatus* (oyster

mushroom), its anti-inflammatory activities have been partially attributed to the presence of amino acids, such as isoleucine, leucine, phenylalanine, and tyrosine (Jedinak et al., 2011).

1.3.2.2.5 Fatty acids

Fatty acids present in *T. boudieri* and *T. claveryi* can support their anti-inflammatory activities because of their high contents of PUFAs. The primary metabolome of both *Terfezia* species was characterized by the abundance of PUFAs, such as linoleic acid (Darwish et al., 2021a; Hamza et al., 2016). PUFAs are the precursors of eicosanoids, which are essential signaling molecules, playing important roles in the proper regulation of inflammatory and anti-inflammatory processes in the cells (Dennis & Norris, 2015). For example, Grzywacz et al. revealed that *Imleria badia* extracts inhibited the expression of COX-2 and prostaglandin E2 synthase (PGES) in LPS-stimulated RAW 264.7 macrophages. Moreover, the *I. badia* extracts reduced the protein levels of NF-κB p50 and p65 subunits. It was suggested that the anti-inflammatory activates of *I. badia* was due to the high contents of unsaturated fatty acids, beside other bioactive compounds (Grzywacz et al., 2016).

1.4 Rationale and Hypothesis

In the present study, the anti-inflammatory properties of two chief desert truffles, *T. boudieri* and *T. claveryi* have been investigated. Both species have been selected for the study based on their metabolomic analyses, which indicated that they contained abundant biologically active compounds, such as polysaccharides, phenolics, terpenoids, proteins, and fatty acids, which can contribute to their anti-inflammatory potential. Nevertheless, the molecular mechanisms underlying their anti-inflammatory activities in RAW264.7 macrophages are not yet characterized. Thus, we hypothesize that *T. boudieri* and *T. claveryi* extracts will attenuate the LPS/IFN-γ-mediated inflammation in RAW 264.7 macrophages through targeting TLR4 and Nrf2 signaling pathways. Furthermore, we hypothesize that their anti-inflammatory characteristics can be attributed to an epigenetic mechanism through targeting specific miRNAs.

1.5 Objectives and Aims

The objective of this study is to holistically compare and examine the anti-inflammatory properties of *T. boudieri* and *T. claveryi* extracts in LPS/IFN-γ-stimulated RAW 264.7 cells as well as identifying the underlying mechanisms related to these properties.

Moreover, the hypothesis will be tested by the following specific aims:

1. Investigate the anti-inflammatory effects of *T. boudieri* and *T. claveryi* extracts on the nitrite production in LPS/IFN-γ-stimulated RAW 264.7 cells.

2. Examine the effects of *T. boudieri* and *T. claveryi* extracts on the mRNA expression level of iNOS, COX-2, TNF-α, and IL-6 in LPS/IFN-γ-stimulated RAW 264.7 cells.
3. Determine whether the anti-inflammatory effects of *T. boudieri* and *T. claveryi* extracts are related to modulation of the Nrf2 signaling pathway through measuring the mRNA expression of the Nrf2 targets, HO-1 and OSGIN1 in LPS/IFN-γ-stimulated RAW 264.7 cells.
4. Investigate whether the anti-inflammatory effects of *T. boudieri* and *T. claveryi* extracts are associated with epigenetic modulation of gene expression through affecting miRNAs, including miR-21, miR-146a, and miR-155 in LPS/IFN-γ-stimulated RAW 264.7 cells.
5. Determine the effects of *T. boudieri* and *T. claveryi* extracts on the protein expression level of iNOS, COX-2, TNF-α, and IL-6 in LPS/IFN-γ-stimulated RAW 264.7 cells.

Chapter 2: Materials and Methods

2.1 Materials

RAW 264.7 cell line (ATCC. No. TIB-71™; RRID: CVCL_0493) was obtained from the National Research Centre (NRC), Cairo, Egypt. *T. boudieri* and *T. claveryi* extracts were obtained from Faculty of Pharmacy, Cairo University, Egypt. Dulbecco's Modified Eagle Medium (DMEM), High Glucose (Cat. No. 41965-039), Fetal Bovine Serum (FBS; Cat. No. 10270-106), Penicillin-Streptomycin (Pen/Strep; Cat. No. 15140122), (3-(4, 5-dimethylthiazol-2-yl)-2, 5-diphenyltetrazolium bromide (MTT; Cat. No. M6494), Griess Reagent Kit (Cat. No. G7921), Isopropanol (HPLC grade; Cat. No. 67-63-0), Ethanol (HPLC grade; Cat. No. 64-17-5), RevertAid First Strand cDNA Synthesis Kit (Cat. No. K16.22), PowerUp™ SYBR™ Green Master Mix (Cat. No. A25741), mRNA primers (iNOS, TNF-α, IL-6, COX-2 and GAPDH), Pierce™ BCA Protein Assay Kit (Cat. No. 23225), NuPAGE™ LDS Sample Buffer (4X; Cat. No. NP0007), NuPAGE™ Sample Reducing Agent (10X; Cat. No. NP0009), NuPAGE™ MES SDS Running Buffer (20X; Cat. No. NP0002), NuPAGE™ 4 to 12%, Bis-Tris, 1.0 mm, Mini Protein Gel, 10-well (Cat. No. NP0321BOX), NuPAGE™ Transfer Buffer (20X; Cat. No. NP0006), Western Blotting Filter Paper, 0.83 mm thick, 8 x 13.5 cm (Cat. No. 84784), Pierce™ 20X TBS Tween™ 20 Buffer (Cat. No. 28360), Blocker™ BSA (10X) in PBS (Cat. No. 37525), Rabbit polyclonal anti-iNOS antibody (Cat. No. PA3-030A), Rabbit polyclonal anti-GAPDH antibody (Cat. No. PA1-987), Goat anti-Rabbit IgG (H+L) secondary antibody, horseradish peroxidase (HRP)-conjugated (Cat. No. 31460), and Pierce™ ECL Western Blotting Substrate (Cat. No. 32106) were all obtained from Thermo Fisher Scientific

(Waltham, MA, USA). HO-1 and OSGIN1 mRNA primers were purchased from Synbio Technologies (Monmouth Junction, NJ, USA). Cell Lysis Buffer (10X; Cat. No. 9803S), Protease Inhibitor Cocktail (100X; Cat. No. 5871), and Prestained Protein Marker, Broad Range (11-190 kDa; Cat. No. 13953S) were purchased from Cell Signaling (Danvers, MA, USA). LPS from Escherichia coli 0111: B4 (Cat. No. L2630) was purchased from Sigma-Aldrich (St. Louis, MO, USA). Recombinant Murine IFN-γ (Cat. No. 315-05) was purchased from PeproTech (Cranbuhry, NJ, USA). Phosphate Buffered Saline (1X PBS; Cat. No. BE17-516F) was purchased from Lonza-Bioscience (Basel, Switzerland). Sulforaphane (Cat. No. 10496) was purchased from Cayman Europe Oü (Tallinn, Estonia). QiAzol lysis reagent (Cat. No. 79306), Nuclease-Free Water (Cat. No. 129114), miScript II RT kit (Cat. No. 218161), miScript SYBR® Green PCR Kit (Cat No. 218073), and miScript primer assays including Hs_RNU6-2_11 (Cat No. MS00033740), Mm_miR-21_2 (Cat. No. MS00011487), Mm-miR-146a*_1 (Cat. No. MS00024220), and Mm_miR-155_1 (Cat. No. MS00001701) were obtained from Qiagen (Hilden, Germany). Dimethyl Sulfoxide (DMSO, research grade; Cat. No. 20385.02), and Chloroform: Isoamyl alcohol 24:1 (molecular biology grade; Cat. No. 39554.02) were purchased from SERVA (Heidelberg, Germany). Rabbit polyclonal anti-COX-2 antibody (Cat. No. E-AB-70031), Mouse TNF-α (Cat. No. E-EL-M0049), and Mouse IL-6 (Cat. No. E-EL-M0044) Enzyme-Linked Immunosorbent Assay (ELISA) Kits were purchased from Elabscience (Wuhan, China).

2.2 Fungal collection and extract preparation

Fungal sporocarps (fruiting bodies) of *T. boudieri* and *T. claveryi* were collected from Marsa Matruh and identified at the Regional Center for Mycology and Biotechnology,

Cairo, Egypt. The materials for extraction were cleaned, dried by lyophilization, and extracted with ethanol. The ethanolic extract (100 mg/mL) of each specimen was separately dissolved in DMSO, filtered with 0.2 μm syringe filter, and stored at 4°C until used.

2.3 Cell culture

RAW 264.7 cells (cell line information is presented in **Table 2.1** and **Figure 2.1**) were cultured in DMEM, high glucose supplemented with 10% heat inactivated FBS and 1% Pen/Strep (100 units/mL penicillin and 100 μg/mL streptomycin) at 37°C in a 5% CO2 incubator.

Table 2.1 RAW 264.7 cell line information

Cell line: RAW 264.7 TIB-71™
Organism: Mus musculus, mouse
Strain: BALB/c
Cell Type: macrophage
Tissue: Ascites
Age: adult
Gender: Male
Morphology: monocyte/macrophage
Growth properties: Adherent
Immortalization method: Abelson murine leukemia virus transformed
Growth medium: DMEM, high glucose supplemented with 10% heat inactivated FBS
Subculturing procedure: 1:3 to 1:6 is recommended
Growth Conditions: 37°C, 5% CO2
Cryopreservation: Complete DMEM supplemented with 5% (v/v) DMSO

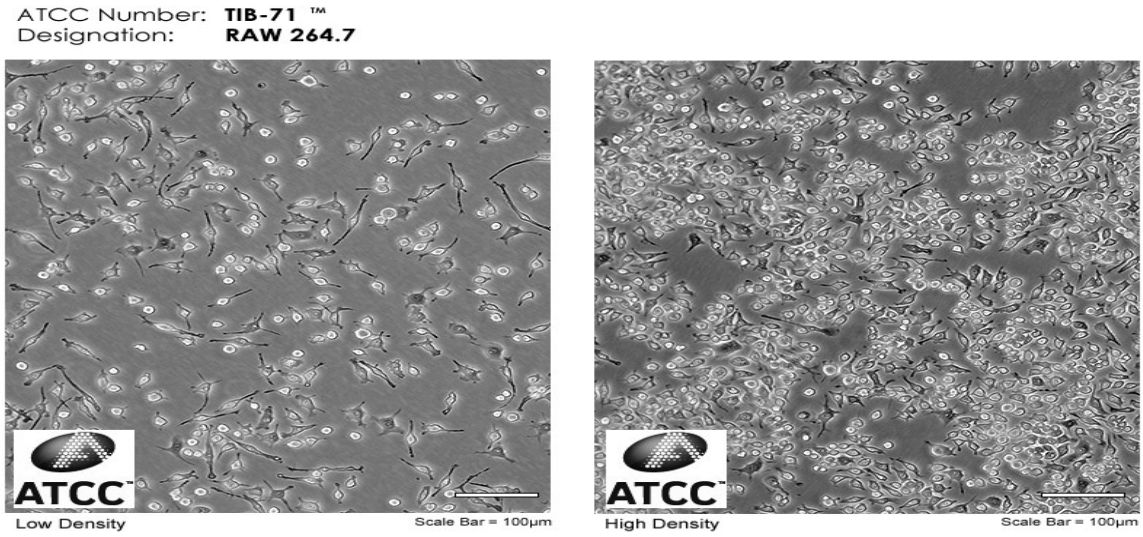

Figure 2.1 RAW 264.7 ATCC® TIB-71TM
(Adapted from ATCC)

2.4 Cell viability assay

The cell viability was measured with the MTT colorimetric assay as previously described (Bahuguna et al., 2017). Briefly, RAW 264.7 cells were seeded at a density of 2 × 10^4 cells/well in a 96-well plate, and cultured in DMEM, high glucose supplemented with 10% heat inactivated FBS and 1% Pen/Strep for 4 h at 37°C in a 5% CO2 incubator. After removing the medium, the cells were treated with increasing concentrations of *T. boudieri* and *T. claveryi* extracts (5, 10, 20, 40, 80, and 160 µg/mL), prepared in serum-free DMEM for 24 h to determine the non-cytotoxic concentrations to be used in the study. After the incubation period, the medium was decanted, and the cells were incubated with 100 µL serum-free DMEM containing 1 mg/mL MTT for 2 hours at 37°C in a 5% CO2 incubator. MTT was reduced by NAD(P)H-dependent cellular oxidoreductase enzymes of the metabolically active cells into formazan crystals, which were then dissolved in 100 µL DMSO. The absorbance of each group was measured at 570 nm using SPECTROstar®

Nano microplate reader (BMG LABTECH, Ortenberg, Germany), and the results were presented as the percentage of the control with the following Equation.

$$\text{Cell viability (\%)} = \frac{(\text{Absorbance sample} - \text{Absorbance blank})}{(\text{Absorbance control} - \text{Absorbance blank})} \times 100$$

In this study, RAW 264.7 cells were stimulated with LPS (100 ng/mL) plus IFN-γ (10 U/mL). Therefore, the cytotoxicity of *T. boudieri* and *T. claveryi* extracts in the presence of LPS/ IFN-γ was also evaluated. RAW 264.7 cells were stimulated with LPS/IFN-γ (100 ng/10 U/mL) and co-incubated with the non-cytotoxic concentrations of *T. boudieri* and *T. claveryi* extracts 5, 10, and 20 µg/mL for 24 h in a 96-well plate. Sulforaphane (SFN) (1 µl) was used as a positive control in all further experiments, so its cytotoxicity on RAW 264.7 cells with or without LPS/ IFN-γ was also examined. The cell viability was then measured with MTT as previously mentioned.

2.5 Nitrite assay

RAW 264.7 cells were seeded at a density of 2×10^5 cells/well in a 96-well plate and incubated for 4 h. The cells were then stimulated with LPS/IFN-γ (100 ng/10 U/mL) and co-incubated with *T. boudieri* and *T. claveryi* extracts at concentrations of 5, 10, and 20 µg/mL for 24 h at 37°C in a 5% CO2 incubator. SFN (1 µM) was used as a positive control. The nitrite accumulated in the culture medium was measured as an indicator of NO production using the Griess Reagent Kit by mixing 150 µL of the culture supernatant from each well with 130 µL deionized water and 20 µL of Griess reagent [1:1 mixture (v/v) of 0.1% N-(1-naphthyl) ethylenediamine dihydrochloride and 1% sulfanilamide in 5% phosphoric acid] and incubating at room temperature for 30 min in the dark according to the manufacturer's instructions. The absorbance of the mixture was measured at 548 nm

using SPECTROstar® Nano microplate reader. The concentration of nitrite in each sample was calculated based on a standard curve prepared with NaNO2 (**Table 2.2**).

Table 2.2 Standard curve of nitrite concentration versus absorbance

Nitrite conc. (μM)	Absorbance
0	0
10	0.1118
20	0.2134
30	0.3168
40	0.4098
50	0.5256

2.6 Total RNA isolation

RAW 264.7 cells were seeded at a density of 1×10^6 cells/well in a 6-well plate and incubated overnight. Then, the cells were stimulated with LPS/IFN-γ (100 ng/10 U/mL) and co-incubated with *T. boudieri* and *T. claveryi* extracts at concentrations of 5, 10, and 20 μg/mL for 6 h at 37°C in a 5% CO2 incubator. SFN (1 μM) was used as a positive control. Total RNA was extracted from the cells using QiAzol lysis reagent according to the manufacturer's instructions. In brief, cells were washed with cold PBS and homogenized with QiAzol lysis reagent (1 mL in each well) followed by incubation for 5 min at room temperature to allow the complete dissociation of the nucleoprotein complexes. Chloroform was then added (0.2 mL of chloroform per 1 mL QiAzol) to each tube containing the homogenized sample and incubated for 2-3 min at room temperature. The sample tubes were then centrifuged at 12,000 x g for 15 min at 4°C. Following centrifugation, the homogenate separated into colorless upper aqueous phase in which the RNA exclusively remains, an interphase and lower red, phenol-chloroform phase. The

upper aqueous phase was then transferred into a new tube and mixed with isopropanol (0.5 mL of isopropanol per 1 mL QiAzol) to precipitate the RNA from the aqueous phase. The sample tubes were incubated for 10 min at room temperature, and centrifuged at 12,000 x g for 15 min at 4°C. After centrifugation, the supernatant was discarded, and the RNA pellet was washed with 75% ethanol (1 mL per 1 mL of QiAzol). This was followed with brief vertexing and centrifugation at 7500 x g for 5 min at 4°C. After that, the supernatant was completely removed, and the RNA pellet was left to air-dry for 5-10 min. RNA pellet was then resuspended in 20 µl RNase-free water and RNA concentration and purity were determined using NanoDrop™ One Microvolume UV-Vis Spectrophotometer (Thermo Fisher Scientific, MA, USA).

2.7 cDNA Synthesis

2.7.1 cDNA synthesis for quantitative analysis of mRNA

For mRNA, cDNA synthesis was prepared from the total RNA using Thermo Scientific™ RevertAid™ First Strand cDNA Synthesis Kit according to the manufacturer's instructions. Briefly, 1µg of total RNA isolated from each sample was diluted with nuclease-free water up to 10 µL. Then, 10 µL from the RevertAid cDNA reaction **(Table 2.3)** were added to each sample for a final volume reaction of 20 µL. The cDNA reaction master mix contains 4.0 µL 5X Reaction Buffer, 2.0 µL 10 mM dNTP Mix, 1.0 µL Oligo (dT)18 primer, 1.0 µL RT Random Hexamer primer, 1.0 µL RiboLock RNase Inhibitor (20 U/µL), and 1.0 µL RevertAid M-MuLV RT (200 U/µL). The cDNA was synthesized under the following conditions: 25 °C for 5 min, followed by 42°C for 60 min, and then 70 °C for 5 min to terminate the reaction, and finally cooled to 4 °C in 96-well Thermal cycler

(Applied Biosystems, CA, USA). The completed reaction was stored at -20°C to prevent cDNA degradation.

Table 2.3 RevertAid cDNA reaction components

Kit component	**Per reaction (µL)**
5X Reaction Buffer	4
10 mM dNTP Mix	2
Oligo (dT)18 primer	1
RT Random Hexamer primer	1
RiboLock RNase Inhibitor (20 U/µL)	1
RevertAid M-MuLV RT (200 U/µL)	1
Total Volume	**10**

2.7.2 cDNA synthesis for quantitative analysis of miRNA

For the miRNA, cDNA synthesis was prepared from the total RNA using miScript® II RT Kit according to the manufacturer's instructions. Briefly, 2 µg of total RNA isolated from each sample were diluted with nuclease-free water up to 12 µL. Then, 8 µL of miScript® II RT cDNA reaction **(Table 2.4)** were added to each sample for a final reaction volume of 20 µL. The cDNA reaction master mix contains 4.0 µL 5x miScript HiSpec Buffer, 2.0 µL 10x miScript Nucleics Mix and 2.0 µL miScript Reverse Transcriptase Mix. The cDNA was synthesized through incubation of the reaction mixture in 96-well Thermal cycler at 37°C for 1 h followed by 5 min at 95ºC to inactivate the miScript Reverse Transcriptase enzyme. The completed reaction was stored at -20°C to prevent cDNA degradation.

Table 2.4 miScript® II RT cDNA reaction components

Kit component	**Per reaction (µL)**
5x miScript HiSpec Buffer	4
10x miScript Nucleics Mix	2
miScript Reverse Transcriptase Mix	2
Total Volume	**8**

2.8 Quantitative real-time polymerase chain reaction (qPCR)

2.8.1 Relative quantification of mRNA using qPCR

The qPCR analysis was performed using PowerUp™ SYBR™ Green Master Mix to quantify the mRNA expression of iNOS, COX-2, TNF-α, IL-6, HO-1, OSGIN1 and GPADH (as a housekeeping gene).

Before quantification by qPCR, the cDNA was firstly diluted with nuclease free water (1:3 dilution) by adding 40 µL nuclease-free water to the 20 µL cDNA reaction, from which 3 µL used as a template for the qPCR reaction. The qPCR reaction mixture **(Table 2.5)** was carried out in a volume of 12.5 µL containing 6.25 µL of PowerUp™ SYBR™ Green Master Mix, 0.375 µL of 10 µM forward primer, 0.375 uL of 10 µM reverse primer, 3 µL of diluted cDNA sample equivalent to 50 ng cDNA, and 2.5 µL of nuclease-free water. qPCR analysis was conducted using ABI Prism 7500 system (Applied Biosystems) under the following conditions: initial activation at 95 °C for 10 min, followed by 40 PCR cycles of denaturation at 95 °C for 15 s and annealing/extension at 60 °C for 1 min. Melting curves were collected at the end of each run to check the primers specificity and the final PCR product purity. mRNA primers used in this study were designed using NCBI Primer-BLAST and are listed in **Table 2.6.**

Table 2.5 qPCR reaction components for relative quantification of mRNA

Component	**Per reaction (µL)**
PowerUp™ SYBR™ Green Master Mix	6.25
Forward primer **(**10 µM)	0.375
Reverse primer **(**10 µM)	0.375
cDNA	3
Nuclease-free water	2.5
Total Volume	**12.5**

Table 2.6 Primer sequences used for the qPCR analysis

Gene	**Forward Primer (5′–3′)**	**Reverse Primer (5′–3′)**
iNOS	GGAACCTACCAGCTCACTCTGG	TGCTGAAACATTTCCTGTGCTGT
COX-2	CTCACGAAGGAACTCAGCAC	GGATTGGAACAGCAAGGATTTG
TNF-α	GAACTCCAGGCGGTGCCTAT	TGAGAGGGAGGCCATTTGGG
IL-6	GATGCTACCAAACTGGATATAATCAG	CTCTGAAGGACTCTGGCTTTG
HO-1	CACAGATGGCGTCACTTCGTC	GTGAGGACCCACTGGAGGAG
OSGIN1	CGGTGACATCGCCCACTAC	GCTCGGACTTAGCCCACTC
GAPDH	CTTTGTCAAGCTCATTTCCTGG	TCTTGCTCAGTGTCCTTGC

Primer's name: Inducible nitric oxide synthase (iNOS), cyclooxygenase-2 (COX-2), tumor necrosis factor-α (TNF-α), interleukin-6 (IL-6), heme oxygenase-1 (HO-1), oxidative stress induced growth inhibitor-1 (OSGIN1), and glyceraldehyde 3-phosphate dehydrogenase (GAPDH).

2.8.2 Relative quantification of miRNA using qPCR

The qPCR analysis was performed using miScript SYBR® Green PCR Kit to quantify the miRNA expression of miR-21, miR-146a, miR-155, and RNU6-6p (as a housekeeping gene).

Before quantification by qPCR, the cDNA was firstly diluted with nuclease free water (1:100 ratio) by taking 2 µL from the 20 µL synthesized cDNA and diluting them with 198 µL of nuclease-free water, from which 2 µL used as a template for the qPCR reaction. The qPCR reaction mixture **(Table 2.7)** was carried out in a volume of 10 µL containing 5 µL of 2x QuantiTect® SYBR Green PCR Master Mix, 1 µL of 10x miScript primer assay, 1 µL of 10x miScript universal primer, 2 µL of diluted cDNA sample, and 1 µL of nuclease-free water. qPCR analysis was conducted using ABI Prism 7500 system (Applied Biosystems) under Qiagen standard protocol: initial activation at 95 °C for 15 min, followed by 40 PCR cycles of denaturation at 94°C for 15 s, annealing at 55°C for 30 s, and extension at 70°C for 30 s. Melting curves were collected at the end of each run to check the primers specificity and the final PCR product purity. miScript primer assays (miRNA-specific forward primers) were designed and purchased from Qiagen. miScript universal primer (miRNA reverse primer) was provided in the miScript SYBR® Green PCR Kit and was applied to all reactions allowing the detection of miRNAs in combination with miScript primer assays. Primer assays used in this study are listed in **Table 2.8**.

Table 2.7 qPCR reaction components for relative quantification of miRNA

Component	**Per reaction (µL)**
2x QuantiTect® SYBR Green PCR Master Mix	5
10x miScript primer assay	1
10x miScript universal primer	1
cDNA	2
Nuclease-free water	1
Total Volume	**10**

Table 2.8 Primer assays (forward primers) used for the qPCR analysis

miRNA	**Primer assay sequence**
miR-21	UAGCUUAUCAGACUGAUGUUGA
miR-146a	CCUGUGAAAUUCAGUUCUUCAG
miR-155	UUAAUGCUAAUUGUGAUAGGGGU
RNU6	Housekeeping gene

2.9 qPCR data analysis

qPCR data was analyzed using the relative quantification method also referred to as the $2^{-\Delta\Delta CT}$ method (Schmittgen & Livak, 2008). The CT (cycle threshold) was calculated based on the number of PCR cycles at which the fluorescent signal crossed the threshold i.e., exceeded the background level. This method calculates relative gene expression in target and reference samples with a reference gene for normalization based on CT information produced from the qPCR machine (X. Rao et al., 2013). The final result of this method is displayed as the fold change of target gene expression in a target sample (treated sample) relative to a reference sample (untreated control), normalized to a reference gene; GAPDH (for mRNA) or RNU6 (for miRNA) as the following:

ΔCT = CT (target gene)−CT (reference gene).

ΔΔCT = ΔCT (treated sample) − ΔCT (untreated control).

Fold change= $2^{-\Delta\Delta CT}$

2.10 Enzyme-Linked Immunosorbent Assay (ELISA) for TNF-α and IL-6

RAW 264.7 cells were seeded at a density of 1×10^6 cells/well in a 6-well plate and incubated overnight. The cells were then stimulated with 100 ng/mL LPS plus 10 U/mL IFN-γ and co-incubated with *T. boudieri* and *T. claveryi* extracts at concentrations of 5 and 20 µg/mL for 24 h at 37°C in a 5% CO2 incubator. SFN (1 µM) was used as a positive control. After incubation, the supernatants were collected, centrifuged at 1000x g for 20 min at 4°C, and then stored at − 80 °C. The samples were subsequently analyzed for TNF-α and IL-6 proteins.

2.10.1 ELISA for TNF-α

The concentration of TNF-α protein secreted into the cell culture supernatant was measured using an ELISA kit according to the manufacturer's instructions.

Reagent preparation

The Reference Standard was diluted to different concentrations with the provided Reference Standard and Sample Diluent to prepare the standard curve of TNF-α concentrations with a detection range of 31.25- 1000 pg/mL. The 25x Concentrated Wash Buffer was also diluted to 1x working solution with deionized water. Moreover, the 100x Concentrated TNF-α Biotinylated Detection Ab was diluted to 1x working solution with the provided Biotinylated Detection Ab Diluent. Finally, the 100x Concentrated HRP Conjugate was diluted to 1x working solution with the provided HRP Conjugate Diluent.

Sample preparation

Samples were brought to room temperature before use followed by brief mixing. Samples were also diluted with Reference Standard and Sample Diluent (1: 200 ratio) for detecting TNF-α protein.

Assay procedures

The TNF-α ELISA kit is based on the Sandwich-ELISA principle in which the ELISA microplate has been pre-coated with an antibody specific to the mouse TNF-α. Briefly, 100µL of the cell culture supernatant (1:200 dilution) were added to the ELISA microplate wells followed by incubation for 90 min at 37°C. The liquid was then removed, and 100µL of 1x Biotinylated Detection Ab specific for Mouse TNF-α were added to each well and incubated for 1 h at 37°C. After that, the solution was decanted and 350µL of 1x wash buffer were added to each well (washing step was repeated 3 times). Then, 100µL of 1x HRP Conjugate were added to each well and incubated for 30 min at 37°C. The solution was decanted again after the incubation time and 350µL of 1x wash buffer were added to each well (washing step was repeated 5 times). This was followed by addition of 90µL substrate reagent to each well and incubation for 15 min at 37°C. Only wells containing mouse TNF-α, biotinylated detection antibody and HRP conjugate appeared blue in color after substrate addition. Finally, the enzyme-substrate reaction was terminated by the addition of 50µL stop solution to each well and the color turned into yellow. The absorbance of each well was immediately measured at 450 nm using SPECTROstar® Nano microplate reader. The concentration of the mouse TNF-α in each sample was calculated by comparing the absorbance of the samples to the standard curve **(Table 2.9).**

Table 2.9 Standard curve of TNF-α concentration versus absorbance

TNF-α (pg/mL)	Absorbance
1000	1.8554
500	1.06735
250	0.5953
125	0.3396
62.5	0.20395
31.25	0.0987
0	0

2.10.2 ELISA for IL-6

The concentration of IL-6 protein secreted into the cell culture supernatant was measured using an ELISA kit according to the manufacturer's instructions.

Reagent preparation

The Reference Standard was diluted to different concentrations with the provided Reference Standard and Sample Diluent to prepare the standard curve of IL-6 concentrations with a detection range of 31.25- 2000 pg/mL. The 25x Concentrated Wash Buffer was also diluted to 1x working solution with deionized water. Moreover, the 100x Concentrated IL-6 Biotinylated Detection Ab was diluted to 1x working solution with the provided Biotinylated Detection Ab Diluent. Finally, the 100x Concentrated HRP Conjugate was diluted to 1x working solution with the provided HRP Conjugate Diluent.

Sample preparation

Samples were brought to room temperature before use followed by brief mixing. Samples were also diluted with Reference Standard and Sample Diluent (1: 20 ratio) for detecting IL-6 protein.

Assay procedures

The IL-6 ELISA kit is based on the Sandwich-ELISA principle in which the ELISA microplate has been pre-coated with an antibody specific to the mouse IL-6. Briefly, 100µL of the cell culture supernatant (1:20 dilution) were added to the ELISA microplate wells followed by incubation for 90 min at 37°C. The liquid was then removed, and 100µL of 1x Biotinylated Detection Ab specific for Mouse IL-6 were added to each well and incubated for 1 h at 37°C. After that, the solution was decanted and 350µL of 1x wash buffer were added to each well (washing step was repeated 3 times). Then, 100µL of 1x HRP Conjugate were added to each well and incubated for 30 min at 37°C. The solution was decanted again after the incubation time and 350µL of 1x wash buffer was added to each well (washing step was repeated 5 times). This was followed by addition of 90µL substrate reagent to each well and incubation for 15 min at 37°C. Only wells containing mouse IL-6, biotinylated detection antibody and HRP conjugate appeared blue in color after substrate addition. Finally, the enzyme-substrate reaction was terminated by the addition of 50µL stop solution to each well and the color turned into yellow. The absorbance of each well was immediately measured at 450 nm using SPECTROstar® Nano microplate reader. The concentration of the mouse IL-6 in each sample was calculated by comparing the absorbance of the samples to the standard curve **(Table 2.10)**.

Table 2.10 Standard curve of IL-6 concentration versus absorbance

IL-6 (pg/mL)	Absorbance
2000	2.35105
1000	1.31855
500	0.63385
250	0.30825
125	0.30385
62.5	0.1525
31.25	0.1124
0	0

2.11 Western Blotting

Preparation of whole cell lysate

RAW 264.7 cells were seeded at a density of 1×10^6 cells/well in a 6-well plate and incubated overnight. The cells were then stimulated with 100 ng/ml LPS plus 10 U/ml IFN-γ and co-incubated with *T. boudieri* and *T. claveryi* extracts at concentrations of 20 µg/mL for 24 h at 37°C in 5% CO2 incubator. SFN (1 µM) was used as a positive control. Briefly, cells were washed with ice-cold PBS and kept on ice throughout. PBS was then discarded and replaced by new ice-cold PBS. Cells were subsequently harvested using cell scraper to dislodge the adherent cells from the plate. This was followed by transferring the cell suspension into pre-cooled microcentrifuge tubes and centrifugation at 125 x g for 10 min at 4°C. The supernatant was then discarded, and the pellet was resuspended in 100 µL of 1x ice-cold cell lysis buffer containing 1x protease inhibitor cocktail. Cell lysates were incubated for 30 min on ice followed by centrifugation at 14,000 x g for 15 min at 4°C. After centrifugation, the supernatant containing the whole cell lysates was collected and

stored at -80°C. The protein concentration was measured using Pierce™ BCA Protein Assay Kit.

Total protein quantification

Pierce™ BCA Protein Assay Kit was used to quantify the total protein in the samples according to the the manufacturer's instructions.

Assay procedures

This method is based on bicinchoninic acid (BCA) for the colorimetric detection and quantification of total protein. Before determining the protein concentration, the protein was firstly diluted with 1x cell lysis buffer (1:5 ratio) by taking 5 µL from the whole cell lysate of each sample and diluting them with 20 µL of 1x cell lysis buffer. Then, 25 µL of each standard or unknown diluted sample were added into a 96-well plate. This was followed by adding 200 µL of the BCA working reagent (50:1, Reagent A: B) to each well and shaking the plate for 30 seconds. The plate was then covered and incubated for 30 min at 37°C. After incubation, the absorbance of each well was measured at 562 nm using the SPECTROstar® Nano microplate reader. The protein concentration of each unknown sample was calculated based on a standard curve prepared with bovine serum albumin **(Table 2.11** and **Table 2.12)**.

Table 2.11 Preparation of diluted BSA standard

Dilution Scheme (Working Range = 20–2,000 µg/mL)			
Vial	**Volume of Diluent (µL)**	**Volume and Source of BSA (µL)**	**Final BSA Concentration (µg/mL)**
A	0	300 of Stock	2000
B	125	375 of Stock	1500
C	325	325 of Stock	1000
D	175	175 of vial B dilution	750
E	325	325 of vial C dilution	500
F	325	325 of vial E dilution	250
G	325	325 of vial F dilution	125
H	400	100 of vial G dilution	25
I	400	0	0 = Blank

Table 2.12 Standard curve of BSA concentration versus absorbance

BSA concentration (µg/ml)	Absorbance
2000	2.0557
1500	1.5747
1000	1.0607
750	0.8505
500	0.5913
250	0.3365
125	0.1880
25	0.0438
0	0

Sample preparation

After measuring the protein concentration for each cell lysate, samples were reduced and denatured for gel electrophoresis. In brief, 10 μg of the protein was added into a microcentrifuge tube containing 5 μL of NuPAGE® LDS Sample Buffer (4X), 2 μL of NuPAGE® Reducing Agent (10X), and Deionized Water up to 13 μL. The reducing and denaturing reaction was carried out in a volume of 20 μL **(Table 2.13)**. Samples were then heated for 10 min at 70°C.

Table 2.13 Reducing and denaturing reaction components for gel electrophoresis

Reagent	**Reduced sample**
Sample	x μL equivalent to 10 μg protein
NuPAGE® LDS Sample Buffer (4X)	5 μL
NuPAGE® Reducing Agent (10X)	2 μL
Deionized Water	to 13 μL
Total Volume	**20 μL**

Buffer preparation

The 20x NuPAGE™ MES SDS Running Buffer was diluted to 1x working solution with deionized water. The 20x NuPAGE™ Transfer Buffer was also diluted to 1x working solution with deionized water and 10% methanol. Furthermore, Pierce™ 20X TBS Tween™ 20 Buffer was diluted to 1x TBST working solution with deionized water. Blocker™ BSA (10X) in PBS was finally diluted with 1x TBST to prepare 5% blocking buffer.

Electrophoresis

Equal volume of protein (20 µl) was loaded into each lane of the NuPAGE™ 4 to 12%, Bis-Tris Gel along with the Prestained Protein Marker. The gel was running into 1x NuPAGE™ MES SDS Running Buffer for 35 min at 200 Volts. The gel electrophoresis was conducted using the XCell SureLock™ Mini-Cell (Thermo Fisher Scientific, MA, USA). After electrophoresis, the protein was transferred into a PVDF membrane through electrotransfer process.

Electrotransfer

Prior to the electrotransfer process, the PVDF membrane was activated with methanol for 30 seconds followed by rinsing in deionized water. The membrane was then placed into 1x NuPAGE™ Transfer Buffer. After membrane activation, the electrotransfer process was performed for 60 min at 30 Volts to transfer the protein from the gel to the PVDF membrane via 1x NuPAGE™ Transfer Buffer using the XCell II™ Blot Module (Thermo Fisher Scientific, MA, USA).

Membrane blocking and antibody incubations

Following transfer, the PVDF membrane was blocked in 5% Blocker™ BSA for 1 h at room temperature. The membrane was then washed three times for 5 min each with 1x TBST. This was followed by incubating the membrane overnight at 4°C with primary antibodies diluted in 1x TBST; Rabbit polyclonal anti-iNOS antibody (1: 2000), Rabbit polyclonal anti-COX-2 antibody (1: 1000), and Rabbit polyclonal anti-GAPDH antibody (1: 2500). After overnight incubation, the membrane was washed three times for 5 min each with 1x TBST. The membrane was then incubated for 1 h at room temperature with

Goat anti-Rabbit IgG (H+L) secondary antibody, horseradish peroxidase (HRP)-conjugated diluted in 5% Blocker™ BSA (1: 15000). After incubation, the membrane was washed three times for 5 min each with 1x TBST and incubated for 1 min with the Pierce™ ECL Western Blotting Substrate. Finally, the membrane was covered with plastic wrap and exposed to chemiluminescence. Proteins were visualized with the Pierce™ ECL Western Blotting Substrate using ChemiDoc MP Imaging System (Bio-Rad Laboratories, CA, USA). The density of western blotting bands was quantified using the ImageLab software (Bio-Rad). The density of the protein bands was normalized to that of GAPDH. The density values were relatively expressed to the average value for the untreated control group, which was designated as 1.0.

2.12 Statistical analysis

Data are expressed as mean ± standard error of the mean (SEM) for the indicated number of independently performed experiments. Statistical analysis was performed using SigmaPlot Version 14.0 (Systat Software, Inc., San Jose, CA, USA). Statistical significance between multiple groups was calculated by one-way ANOVA followed by Student–Newman–Keuls (SNK) post-hoc test, where P-value < 0.05 was considered statistically significant. All values obtained from the Griess assay, ELISA, and BCA assay were subjected to linear regression analysis.

Chapter 3: Results

3.1 Effect of *T. boudieri* and *T. claveryi* extracts on the viability of RAW 264.7 cells

Before examining the effect of *T. boudieri* and *T. claveryi* extracts on LPS/IFN-γ-induced inflammation in RAW 264.7 cells, MTT assay was performed to determine the optimal concentrations to be used in the study i.e., effective in providing anti-inflammatory with minimum cytotoxicity. RAW 264.7 cells were incubated with increasing concentrations of *T. boudieri* and *T. claveryi* extracts (5–160 µg/mL) in the presence or absence of LPS/IFN-γ (100 ng/10 U/mL) for 24 h. SFN (1 µM) was used as a positive control. Both extracts did not significantly affect the cell viability at concentrations below 40 µg/mL compared to the untreated control. However, cell viability was decreased by approximately 63% with *T. boudieri* and 46% with *T. claveryi* when the concentration was increased to 160 µg/mL, revealing that *T. boudieri* has more cytotoxic effect on RAW 264.7 cells **(Figure 3.1A,B).** When the cells were incubated with LPS/IFN-γ, similar results were observed with no cytotoxicity at concentrations of 5, 10, and 20 µg/mL for both extracts **(Figure 3.1C).** SFN (1 µM) alone and in combination with LPS/IFN-γ did not show any cytotoxicity on RAW 264.7 cells **(Figure 3.1D)**. Therefore, *T. boudieri* and *T. claveryi* extracts were used at concentrations of 5, 10, 20 µg/mL in all subsequent experiments to investigate their effects on inflammation induced by LPS/IFN-γ in RAW 264.7 cells.

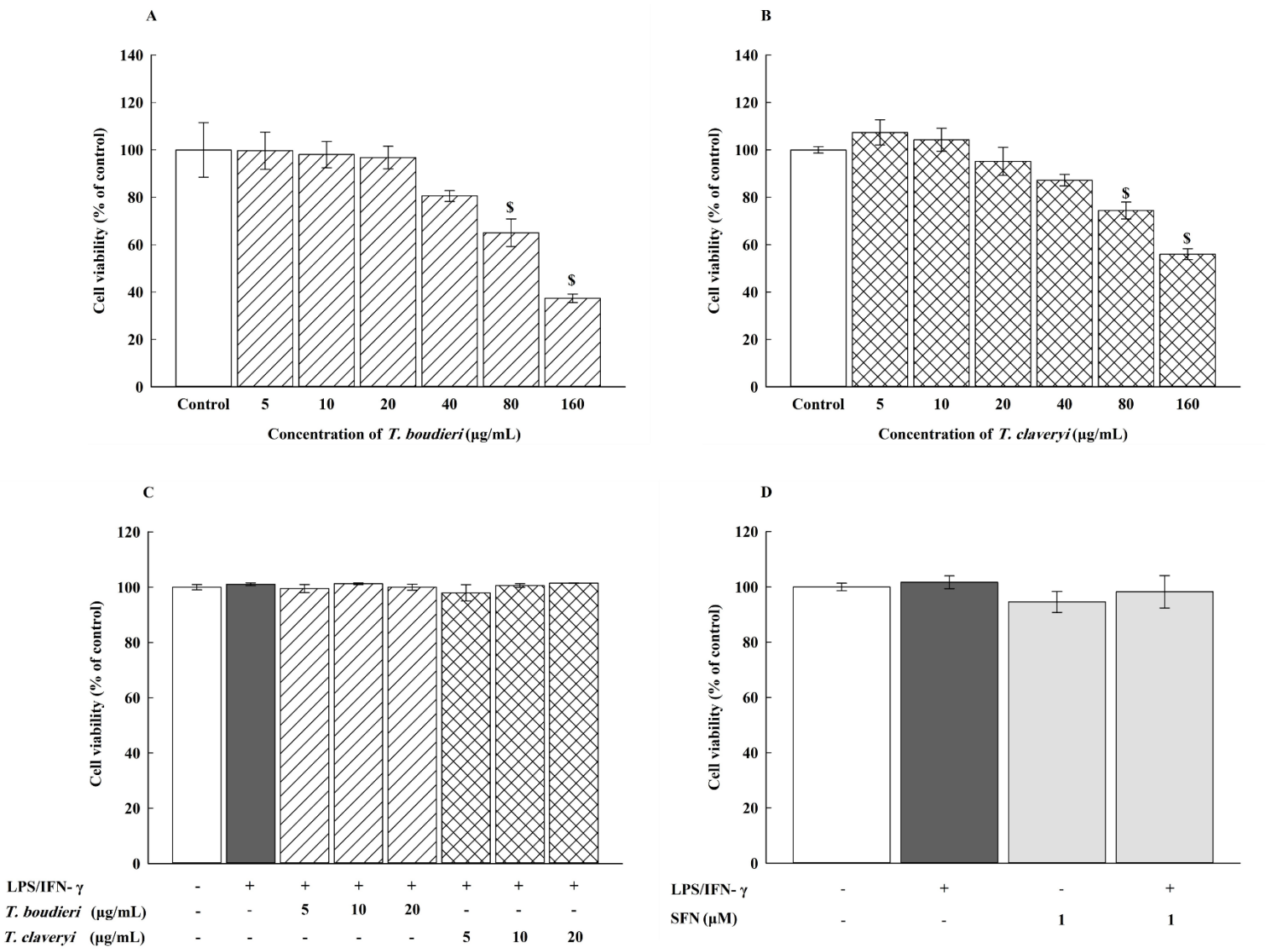

Figure 3.1 Effect of *T. boudieri* and *T. claveryi* extracts on the viability of RAW 264.7 cells. RAW 264.7 cells were separately incubated with increasing concentrations (5–160 μg/mL) of *T. boudieri* (A) and *T. claveryi* (B) extracts or with LPS/IFN-γ (100 ng/10 U/mL) (C), and SFN (1 μM) as a positive control (D) for 24 h. Cell viability was measured using MTT assay. Data are expressed as a percentage of control (100%) ± SEM (n = 8). Statistical significance was calculated by one-way ANOVA followed by Student–Newman–Keuls (SNK) post-hoc test. $ $P < 0.05$ vs. control.

3.2 Effect of *T. boudieri* and *T. claveryi* extracts on nitrite production in LPS/IFN-γ-stimulated RAW 264.7 cells

To investigate the anti-inflammatory effects of *T. boudieri* and *T. claveryi* extracts on nitrite production, RAW 264.7 cells were treated with *T. boudieri* and *T. claveryi* extracts at concentrations of 5, 10, and 20 µg/mL in the presence of LPS/IFN-γ (100 ng/10 U/mL) for 24 h. SFN (1 µM) was used as a positive control. As shown in **Figure 3.2,** the nitrite levels in the cell culture medium were measured using the Griess Reagent Kit. Nitrite levels exhibited a substantial increase by 200% compared to the untreated control after stimulating cells with LPS/IFN-γ. However, treatment with both *Terfezia* extracts inhibited nitrite production in LPS/IFN-γ-stimulated cells in a dose-dependent manner. *T. boudieri* extract at concentrations of 5, 10, and 20 µg/mL significantly inhibited nitrite production by 11, 31, and 45%, respectively, and *T. claveryi* at concentrations of 10 and 20 µg/mL showed a statistically significant inhibition of nitrite production by 38 and 41%, respectively. SFN (1 µM) also decreased nitrite levels by 29%.

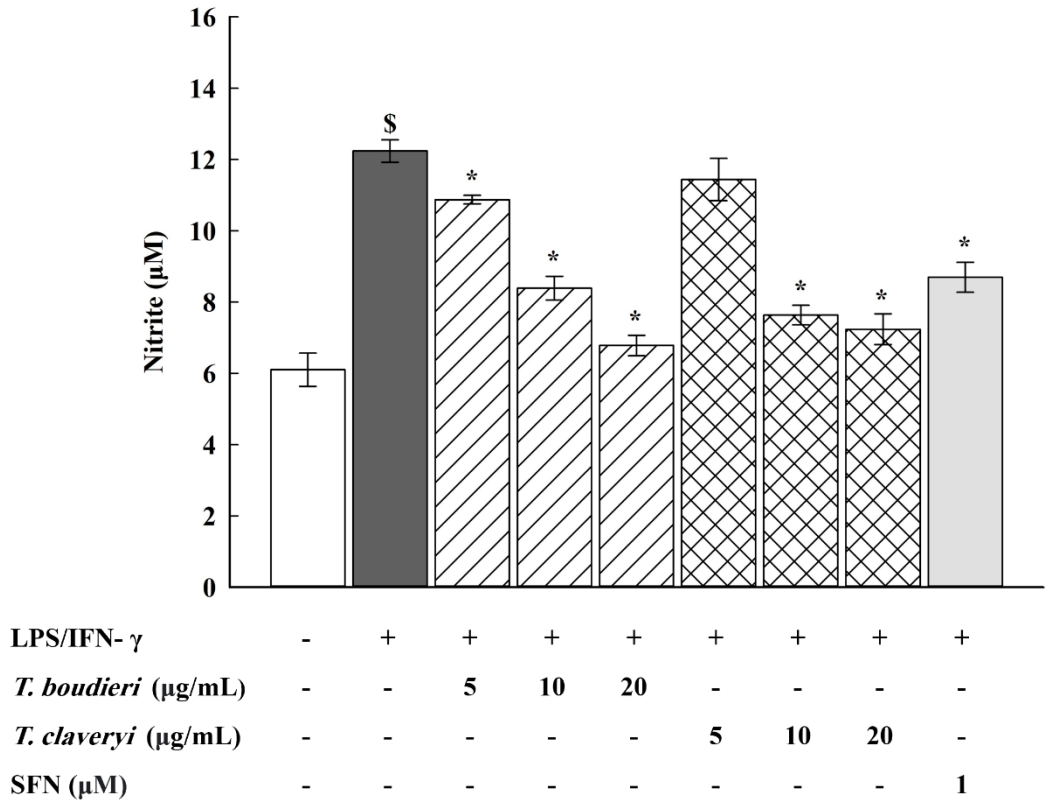

Figure 3.2 Effect of *T. boudieri* and *T. claveryi* extracts on nitrite production in LPS/IFN-γ-stimulated RAW 264.7 cells. RAW 264.7 cells were stimulated with LPS/IFN-γ (100 ng/10 U/mL) and co-incubated with *T. boudieri* and *T. claveryi* extracts at concentrations of 5, 10, and 20 μg/mL for 24 h. SFN (1 μM) was used as a positive control. Nitrite levels were analyzed by the Griess Reagent Kit. Data are expressed as mean ± SEM (n = 8). Statistical significance was calculated by one-way ANOVA followed by Student–Newman–Keuls (SNK) post-hoc test. $ $P < 0.05$ vs. control. * $P < 0.05$ vs. LPS/IFN-γ.

3.3 Effect of *T. boudieri* and *T. claveryi* extracts on the mRNA expression of iNOS in LPS/IFN-γ-stimulated RAW 264.7 cells

To investigate whereas the reduction of nitrite production following treatment with *Terfezia* extracts was due to suppression of iNOS gene expression, RAW 264.7 cells were treated with *T. boudieri* and *T. claveryi* extracts at concentrations of 5, 10, and 20 μg/mL in the presence of LPS/IFN-γ (100 ng/10 U/mL) for 6 h. SFN (1 μM) was used as a positive control. iNOS mRNA expression was then determined using qPCR. As shown in **Figure 3.3**, LPS/IFN-γ remarkably upregulated the mRNA expression of iNOS by 354% compared to the untreated control. Nevertheless, when the LPS/IFN-γ-stimulated cells were co-treated with *Terfezia* extracts, *T. boudieri* at concentrations of 5, 10, and 20 μg/mL dose-dependently suppressed the upregulation of iNOS mRNA expression by 23, 28, and 30%, respectively, and *T. claveryi* extract at concentrations of 5, 10, and 20 μg/mL downregulated iNOS mRNA expression by 24, 34, and 42%, respectively, in a dose-dependent manner. SFN (1 μM) also inhibited the iNOS mRNA expression by 38%. These results indicate that *Terfezia* extracts decreased nitrite production in LPS/IFN-γ-stimulated macrophages by downregulating iNOS transcription.

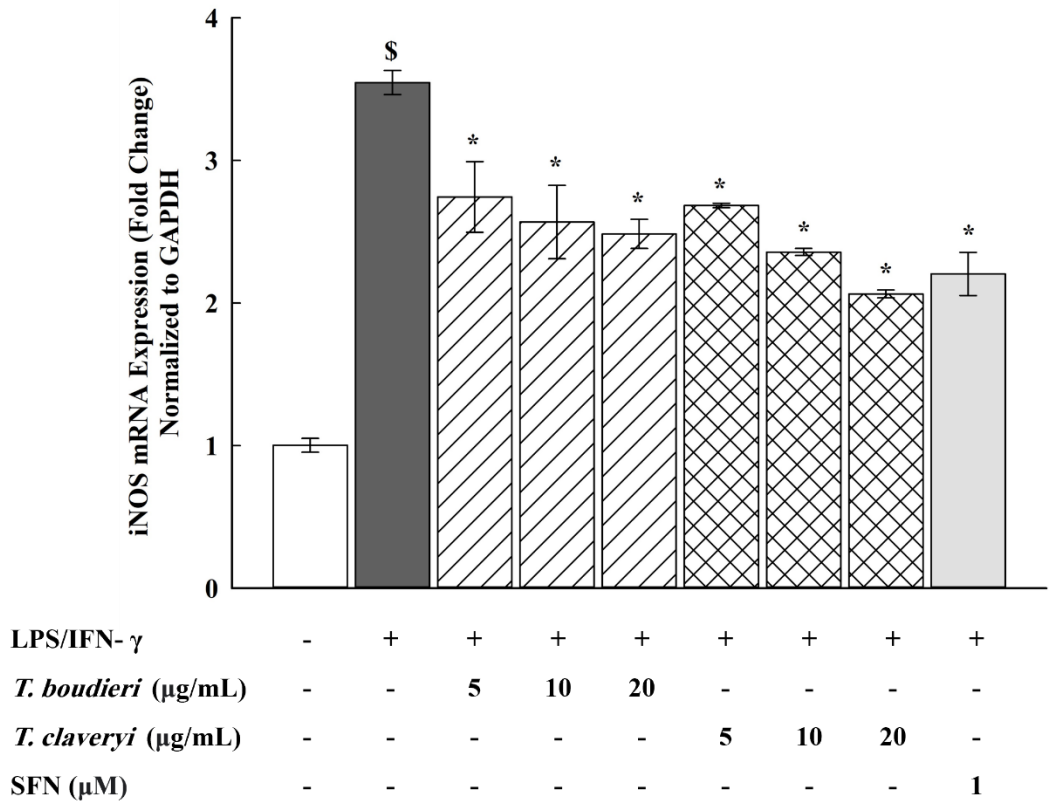

Figure 3.3 Effect of *T. boudieri* and *T. claveryi* extracts on the mRNA expression of iNOS in LPS/IFN-γ-stimulated RAW 264.7 cells. RAW 264.7 cells were stimulated with LPS/IFN-γ (100 ng/10 U/mL) and co-incubated with *T. boudieri* and *T. claveryi* extracts at concentrations of 5, 10, and 20 μg/mL for 6 h. SFN (1 μM) was used as a positive control. iNOS mRNA expression level was analyzed by qPCR. Data are expressed as mean ± SEM (n = 3). Statistical significance was calculated by one-way ANOVA followed by Student–Newman–Keuls (SNK) post-hoc test. $ $P < 0.05$ vs. control. * $P < 0.05$ vs. LPS/IFN-γ.

3.4 Effect of *T. boudieri* and *T. claveryi* extracts on the mRNA expression of COX-2 in LPS/IFN-γ-stimulated RAW 264.7 cells

To examine the suppressive effect of *Terfezia* extracts on the COX-2 mRNA expression, RAW 264.7 cells were treated with *T. boudieri* and *T. claveryi* extracts at concentrations of 5, 10, and 20 μg/mL in the presence of LPS/IFN-γ (100 ng/10 U/mL) for 6 h. SFN (1 μM) was used as a positive control. COX-2 mRNA expression was then determined using qPCR. **Figure 3.4** shows that the mRNA expression of COX-2 was significantly induced by 409% compared to the untreated control following stimulation by LPS/IFN-γ. However, when the LPS/IFN-γ-stimulated cells were co-treated with *Terfezia* extracts, *T. boudieri* strongly downregulated the mRNA expression of COX-2 by approximately 60% (5 –20 μg/mL), and *T. claveryi* extract at only 20 μg/mL significantly downregulated the mRNA expression of COX-2 by 35%. Significant differences were also observed in the inhibitory effects of both *Terfezia* extracts on the COX-2 mRNA expression, with *T. boudieri* being statistically significant compared to *T. claveryi* at 5, 10, and 20 μg/mL. SFN (1 μM) also inhibited the COX-2 mRNA expression by 31%.

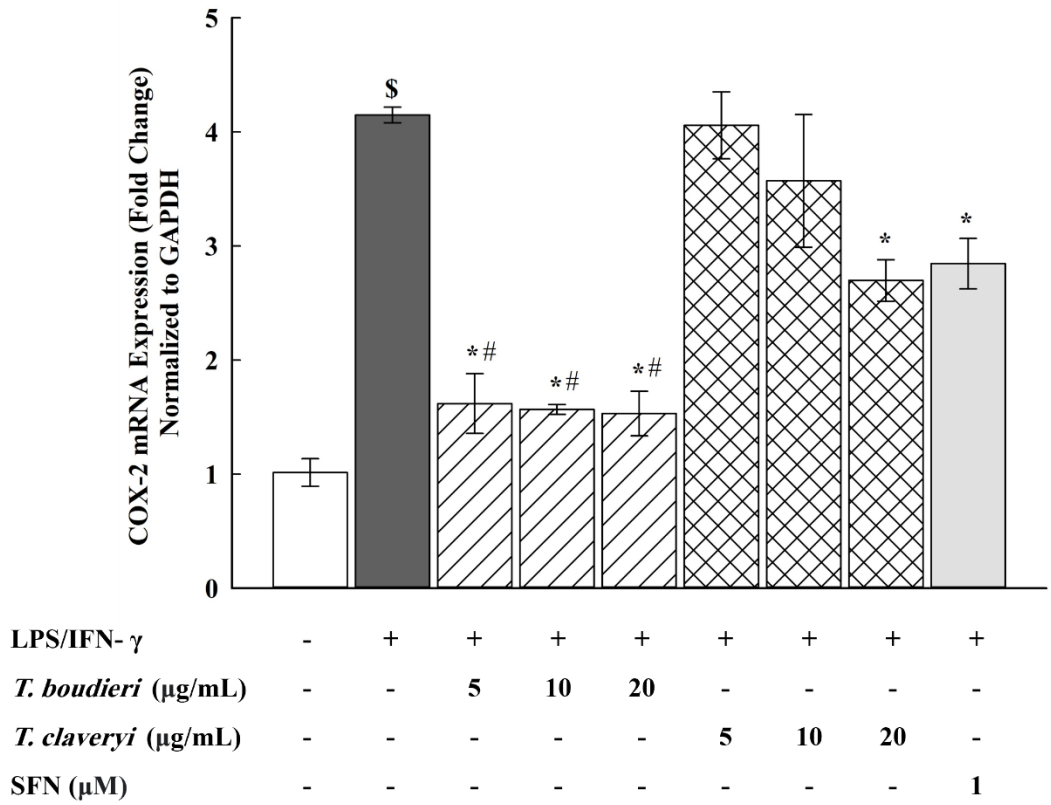

Figure 3.4 Effect of *T. boudieri* and *T. claveryi* extracts on the mRNA expression of COX-2 in LPS/IFN-γ-stimulated RAW 264.7 cells. RAW 264.7 cells were stimulated with LPS/IFN-γ (100 ng/10 U/mL) and co-incubated with *T. boudieri* and *T. claveryi* extracts at concentrations of 5, 10, and 20 μg/mL for 6 h. SFN (1 μM) was used as a positive control. COX-2 mRNA expression level was analyzed by qPCR. Data are expressed as mean ± SEM (n = 3). Statistical significance was calculated by one-way ANOVA followed by Student–Newman–Keuls (SNK) post-hoc test. $ $P < 0.05$ vs. control. * $P < 0.05$ vs. LPS/IFN- γ. # $P < 0.05$, *T. boudieri* at any given concentration vs. *T. claveryi* at the corresponding concentration.

3.5 Effect of *T. boudieri* and *T. claveryi* extracts on the mRNA expression of TNF-α and IL-6 in LPS/IFN-γ-stimulated RAW 264.7 cells

To examine the potential anti-inflammatory effects of *Terfezia* extracts on the mRNA expression of pro-inflammatory cytokines TNF-α and IL-6, RAW 264.7 cells were treated with *T. boudieri* and *T. claveryi* extracts at concentrations of 5, 10, and 20 µg/mL in the presence of LPS/IFN-γ (100 ng/10 U/mL) for 6 h. SFN (1 µM) was used as a positive control. The mRNA expression of TNF-α and IL-6 was then determined using qPCR. **Figure 3.5** shows that incubation with LPS/IFN-γ significantly increased the mRNA expression of TNF-α and IL-6 by 447 and 5278%, respectively, compared to the untreated controls. However, when the LPS/IFN-γ-stimulated cells were co-treated with *Terfezia* extracts, *T. boudieri* and *T. claveryi* at only 20 µg/mL significantly reduced the mRNA expression of TNF-α by 23, and 30%, respectively **(Figure 3.5A).** Moreover, the mRNA expression of IL-6 was significantly downregulated by treatment with *T. boudieri* (5, 10, and 20 µg/mL) by 23, 25, and 30%, respectively, and also downregulated by treatment with *T. claveryi* (5, 10, and 20 µg/mL) by 20, 27, and 40%, respectively, as shown in **Figure 3.5B.** Both extracts suppressed the LPS/IFN-γ-induced upregulation of TNF-α and IL-6 mRNA expression levels in a concentration-dependent manner. SFN (1 µM) also achieved a statistically significant inhibition of TNF-α and IL-6 by 58%.

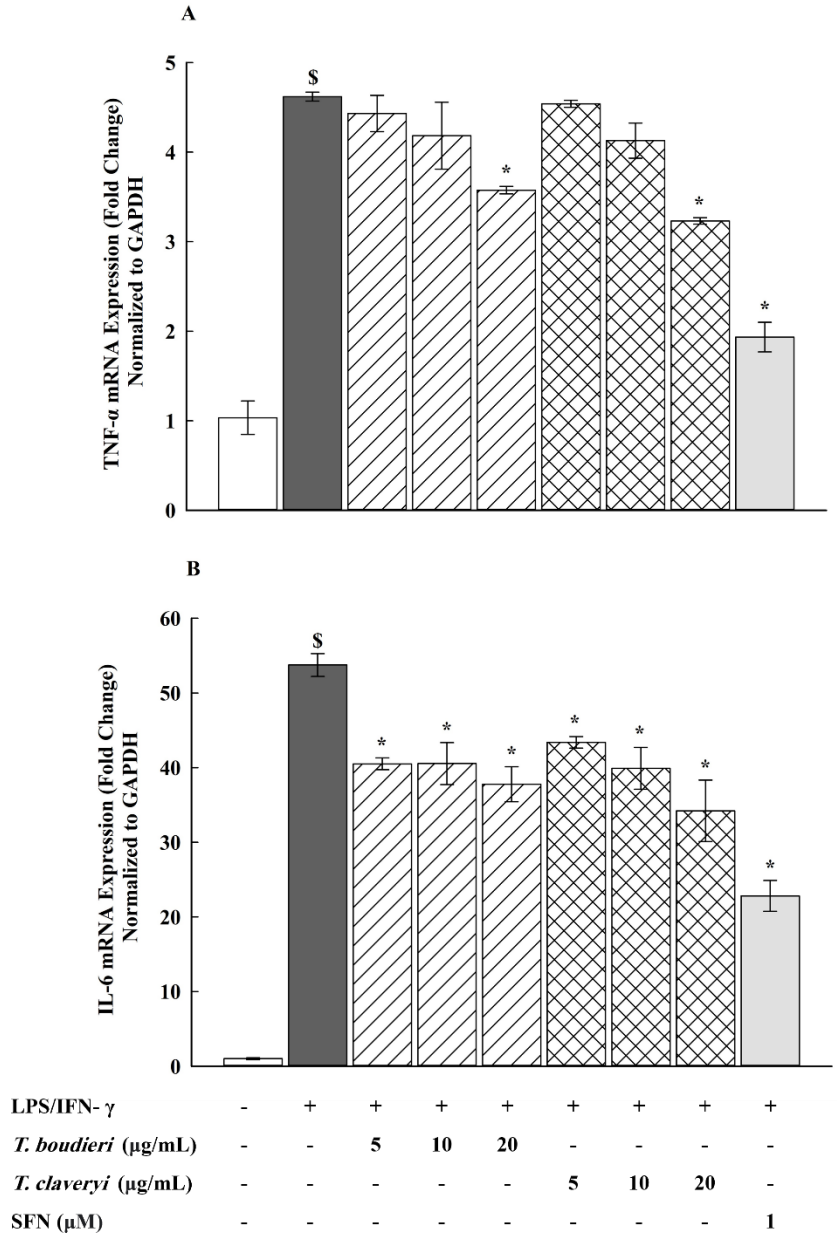

Figure 3.5 Effect of *T. boudieri* and *T. claveryi* extracts on the mRNA expression of TNF-α and IL-6 in LPS/IFN-γ-stimulated RAW 264.7 cells. RAW 264.7 cells were stimulated with LPS/IFN-γ (100 ng/10 U/mL) and co-incubated with *T. boudieri* and *T. claveryi* extracts at concentrations of 5, 10, and 20 μg/mL for 6 h. SFN (1 μM) was used as a positive control. TNF-α (A) and IL-6 (B) mRNA expression levels were analyzed by qPCR. Data are expressed as mean ± SEM (n = 3). Statistical significance was calculated by one-way ANOVA followed by Student–Newman–Keuls (SNK) post-hoc test. $ $P <$ 0.05 vs. control. * $P < 0.05$ vs. LPS/IFN-γ.

3.6 Effect of *T. boudieri* and *T. claveryi* extracts on the mRNA expression of HO-1 and OSGIN1 in LPS/IFN-γ-stimulated RAW 264.7 cells

To determine whether the anti-inflammatory effects of *Terfezia* extracts were related to modulation of the Nrf2 signaling pathway, RAW 264.7 cells were firstly treated with *T. boudieri* and *T. claveryi* extracts at concentrations of 5, 10, and 20 μg/mL in the presence of LPS/IFN-γ (100 ng/10 U/mL) for 6 h. SFN (1 μM) was used as a positive control. qPCR was then performed to measure the mRNA expression of Nrf2 targets (HO-1 and OSGIN1). **Figure 3.6A,C** shows that *T. boudieri*, *T. claveryi* and SFN did not shown any significant upregulation on the mRNA expression of HO-1 and OSGIN1 at any tested concentration. Consequently, the concentration of *T. boudieri* and *T. claveryi* was increased to a non-cytotoxic concentration of 40 μg/mL. SFN was also increased up to 5 μM. As shown in **Figure 3.6B,D**, SFN (5 μM) significantly upregulated the mRNA expression of HO-1 and OSGIN1 by 407 and 248%, respectively, whereas *T. boudieri* and *T. claveryi* (40 μg/mL) did not show any significant effect on either HO-1 or OSGIN1 mRNA expression.

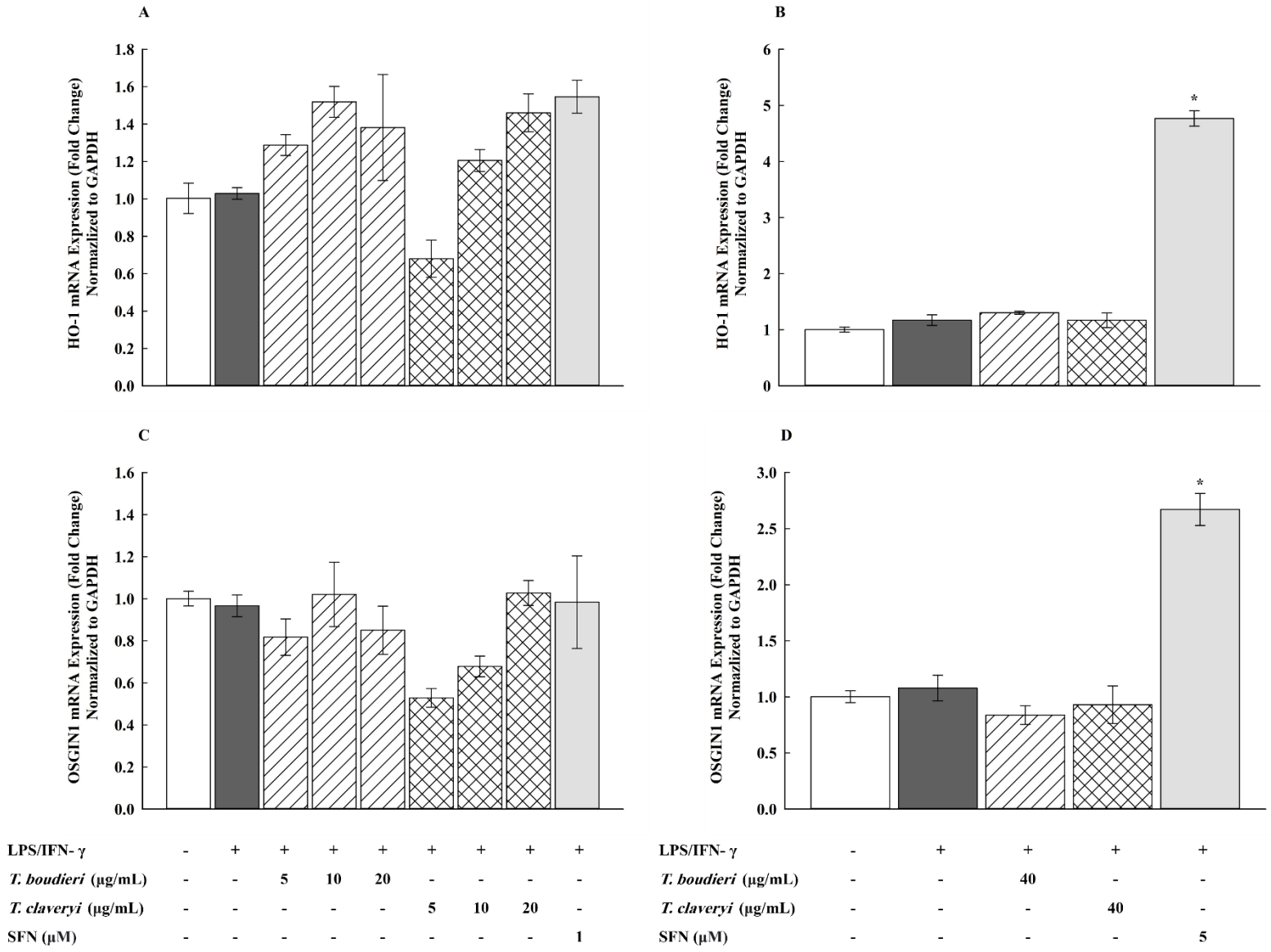

Figure 3.6 Effect of *T. boudieri* and *T. claveryi* extracts on the mRNA expression of HO-1 and OSGIN1 in LPS/IFN-γ-stimulated RAW 264.7 cells. RAW 264.7 cells were stimulated with LPS/IFN-γ (100 ng/10 U/mL) and co-incubated with *T. boudieri* and *T. claveryi* extracts at concentrations of 5, 10, 20 and 40 µg/mL for 6 h. SFN at concentrations of 1 and 5 µM was used as a positive control. The mRNA expression levels of HO-1 (A, B) and OSGIN1 (C, D) were analyzed by qPCR. Data are expressed as mean ± SEM (n = 3). Statistical significance was calculated by one-way ANOVA followed by Student–Newman–Keuls (SNK) post-hoc test. $ $P < 0.05$ vs. control. * $P < 0.05$ vs. LPS/IFN-γ.

3.7 Effect of *T. boudieri* and *T. claveryi* extracts on the miRNA expression of miR-21, miR-146a, and miR-155 in LPS/IFN-γ-stimulated RAW 264.7 cells

To investigate whether the anti-inflammatory effects of *Terfezia* extracts were associated with epigenetic modulation of gene expression, RAW 264.7 cells were treated with *T. boudieri* and *T. claveryi* extracts at concentrations of 5, 10, and 20 µg/mL in the presence of LPS/IFN-γ (100 ng/10 U/mL) for 6 h. SFN (1 µM) was used as a positive control. qPCR was then performed to measure the miRNA expression of miR-21, miR-146a, and miR-155. As shown in **Figure 3.7,** miR-21, miR-146a, and miR-155 were significantly upregulated by 206, 263, and 247%, respectively, in LPS/IFN-γ-induced cells compared to the untreated controls, and significantly reduced by treatment with *Terfezia* extracts in a dose-dependent manner. Significant differences were also observed in the inhibitory effects of *Terfezia* extracts on the miR-21, and miR-146a, with *T. claveryi* (20 µg/mL) being statistically significant compared to *T. boudieri* (20 µg/mL). **Figure 3.7A** illustrates that *T. boudieri* (10 and 20 µg/mL) significantly reduced the upregulation of miR-21 by approximately 35%, and *T. claveryi* (5, 10, and 20 µg/mL) showed a significant inhibition of the upregulated miR-21 by 21, 50, and 64%, respectively. **Figure 3.7B** demonstrates that *T. boudieri* (5, 10, and 20 µg/mL) significantly reduced the upregulation of miR-146a by 28, 54, and 58%, respectively, and *T. claveryi* (5, 10, and 20 µg/mL) showed a highly significant inhibition of the upregulated miR-146a by 46, 70, and 85%, respectively. **Figure 3.7C** shows that *T. boudieri* and *T. claveryi* at only 20 µg/mL significantly decreased the upregulation of miR-155 by 28 and 35%, respectively. SFN (1 µM) also downregulated the expression of miR-21, miR-146a, and miR-155 by 55, 72 and 36%, respectively.

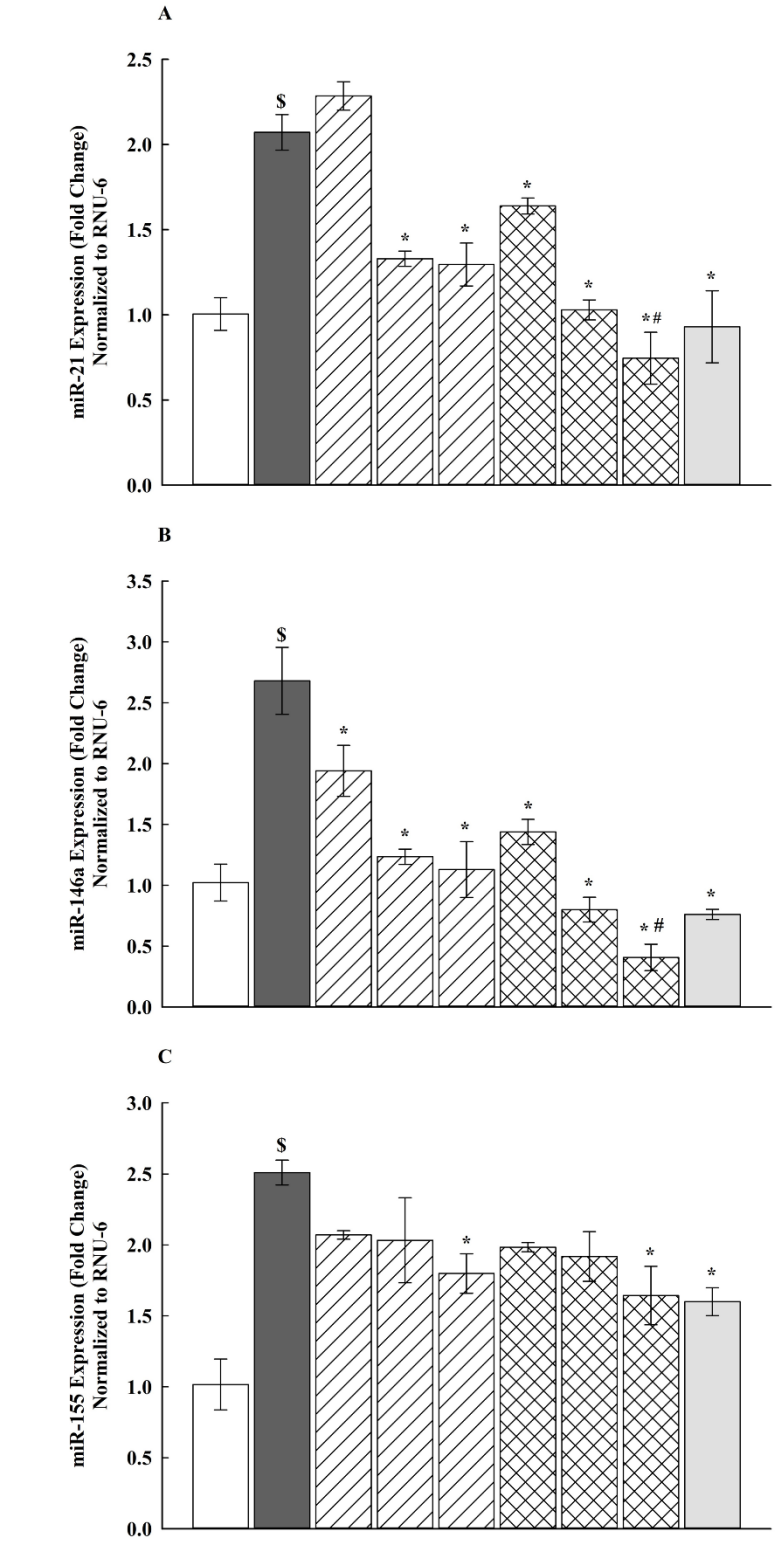
A
miR-21 Expression (Fold Change) Normalized to RNU-6
2.5
2.0
1.5
1.0
0.5
0.0
$
*
*
*
*
*
*#
*
B
miR-146a Expression (Fold Change) Normalized to RNU-6
3.5
3.0
2.5
2.0
1.5
1.0
0.5
0.0
$
*
*
*
*
*
*#
*
C
miR-155 Expression (Fold Change) Normalized to RNU-6
3.0
2.5
2.0
1.5
1.0
0.5
0.0
$
*
*
*
*
LPS/IFN- γ - + + + + + + + +
T. boudieri (µg/mL) - - 5 10 20 - - - -
T. claveryi (µg/mL) - - - - - 5 10 20 -
SFN (µM) - - - - - - - - 1

Figure 3.7 Effect of *T. boudieri* and *T. claveryi* extracts on the miRNA expression of miR-21, miR-146a, and miR-155 in LPS/IFN-γ-stimulated RAW 264.7 cells. RAW 264.7 cells were stimulated with LPS/IFN-γ (100 ng/10 U/mL) and co-incubated with *T. boudieri* and *T. claveryi* extracts at concentrations of 5, 10, and 20 µg/mL for 6 h. SFN (1 µM) was used as a positive control. The miRNA expression levels of miR-21 (A), miR-146a (B), and miR-155 (C) were analyzed by qPCR. Data are expressed as mean ± SEM (n = 3). Statistical significance was calculated by one-way ANOVA followed by Student–Newman–Keuls (SNK) post-hoc test. $ $P < 0.05$ vs. control. * $P < 0.05$ vs. LPS/IFN- γ. # $P < 0.05$, *T. boudieri* at any given concentration vs. *T. claveryi* at the corresponding concentration.

Effect of *T. boudieri* and *T. claveryi* extracts on the secretion of TNF-α and IL-6 proteins in LPS/IFN-γ-stimulated RAW 264.7 cells

To relate *Terfezia*-mediated inhibition of the mRNA expression of cytokines TNF-α and IL-6 to cytokines secretion, RAW 264.7 cells were treated with *T. boudieri* and *T. claveryi* extracts at concentrations of 5 and 20 µg/mL in the presence of LPS/IFN-γ (100 ng/10 U/mL) for 24 h. SFN (1 µM) was used as a positive control. The concentration of TNF-α and IL-6 proteins secreted into the cell culture supernatant was measured using ELISA. As shown i**n Figure 3.8**, the production of TNF-α and IL-6 proteins was significantly increased in the cell culture medium of LPS/IFN-γ-induced cells, compared to the untreated controls. However, when the cells were co-treated with *Terfezia* extracts, *T. boudieri* at 20 µg/mL significantly reduced TNF-α and IL-6 production by 24, and 14%, respectively. It was also found that *T. claveryi* at 20 µg/mL and SFN (1 µM) displayed a significant decrease in TNF-α production by 27, and 34%, respectively, but they did not show any significant inhibition on IL-6 production **(Figure 3.8A,B).**

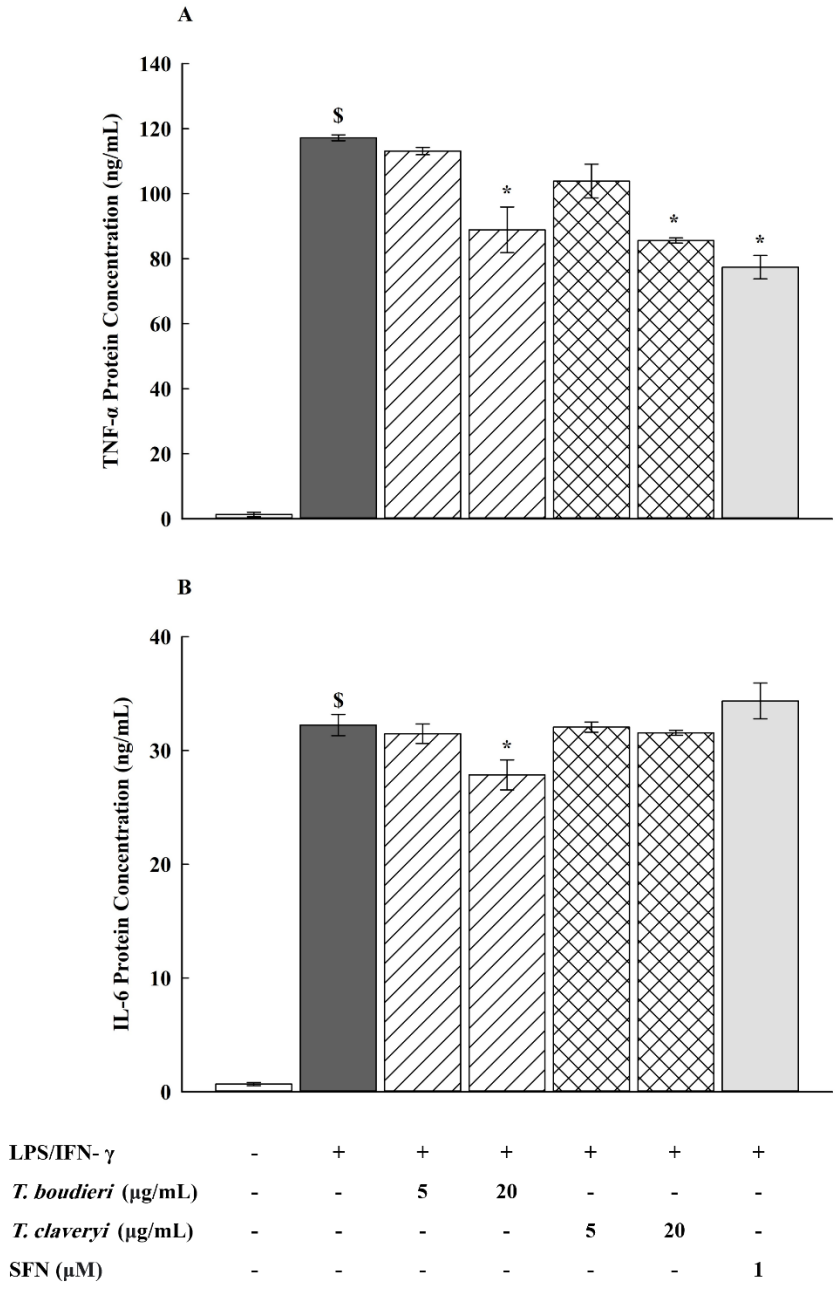

Figure 3.8 Effect of *T. boudieri* and *T. claveryi* extracts on the secretion of TNF-α and IL-6 proteins in LPS/IFN-γ-stimulated RAW 264.7 cells. RAW 264.7 cells were stimulated with LPS/IFN-γ (100 ng/10 U/mL) and co-incubated with *T. boudieri* and *T. claveryi* extracts at concentrations of 5 and 20 µg/mL for 24 h. SFN (1 µM) was used as a positive control. TNF-α (A) and IL-6 (B) protein concentrations were quantified by ELISA. Data are expressed as mean ± SEM (n = 3). Statistical significance was calculated by one-way ANOVA followed by Student–Newman–Keuls (SNK) post-hoc test. $ $P < 0.05$ vs. control. * $P < 0.05$ vs. LPS/IFN-γ.

3.8 Effect of *T. boudieri* and *T. claveryi* extracts on the expression of iNOS and COX-2 proteins in LPS/IFN-γ-stimulated RAW 264.7 cells

To confirm the inhibitory effect of *Terfezia* extracts on the iNOS and COX-2 expression at the protein level, RAW 264.7 cells were treated with *T. boudieri* and *T. claveryi* extracts at concentrations of 20 µg/mL in the presence of LPS/IFN-γ (100 ng/10 U/mL) for 24 h. SFN (1 µM) was used as a positive control. The expression of iNOS and COX-2 proteins were examined using western blotting. As shown in **Figure 3.9**, LPS/IFN-γ significantly increased the expression of iNOS and COX-2 proteins by 292 and 279%, respectively, compared to the untreated controls. However, when the LPS/IFN-γ-stimulated cells were co-treated with *Terfezia* extracts, *T. boudieri* (20 µg/mL) significantly inhibited the iNOS and COX-2 expression by 41 and 30% respectively. Furthermore, *T. claveryi* (20 µg/mL) suppressed the expression of iNOS by 46%, but it did not show any significant effect on the COX-2 expression. SFN (1 µM) also inhibited the iNOS and COX-2 expression by 43 and 35%, respectively. The expression of the GAPDH, which was used as a loading control was not changed **(Figure 3.9A,B).**

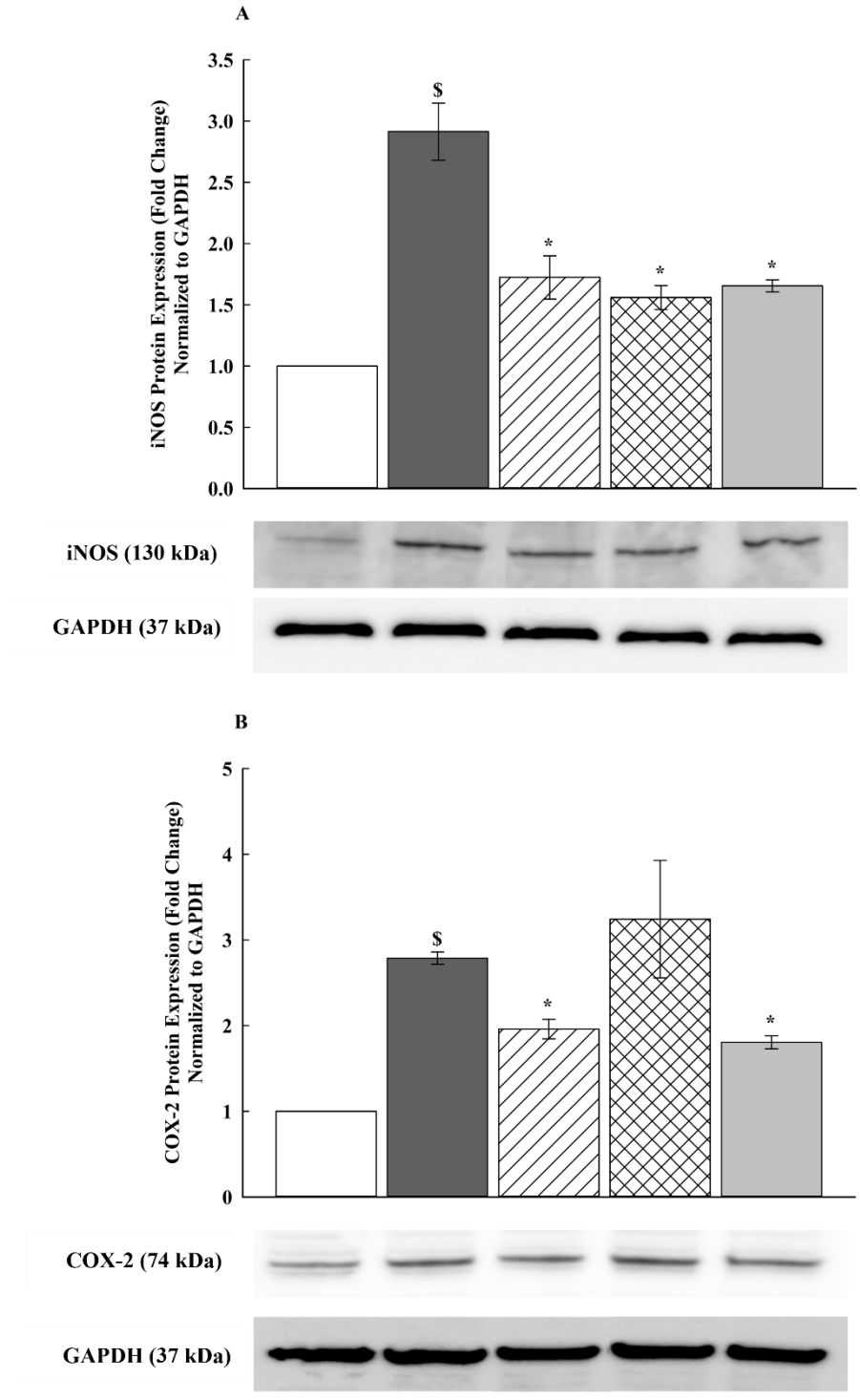
A
iNOS Protein Expression (Fold Change) Normalized to GAPDH
3.5
3.0
2.5
2.0
1.5
1.0
0.5
0.0
$
*
*
*
iNOS (130 kDa)
GAPDH (37 kDa)
B
COX-2 Protein Expression (Fold Change) Normalized to GAPDH
5
4
3
2
1
0
$
*
*
COX-2 (74 kDa)
GAPDH (37 kDa)
LPS/IFN- γ - + + + +
T. boudieri (µg/mL) - - 20 - -
T. claveryi (µg/mL) - - - 20 -
SFN (µM) - - - - 1

Figure 3.9 Effect of *T. boudieri* and *T. claveryi* extracts on the expression of iNOS and COX-2 proteins in LPS/IFN-γ-stimulated RAW 264.7 cells. RAW 264.7 cells were stimulated with LPS/IFN-γ (100 ng/10 U/mL) and co-incubated with *T. boudieri* and *T. claveryi* extracts at concentrations of 20 µg/mL for 24 h. SFN (1 µM) was used as a positive control. iNOS (A) and COX-2 (B) protein expression levels were determined by western blotting. GAPDH was used as a loading control. Data are expressed as mean ± SEM (n = 3). Statistical significance was calculated by one-way ANOVA followed by Student–Newman–Keuls (SNK) post-hoc test. $ $P < 0.05$ vs. control. * $P < 0.05$ vs. LPS/IFN-γ.

Chapter 4: Discussion

Inflammation is a protective immune response that can be triggered by noxious stimuli, such as pathogens and toxins. Inflammation is therefore the first immunological line of defense through which the body can remove infection and repair tissue damage. The extent of the inflammatory response has critical importance because failure to eliminate the inflammatory trigger during acute inflammation leads to chronic inflammation, autoimmune responses, and severe tissue damage. NSAIDs are the most used drugs in the treatment of inflammation-associated diseases but have serious side effects (Abdulkhaleq et al., 2018). Thus, multiple studies have been performed in order to explore alternative anti-inflammatory drugs of natural origin without the side effects of NSAIDs. The natural products are considered potential sources of novel anti-inflammatory agents, which can contribute to the development of innovative therapeutics (Beg et al., 2011). Desert truffles were reported to treat several inflammatory diseases (H. El Enshasy et al., 2013). Nevertheless, the mechanisms behind their anti-inflammatory activities in RAW 264.7 macrophages remain unclear. Hence, in the present study, the anti-inflammatory properties of two major desert truffles, *T. boudieri* and *T. claveryi* have been examined. Both species have been selected for the study based on the abundance of functional anti-inflammatory compounds in their chemical profile.

SFN was used a positive control in this study because it possesses a potent anti-inflammatory activity, which is mediated through suppressing TLR4 oligomerization (Youn et al., 2010). Furthermore, Heiss et al. indicated that SFN reduced production of the

inflammatory mediators, including NO, PGE_2, and TNF-α along with downregulation of iNOS, and COX-2 proteins in LPS-induced RAW 264.7 cells (Heiss et al., 2001). SFN-mediated anti-inflammatory activity has been attributed in part to the activation of the Nrf2 as reported by Lin et al (W. Lin et al., 2008). In addition to the previous studies, Saleh et al. demonstrated that SFN modulated the TLR-associated miRNAs, such as miR-146a and miR-155 in LPS/IFN-γ-induced RAW 264.7 cells (Saleh et al., 2021). Therefore, SFN represents an ideal positive control in evaluating the anti-inflammatory properties of other drugs.

Macrophages play pivotal roles during the inflammatory response, such as phagocytosis of microbes, antigen presentation, and secretion of inflammatory mediators (Shapouri-Moghaddam et al., 2018). Moreover, macrophages are essential for maintaining homeostasis and tissue regeneration after injury (Watanabe et al., 2019; Wynn et al., 2013). Therefore, *In vitro* models of macrophages are important tools in evaluating the efficacy of the anti-inflammatory drugs through assessing the inflammatory response and cytotoxicity. RAW 264.7 macrophage cells are generally used to investigate the anti-inflammatory properties of drugs, and significantly activated by LPS and/or IFN-γ (Martinez & Gordon, 2014). IFN-γ is included in combination with LPS in the macrophage polarization, and the induction of macrophages with either one of them, leads to the secretion of several inflammatory mediators (Cassetta et al., 2011; Shapouri-Moghaddam et al., 2018; Sica et al., 2015). In the current study, to examine the effects of *T. boudieri* and *T. claveryi* extracts on the inflammatory pathways, RAW264.7 cells were stimulated with LPS (100 ng/mL) plus IFN-γ (10 U/mL). Our results demonstrated that LPS and IFN-γ produced a significant inflammatory response in RAW 264.7 cells, which is similar to

the findings of Saleh et al (Saleh et al., 2021). We first determined the non-cytotoxic concentrations of *T. boudieri* and *T. claveryi* extracts with or without LPS/IFN-γ in RAW 264.7 cells using MTT assay. Our data showed that treatment of RAW 264.7 cells with *T. boudieri* and *T. claveryi* extracts in the presence or absence of LPS/IFN-γ was not associated with a decrease in the cellular viability at concentrations between 5-20 μg/mL. Therefore, the concentrations of 5, 10, and 20 μg/mL were selected for both extracts in all further experiments.

The inflammatory response is mediated by a wide range of mediators forming complex regulatory networks that prevent further tissue damage and restore the normal physiology of the inflamed tissues (Medzhitov, 2008). Once macrophages are activated by LPS/IFN-γ, production of inflammatory mediators including cytokines (e.g., TNF-α and IL-6), eicosanoids (e.g., prostaglandins), and NO are increased (Ahmad et al., 2006; Hong et al., 2021). NO is a key signaling molecule that play an important role in the inflammatory response. NO is released as a cellular signaling molecule to increase the vasodilation in blood vessels by the activation of iNOS, which subsequently leads to apparent increase in the blood flow and recruitment of leukocytes to the region of inflammation (Alderton et al., 2001; K. Newton & Dixit, 2012; Tasneem et al., 2019). Therefore, to investigate the anti-inflammatory effects of *T. boudieri* and *T. claveryi* extracts, we analyzed the NO production, and the iNOS expression at the mRNA and protein levels in LPS/IFN-γ-stimulated RAW 264.7 cells. Since NO is rapidly oxidized to nitrite, the nitrite level in the culture medium was measured as an indicator of NO production (Sun et al., 2003). Here, we found that *T. boudieri* and *T. claveryi* extracts inhibited NO production in a dose-dependent manner, which was accompanied by a simultaneous reduction in the iNOS

mRNA expression. These data were consistent with our Western blotting analysis, in which both extracts exhibited a significant inhibition on the expression of iNOS protein. Our results indicate that *Terfezia* extracts effectively improve inflammatory conditions through inhibiting the overproduction of NO and the expression of iNOS in LPS/IFN-γ-stimulated RAW 264.7 cells.

Prostaglandins are eicosanoid-derived molecules that participate in modulating numerous physiological processes, particularly during the immune responses. Prostaglandins are produced through metabolism of arachidonic acid by cyclooxygenases, which exist into two isoforms: COX-1 and COX-2. COX-1 is produced constitutively in most cells, whereas COX-2 is induced in response to inflammatory stimuli (Khanapure et al., 2007; Ricciotti & FitzGerald, 2011). Consequently, numerous anti-inflammatory drugs attempt to inhibit COX-2. Thus, to examine the suppressive effect of *T. boudieri* and *T. claveryi* extracts, we measured the mRNA and protein expression of COX-2 in LPS/IFN-γ-stimulated RAW 264.7 cells. Our study revealed that both extracts downregulated the mRNA expression of COX-2, with *T. boudieri* being more potent in its action on the mRNA and protein levels. Taken together, these data suggest that the anti-inflammatory properties of *Terfezia* extracts are associated with the suppression of COX-2 expression in LPS/IFN-γ-stimulated macrophages.

Cytokines are key signaling proteins, regulating the crosstalk between different cell types involved in the immune and inflammatory response (Turner et al., 2014). Among cytokines, TNF-α is the major mediator of inflammation with several effects, including stimulating other cytokines secretion, activating of cell adhesion molecules, and promoting cell growth and proliferation (Germolec et al., 2018; Turner et al., 2014). IL-6 is another

important cytokine released during inflammation, and its dysregulation causes a variety of inflammatory disorders (Balkwill & Mantovani, 2010). Hence, the dysregulation in the inflammatory cytokines production is commonly related to inflammatory diseases, making them potential therapeutic targets. In the current study, we assessed the expression of pro-inflammatory cytokines TNF-α and IL-6 at the mRNA and protein levels in an attempt to identify the possible effects of *T. boudieri* and *T. claveryi* extracts on the inflammation mediated by LPS/IFN-γ in RAW 264.7 cells. Interestingly, *T. boudieri* extract decreased the expression of TNF-α and IL-6 in a dose-dependent manner at the mRNA and protein levels. On the other hand, *T. claveryi* reduced the mRNA expression of TNF-α and IL-6 beside the suppression of TNF-α protein production, whereas IL-6 at the protein level was not reduced. Consistent with our results, Darwish et al. revealed that *T. claveryi* displayed anti-inflammatory activity by reducing the levels of TNF-α, IL-1*β, and* IFN-γ in LPS-stimulated WBCs (Darwish et al., 2021b). In a previous study of subarachnoid hemorrhage, Echigo et al. reported that trehalose, a predominant disaccharide in *T. boudieri* and *T. claveryi*, decreased the levels of cytokines (TNF-α, IL-1α, IL-1β, and IL-6), and the expression of iNOS and COX-2 in blood-induced inflammation in RAW264.7 cells (Echigo et al., 2012). Previous studies showed that terpenoids presented anti-inflammatory properties. Monoterpenes (e.g., α-Pinene) and sesquiterpenes (e.g., α-humulene and β-caryophyllene) were reported in the chemical profile of *T. boudieri* and *T. claveryi*. α-pinene monoterpene suppressed the production of NO, TNF-α, and IL-6 in mouse peritoneal macrophages. Moreover, α-pinene downregulated the expression of iNOS and COX-2 along with inhibition of the NF-κB and MAPK signaling pathways as confirmed by Kim et al (D.-S. Kim et al., 2015). In an *in vivo* study to evaluate the anti-inflammatory

activities of α-humulene and (−)-trans-caryophyllene sesquiterpenes extracted from the essential oil of *Cordia verbenacea*, it was reported that both compounds inhibited PGE2 production, iNOS, and COX-2 expression in carrageenan-treated rats. Furthermore, α-Humulene suppressed TNFα and IL-1β production, while –(-)trans-caryophyllene reduced only TNFα secretion (Fernandes et al., 2007). Moreover, phenolics found in the metabolome of both extracts, such as catechin, the major phenolic compound in *T. boudieri*, suppressed the production of NO, TNF-α, IL-1β, and IL-6 in LPS-treated rats (Ganeshpurkar & Saluja, 2020). These results suggest that *Terfezia* extracts exert anti-inflammatory properties via suppressing the pro-inflammatory cytokines involved in the inflammatory process.

Nrf2 is a key transcription factor, playing a central role in the inflammation signaling pathways and oxidative stress responses. Therefore, the present study examined whether the anti-inflammatory effects of *T. boudieri* and *T. claveryi* extracts were related to activation of the Nrf2 signaling pathway in RAW 264.7 cells induced by LPS/IFN-γ through assessing the gene expression of Nrf2 target genes, HO-1 and OSGIN1. Inflammatory cells produce numerous inflammatory mediators, which subsequently attract more inflammatory cells to the site of injury, leading to increase in the level of oxidative stress (Saha et al., 2020). Meanwhile, persistent oxidative stress has been found to be associated with chronic inflammation (Tu et al., 2019). Nrf2 signaling pathway is also important in reducing inflammation-related disorders, including atherosclerosis, asthma, autoimmune diseases, and rheumatoid arthritis (J. Kim et al., 2010). Several studies have reported that the activation of Nrf2 signaling pathway suppressed cytokines, chemokine, iNOS, COX-2 secretion, which in turn modulate the NF-kB and other inflammatory

cascades that regulate the transcription and activity of downstream target proteins during the inflammation process (Ahmed et al., 2017; Kobayashi et al., 2016). Our initial findings showed that *T. boudieri*, *T. claveryi* (5, 10, and 20 µg/mL), and SFN (1 µM) did not induce the mRNA expression of HO-1 and OSGIN1. Considering the fact that SFN is a potent activator of Nrf2, but it did not show any significant effect on the Nrf2 targets in our study at concentration of 1 µM. Thus, we increased its concentration to 5 µM, and the concentration of *T. boudieri* and *T. claveryi* was also increased to a non-cytotoxic concentration of 40 µg/mL, as assessed by MTT assay. Here, we clearly showed that SFN (5 µM) activated the gene expression of HO-1 and OSGIN1. On the other hand, *T. boudieri* and *T. claveryi* (40 µg/mL) did not show any significant induction on the gene expression of HO-1 and OSGIN. Similarly, a study by Doss et al. indicated that SFN (5 µM) significantly increased the mRNA level of HO-1 in erythroid cells, while it did not display the same effect at lower concentrations between 100 nM-1 µM (Doss et al., 2016). These results illustrate that *Terfezia*-mediated anti-inflammatory effects are not Nrf2-dependent.

To further elucidate the *Terfezia*-mediated anti-inflammatory mechanisms, the current study investigated the regulatory effects of *T. boudieri* and *T. claveryi* extracts on the expression of inflammatory miRNAs, such as miR-21, miR-146a, and miR-155 in the LPS/IFN-γ-activated RAW 264.7 cells. These miRNAs were selected in this study based on their significant relevance to the TLR4 signaling pathway (Quinn & O'Neill, 2011). miRNAs play major roles in regulation of immune cell functions of both the innate and adaptive systems through targeting inflammation-related pathways, such as TLR4 (Fabbri et al., 2013; Mehta & Baltimore, 2016). miR-21 is a negative regulator of the TLR4-induced immune response that suppresses the NF-κB activity and promotes the production

of the anti-inflammatory cytokine IL-10 through targeting of the programmed cell death protein 4 (PDCD4) (Sheedy et al., 2010). Furthermore, miR-146a was identified to be a NF-κB-dependent gene that targets interleukin-1 receptor-associated kinases1 (IRAK1) and TNF receptor associated factor 6 (TRAF6) in the TLR4 signaling pathway, suggesting it as a negative regulator of the innate immune response (Taganov et al., 2006). Additionally, miR-155 has a well-characterized role in inflammation through targeting multiple proteins involved in the TLR4 signaling pathway (Ferrajoli et al., 2013; X. He et al., 2014). Ceppi et al. reported that miR-155 negatively regulated the inflammatory response to LPS in monocyte-derived dendritic cells. This negative regulation by miR-155 was related to its ability to target TAB2, suppressing its activation of TAK1, and thus the NF-κB and MAPK (Ceppi et al., 2009). The results of the present study demonstrated upregulation of miR-21, miR-146a, and miR-155 in response to LPS/IFN-γ stimulation, consistent with previous studies (Bala et al., 2011; Feng et al., 2014; Y. He et al., 2014). Interestingly, treatment with *T. boudieri* and *T. claveryi* extracts was observed to inhibit the LPS/IFN-γ-induced upregulation of these miRNAs in a concentration-dependent manner, suggesting that both *Terfezia* extracts suppress the inflammatory response in activated macrophages through regulating the expression of miR-21, miR-146a, and miR-155.

Chapter 5: Conclusion and Future Perspectives

In conclusion, TLR4-mediated signaling is associated with the LPS/IFN-γ-induced inflammation in RAW 264.7 macrophages, and inhibition of specific inflammatory mediators represents a highly relevant therapeutic strategy. In the present study, we demonstrated that *T. boudieri* and *T. claveryi* extracts inhibited the inflammatory response in LPS/IFN-γ-stimulated RAW 264.7 macrophages through modulating the TLR4 activation. *T. boudieri* reduced the production of NO and the expression of iNOS, COX-2, TNF-α, and IL-6 at the mRNA and protein levels. Although *T. claveryi* showed similar results, it did not show any inhibitory effect on the IL-6 and COX-2 at the protein level. Moreover, this study provided the first insight into the epigenetically suppressive properties of *T. boudieri* and *T. claveryi* extracts on the expression of miR-21, miR-146a, and miR-155 in LPS/IFN-γ-induced RAW 264.7 macrophages, suggesting that *Terfezia* extracts may have anti-inflammatory activities through inhibiting the miRNAs associated with the TLR4 signaling pathway. Next, our results demonstrated that *T. boudieri* and *T. claveryi* mediate anti-inflammatory characteristics via an Nrf2-independent manner. The results of the present study show that *T. boudieri* and *T. claveryi* may be useful alternative agents for the treatment of inflammation. However, further *in vivo* studies are required to confirm our findings using appropriate animal models.

Supplementary Figures

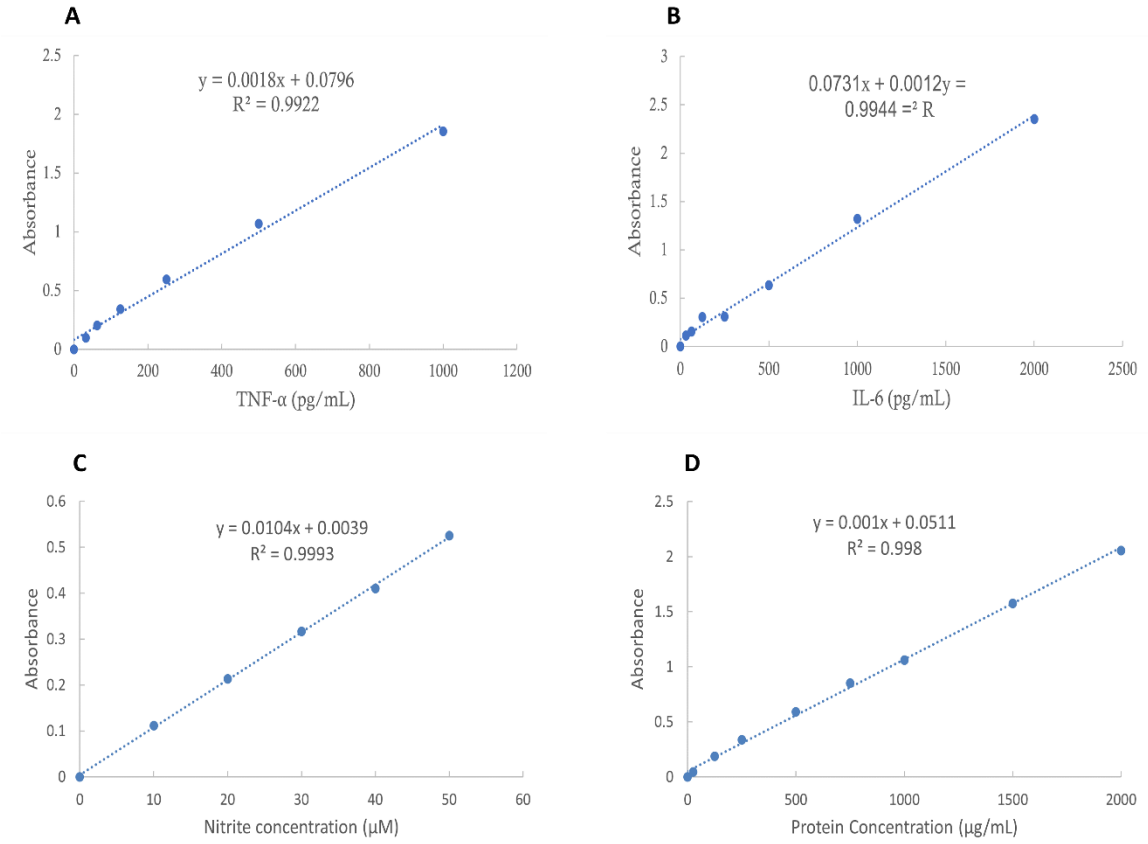

Figure 5.1 (A) Standard curve of TNF-α protein, (B) Standard curve of IL-6 (C) Nitrite standard curve, (D) BSA standard curve

References

Abdulkhaleq, L. A., Assi, M. A., Abdullah, R., Zamri-Saad, M., Taufiq-Yap, Y. H., & Hezmee, M. N. M. (2018). The crucial roles of inflammatory mediators in inflammation: A review. *Veterinary World*, *11*(5), 627–635. https://doi.org/10.14202/vetworld.2018.627-635

Ahmad, S., Israf, D. A., Lajis, N. Hj., Shaari, K., Mohamed, H., Wahab, A. A., Ariffin, K. T., Hoo, W. Y., Aziz, N. A., Kadir, A. A., Sulaiman, M. R., & Somchit, M. N. (2006). Cardamonin, inhibits pro-inflammatory mediators in activated RAW 264.7 cells and whole blood. *European Journal of Pharmacology*, *538*(1), 188–194. https://doi.org/10.1016/j.ejphar.2006.03.070

Ahmed, S. M. U., Luo, L., Namani, A., Wang, X. J., & Tang, X. (2017). Nrf2 signaling pathway: Pivotal roles in inflammation. *Biochimica et Biophysica Acta (BBA) - Molecular Basis of Disease*, *1863*(2), 585–597. https://doi.org/10.1016/j.bbadis.2016.11.005

Akyüz, M. (2013). Nutritive value, flavonoid content and radical scavenging activity of the truffle (Terfezia boudieri Chatin). *Journal of Soil Science and Plant Nutrition*, *13*(1), 143–151. https://doi.org/10.4067/S0718-95162013005000013

AlAhmed, A., & Khalil, H. E. (2019). Antidiabetic Activity of Terfezia Claveryi; An In Vitro and In Vivo Study. *Biomedical and Pharmacology Journal*, *12*(2), 603–608.

Alderton, W. K., Cooper, C. E., & Knowles, R. G. (2001). Nitric oxide synthases: Structure, function and inhibition. *Biochemical Journal*, *357*(Pt 3), 593–615.

Badalyan, S. (2012). Medicinal Aspects of Edible Ectomycorrhizal Mushrooms. In A. Zambonelli & G. M. Bonito (Eds.), *Edible Ectomycorrhizal Mushrooms: Current Knowledge and Future Prospects* (pp. 317–334). Springer. https://doi.org/10.1007/978-3-642-33823-6_18

Bahuguna, A., Khan, I., Bajpai, V. K., & Kang, S. C. (2017). MTT assay to evaluate the cytotoxic potential of a drug. *Bangladesh Journal of Pharmacology*, *12*(2), 8. https://doi.org/10.3329/bjp.v12i2.30892

Bala, S., Marcos, M., Kodys, K., Csak, T., Catalano, D., Mandrekar, P., & Szabo, G. (2011). Up-regulation of MicroRNA-155 in Macrophages Contributes to Increased Tumor Necrosis Factor α (TNFα) Production via Increased mRNA Half-life in Alcoholic Liver Disease. *The Journal of Biological Chemistry*, *286*(2), 1436–1444. https://doi.org/10.1074/jbc.M110.145870

Balkwill, F., & Mantovani, A. (2010). Cancer and Inflammation: Implications for Pharmacology and Therapeutics. *Clinical Pharmacology & Therapeutics*, *87*(4), 401–406. https://doi.org/10.1038/clpt.2009.312

Beara, I. N., Lesjak, M. M., Četojević-Simin, D. D., Marjanović, Ž. S., Ristić, J. D., Mrkonjić, Z. O., & Mimica-Dukić, N. M. (2014). Phenolic profile, antioxidant, anti-inflammatory and cytotoxic activities of black (Tuber aestivum Vittad.) and white (Tuber magnatum Pico) truffles. *Food Chemistry*, *165*, 460–466. https://doi.org/10.1016/j.foodchem.2014.05.116

Beg, S., Swain, S., Hasan, H., Barkat, M. A., & Hussain, M. S. (2011). Systematic review of herbals as potential anti-inflammatory agents: Recent advances, current clinical status and future perspectives. *Pharmacognosy Reviews*, *5*(10), 120–137. https://doi.org/10.4103/0973-7847.91102

Berch, S. M., & Bonito, G. (2016). Truffle diversity (Tuber, Tuberaceae) in British Columbia. *Mycorrhiza*, *26*(6), 587–594. https://doi.org/10.1007/s00572-016-0695-2

Berczi, I., & Szentivanyi, A. (2003). Cytokines and chemokines. In I. Berczi & A. Szentivanyi (Eds.), *NeuroImmune Biology* (Vol. 3, pp. 191–220). Elsevier. https://doi.org/10.1016/S1567-7443(03)80049-2

Beutler, B. (2001). Sepsis begins at the interface of pathogen and host. *Biochemical Society Transactions*, *29*(6), 853–859. https://doi.org/10.1042/bst0290853

Beutler, B. (2002). TLR4 as the Mammalian Endotoxin Sensor. In B. Beutler & H. Wagner (Eds.), *Toll-Like Receptor Family Members and Their Ligands* (pp. 109–120). Springer. https://doi.org/10.1007/978-3-642-59430-4_7

Beutler, B., Du, X., & Poltorak, A. (2001). Identification of Toll-like receptor 4 (Tlr4) as the sole conduit for LPS signal transduction: Genetic and evolutionary studies. *Journal of Endotoxin Research*, *7*(4), 277–280. https://doi.org/10.1177/09680519010070040901

Bhaumik, D., Scott, G. K., Schokrpur, S., Patil, C. K., Campisi, J., & Benz, C. C. (2008). Expression of microRNA-146 suppresses NF-κB activity with reduction of metastatic potential in breast cancer cells. *Oncogene*, *27*(42), 5643–5647. https://doi.org/10.1038/onc.2008.171

Bokhary, H. A., & Parvez, S. (1993). Chemical Composition of Desert Truffles Terfezia claveryi. *Journal of Food Composition and Analysis*, *6*(3), 285–293. https://doi.org/10.1006/jfca.1993.1031

Bonilla, F. A., & Oettgen, H. C. (2010). Adaptive immunity. *Journal of Allergy and Clinical Immunology*, *125*(2, Supplement 2), S33–S40. https://doi.org/10.1016/j.jaci.2009.09.017

Bradai, L., Bissati, S., Chenchouni, H., & Amrani, K. (2015). Effects of climate on the productivity of desert truffles beneath hyper-arid conditions. *International Journal of Biometeorology*, *59*(7), 907–915. https://doi.org/10.1007/s00484-014-0891-8

Brennan, M. S., Matos, M. F., Richter, K. E., Li, B., & Scannevin, R. H. (2017). The NRF2 transcriptional target, OSGIN1, contributes to monomethyl fumarate-mediated cytoprotection in human astrocytes. *Scientific Reports*, *7*(1), 42054. https://doi.org/10.1038/srep42054

Cassetta, L., Cassol, E., & Poli, G. (2011). Macrophage Polarization in Health and Disease. *TheScientificWorldJOURNAL*, *11*, 2391–2402. https://doi.org/10.1100/2011/213962

Ceppi, M., Pereira, P. M., Dunand-Sauthier, I., Barras, E., Reith, W., Santos, M. A., & Pierre, P. (2009). MicroRNA-155 modulates the interleukin-1 signaling pathway in activated human monocyte-derived dendritic cells. *Proceedings of the National Academy of Sciences*, *106*(8), 2735–2740. https://doi.org/10.1073/pnas.0811073106

Chamberlain, L. M., Godek, M. L., Gonzalez-Juarrero, M., & Grainger, D. W. (2009). Phenotypic non-equivalence of murine (monocyte-) macrophage cells in biomaterial and inflammatory models. *Journal of Biomedical Materials Research Part A*, *88A*(4), 858–871. https://doi.org/10.1002/jbm.a.31930

Chaplin, D. D. (2010). Overview of the immune response. *Journal of Allergy and Clinical Immunology*, *125*(2, Supplement 2), S3–S23. https://doi.org/10.1016/j.jaci.2009.12.980

Chen, X.-L., Dodd, G., Thomas, S., Zhang, X., Wasserman, M. A., Rovin, B. H., & Kunsch, C. (2006). Activation of Nrf2/ARE pathway protects endothelial cells from oxidant injury and inhibits inflammatory gene expression. *American Journal of Physiology-Heart and Circulatory Physiology*, *290*(5), H1862–H1870. https://doi.org/10.1152/ajpheart.00651.2005

Cheng, J.-J., Chao, C.-H., Chang, P.-C., & Lu, M.-K. (2016). Studies on anti-inflammatory activity of sulfated polysaccharides from cultivated fungi Antrodia cinnamomea. *Food Hydrocolloids*, *53*, 37–45. https://doi.org/10.1016/j.foodhyd.2014.09.035

Cho, M., Yang, C., Kim, S. M., & You, S. (2010). Molecular characterization and biological activities of watersoluble sulfated polysaccharides from Enteromorpha prolifera. *Food Science and Biotechnology*, *19*(2), 525–533. https://doi.org/10.1007/s10068-010-0073-3

Dahham, S. S., Al-Rawi, S. S., Ibrahim, A. H., Abdul Majid, A. S., & Abdul Majid, A. M. S. (2018). Antioxidant, anticancer, apoptosis properties and chemical composition of black truffle Terfezia claveryi. *Saudi Journal of Biological Sciences*, *25*(8), 1524–1534. https://doi.org/10.1016/j.sjbs.2016.01.031

Darwish, R. S., Shawky, E., Nassar, K. M., Rashad ElSayed, R. M., Hussein, D. E., Ghareeb, D. A., & El Sohafy, S. M. (2021a). Differential anti-inflammatory biomarkers of the desert truffles Terfezia claveryi and Tirmania nivea revealed via UPLC-QqQ-MS-based metabolomics combined to chemometrics. *LWT*, *150*, 111965. https://doi.org/10.1016/j.lwt.2021.111965

Darwish, R. S., Shawky, E., Nassar, K. M., Rashad ElSayed, R. M., Hussein, D. E., Ghareeb, D. A., & El Sohafy, S. M. (2021b). Differential anti-inflammatory biomarkers of the desert truffles Terfezia claveryi and Tirmania nivea revealed via UPLC-QqQ-MS-based metabolomics combined to chemometrics. *LWT*, *150*, 111965. https://doi.org/10.1016/j.lwt.2021.111965

De Cássia da Silveira e Sá, R., Andrade, L. N., & De Sousa, D. P. (2013). A Review on Anti-Inflammatory Activity of Monoterpenes. *Molecules*, *18*(1), 1227–1254. https://doi.org/10.3390/molecules18011227

Delves, P. J., & Roitt, I. M. (2009, August 20). *The Immune System* (world) [Review-article]. Http://Dx.Doi.Org/10.1056/NEJM200007063430107; Massachusetts Medical Society. https://doi.org/10.1056/NEJM200007063430107

Dennis, E. A., & Norris, P. C. (2015). Eicosanoid storm in infection and inflammation. *Nature Reviews Immunology*, *15*(8), 511–523. https://doi.org/10.1038/nri3859

Doğan, H. H., & Aydın, S. (2013). Determination of antimicrobial effect, antioxidant activity and phenolic contents of desert truffle in Turkey. *African Journal of Traditional, Complementary, and Alternative Medicines: AJTCAM*, *10*(4), 52–58.

Doss, J. F., Jonassaint, J. C., Garrett, M. E., Ashley-Koch, A. E., Telen, M. J., & Chi, J.-T. (2016). Phase 1 Study of a Sulforaphane-Containing Broccoli Sprout Homogenate for Sickle Cell Disease. *PLoS ONE*, *11*(4), e0152895. https://doi.org/10.1371/journal.pone.0152895

Du, B., Lin, C., Bian, Z., & Xu, B. (2015). An insight into anti-inflammatory effects of fungal beta-glucans. *Trends in Food Science & Technology*, *41*(1), 49–59. https://doi.org/10.1016/j.tifs.2014.09.002

Dundar, A., Yesil, O. F., Acay, H., Okumus, V., Ozdemir, S., & Yildiz, A. (2012). Antioxidant properties, chemical composition and nutritional value of Terfezia boudieri (Chatin) from Turkey: *Food Science and Technology International*. https://doi.org/10.1177/1082013211427954

Echigo, R., Shimohata, N., Karatsu, K., Yano, F., Kayasuga-Kariya, Y., Fujisawa, A., Ohto, T., Kita, Y., Nakamura, M., Suzuki, S., Mochizuki, M., Shimizu, T., Chung, U., & Sasaki, N. (2012). Trehalose treatment suppresses inflammation, oxidative stress, and vasospasm induced by experimental subarachnoid hemorrhage. *Journal of Translational Medicine*, *10*(1), 80. https://doi.org/10.1186/1479-5876-10-80

El Enshasy, H. A., & Hatti-Kaul, R. (2013). Mushroom immunomodulators: Unique molecules with unlimited applications. *Trends in Biotechnology*, *31*(12), 668–677. https://doi.org/10.1016/j.tibtech.2013.09.003

El Enshasy, H., Elsayed, E. A., Aziz, R., & Wadaan, M. A. (2013). Mushrooms and Truffles: Historical Biofactories for Complementary Medicine in Africa and in the Middle East. *Evidence-Based Complementary and Alternative Medicine*, *2013*, e620451. https://doi.org/10.1155/2013/620451

Elkhateeb, W., Daba, G., Thomas, P., & Wen, T.-C. (2019). Antiviral Potential of Mushrooms in the Light of their Biological Active Compounds. *Journal of Pharmaceutical Sciences*, *5*, 8–12.

Elsayed, E. A., El Enshasy, H., Wadaan, M. A. M., & Aziz, R. (2014). Mushrooms: A Potential Natural Source of Anti-Inflammatory Compounds for Medical Applications. *Mediators of Inflammation*, *2014*, e805841. https://doi.org/10.1155/2014/805841

Epelman, S., Lavine, K. J., & Randolph, G. J. (2014). Origin and Functions of Tissue Macrophages. *Immunity*, *41*(1), 21–35. https://doi.org/10.1016/j.immuni.2014.06.013

Fabbri, M., Paone, A., Calore, F., Galli, R., & Croce, C. M. (2013). A new role for microRNAs, as ligands of Toll-like receptors. *RNA Biology*, *10*(2), 169–174. https://doi.org/10.4161/rna.23144

Farag, M. A., Fathi, D., Shamma, S., Shawkat, M. S. A., Shalabi, S. M., El Seedi, H. R., & Afifi, S. M. (2021). Comparative metabolome classification of desert truffles Terfezia claveryi and Terfezia boudieri via its aroma and nutrients profile. *LWT*, *142*, 111046. https://doi.org/10.1016/j.lwt.2021.111046

Feng, J., Li, A., Deng, J., Yang, Y., Dang, L., Ye, Y., Li, Y., & Zhang, W. (2014). miR-21 attenuates lipopolysaccharide-induced lipid accumulation and inflammatory response: Potential role in cerebrovascular disease. *Lipids in Health and Disease*, *13*, 27. https://doi.org/10.1186/1476-511X-13-27

Fernandes, E. S., Passos, G. F., Medeiros, R., da Cunha, F. M., Ferreira, J., Campos, M. M., Pianowski, L. F., & Calixto, J. B. (2007). Anti-inflammatory effects of compounds alpha-humulene and (−)-trans-caryophyllene isolated from the essential oil of Cordia verbenacea. *European Journal of Pharmacology*, *569*(3), 228–236. https://doi.org/10.1016/j.ejphar.2007.04.059

Fernando, I. P. S., Sanjeewa, K. K. A., Samarakoon, K. W., Lee, W. W., Kim, H.-S., & Jeon, Y.-J. (2018). Squalene isolated from marine macroalgae Caulerpa racemosa and its potent antioxidant and anti-inflammatory activities. *Journal of Food Biochemistry*, *42*(5), e12628. https://doi.org/10.1111/jfbc.12628

Ferrajoli, A., Shanafelt, T. D., Ivan, C., Shimizu, M., Rabe, K. G., Nouraee, N., Ikuo, M., Ghosh, A. K., Lerner, S., Rassenti, L. Z., Xiao, L., Hu, J., Reuben, J. M., Calin, S., You, M. J., Manning, J. T., Wierda, W. G., Estrov, Z., O'Brien, S., … Calin, G. A. (2013). Prognostic value of miR-155 in individuals with monoclonal B-cell lymphocytosis and patients with B chronic lymphocytic leukemia. *Blood*, *122*(11), 1891–1899. https://doi.org/10.1182/blood-2013-01-478222

Ferrao, R., Zhou, H., Shan, Y., Li, Q., Shaw, D. E., Li, X., & Wu, H. (2014). IRAK4 Dimerization and Trans-autophosphorylation are Induced by Myddosome Assembly. *Molecular Cell*, *55*(6), 891–903. https://doi.org/10.1016/j.molcel.2014.08.006

Friedman, M. (2016). Mushroom Polysaccharides: Chemistry and Antiobesity, Antidiabetes, Anticancer, and Antibiotic Properties in Cells, Rodents, and Humans. *Foods*, *5*(4), 80. https://doi.org/10.3390/foods5040080

Ganeshpurkar, A., & Saluja, A. (2020). Immunomodulatory effect of rutin, catechin, and hesperidin on macrophage function. *Indian Journal of Biochemistry and Biophysics (IJBB)*, *57*(1), 58–63.

Gençcelep, H., Uzun, Y., Tunçtürk, Y., & Demirel, K. (2009). Determination of mineral contents of wild-grown edible mushrooms. *Food Chemistry*, *113*(4), 1033–1036. https://doi.org/10.1016/j.foodchem.2008.08.058

Germolec, D. R., Shipkowski, K. A., Frawley, R. P., & Evans, E. (2018). Markers of Inflammation. In J. C. DeWitt, C. E. Rockwell, & C. C. Bowman (Eds.), *Immunotoxicity Testing: Methods and Protocols* (pp. 57–79). Springer. https://doi.org/10.1007/978-1-4939-8549-4_5

Gilmore, T. D. (2006). Introduction to NF-κB: Players, pathways, perspectives. *Oncogene*, *25*(51), 6680–6684. https://doi.org/10.1038/sj.onc.1209954

Grzywacz, A., Argasinska, J. G., Kala, K., Opoka, W., & Muszynska, B. (2016). Anti-Inflammatory Activity of Biomass Extracts of the Bay Mushroom, *Imleria badia* (Agaricomycetes), in RAW 264.7 Cells. *International Journal of Medicinal Mushrooms*, *18*(9). https://doi.org/10.1615/IntJMedMushrooms.v18.i9.20

Gunawardena, D., Bennett, L., Shanmugam, K., King, K., Williams, R., Zabaras, D., Head, R., Ooi, L., Gyengesi, E., & Münch, G. (2014). Anti-inflammatory effects of five commercially available mushroom species determined in lipopolysaccharide and interferon-γ activated murine macrophages. *Food Chemistry*, *148*, 92–96. https://doi.org/10.1016/j.foodchem.2013.10.015

Guo, L., Ma, R., Sun, H., Raza, A., Tang, J., & Li, Z. (2018). Anti-Inflammatory Activities and Related Mechanism of Polysaccharides Isolated from Sargentodoxa cuneata. *Chemistry & Biodiversity*, *15*(11), e1800343. https://doi.org/10.1002/cbdv.201800343

Gupta, S. (2002). Tumor necrosis factor-α-induced apoptosis in T cells from aged humans: A role of TNFR-I and downstream signaling molecules. *Experimental Gerontology*, *37*(2), 293–299. https://doi.org/10.1016/S0531-5565(01)00195-4

Gupta, S. C., Kim, J. H., Kannappan, R., Reuter, S., Dougherty, P. M., & Aggarwal, B. B. (2011). Role of nuclear factor-κB-mediated inflammatory pathways in cancer-related symptoms and their regulation by nutritional agents. *Experimental Biology and Medicine (Maywood, N.J.)*, *236*(6), 658–671. https://doi.org/10.1258/ebm.2011.011028

Hamza, A., Zouari, N., Zouari, S., Jdir, H., Zaidi, S., Gtari, M., & Neffati, M. (2016). Nutraceutical potential, antioxidant and antibacterial activities of Terfezia boudieri Chatin, a wild edible desert truffle from Tunisia arid zone. *Arabian Journal of Chemistry*, *9*(3), 383–389. https://doi.org/10.1016/j.arabjc.2013.06.015

Hayden, M. S., & Ghosh, S. (2008). Shared Principles in NF-κB Signaling. *Cell*, *132*(3), 344–362. https://doi.org/10.1016/j.cell.2008.01.020

He, X., Jing, Z., & Cheng, G. (2014). MicroRNAs: New Regulators of Toll-Like Receptor Signalling Pathways. *BioMed Research International*, *2014*, e945169. https://doi.org/10.1155/2014/945169

He, Y., Sun, X., Huang, C., Long, X., Lin, X., Zhang, L., Lv, X., & Li, J. (2014). MiR-146a Regulates IL-6 Production in Lipopolysaccharide-Induced RAW264.7 Macrophage Cells by Inhibiting Notch1. *Inflammation*, *37*(1), 71–82. https://doi.org/10.1007/s10753-013-9713-0

Heiss, E., Herhaus, C., Klimo, K., Bartsch, H., & Gerhäuser, C. (2001). Nuclear Factor κB Is a Molecular Target for Sulforaphane-mediated Anti-inflammatory Mechanisms *. *Journal of Biological Chemistry*, *276*(34), 32008–32015. https://doi.org/10.1074/jbc.M104794200

Hong, X., Ajat, M., Fakurazi, S., Noor, A. M., & Ismail, I. S. (2021). Anti-inflammatory evaluation of Scurrula ferruginea (jack) danser parasitizing on Tecoma stans (L.) H.B.K. in LPS/IFN-γ-induced RAW 264.7 macrophages. *Journal of Ethnopharmacology*, *268*, 113647. https://doi.org/10.1016/j.jep.2020.113647

Hou, C., Chen, L., Yang, L., & Ji, X. (2020). An insight into anti-inflammatory effects of natural polysaccharides. *International Journal of Biological Macromolecules*, *153*, 248–255. https://doi.org/10.1016/j.ijbiomac.2020.02.315

İbrahim Kıvrak. (2015). Analytical Methods Applied to Assess Chemical Composition, Nutritional Value and In Vitro Bioactivities of Terfezia olbiensis and Terfezia claveryi from Turkey. *Food Analytical Methods*, *8*(5), 1279–1293. https://doi.org/10.1007/s12161-014-0009-2

Iwasaki, A., & Medzhitov, R. (2015). Control of adaptive immunity by the innate immune system. *Nature Immunology*, *16*(4), 343–353. https://doi.org/10.1038/ni.3123

Jamali, S. (2014). Taxonomy of the Truffles. *Plant Science Today*, *1*(4), 219–222. https://doi.org/10.14719/pst.2014.1.4.55

Janakat, S., Al-Fakhiri, S., & Sallal, A.-K. (2004). A promising peptide antibiotic from Terfezia claveryi aqueous extract against Staphylococcus aureus in vitro. *Phytotherapy Research*, *18*(10), 810–813. https://doi.org/10.1002/ptr.1563

Jedinak, A., Dudhgaonkar, S., Wu, Q., Simon, J., & Sliva, D. (2011). Anti-inflammatory activity of edible oyster mushroom is mediated through the inhibition of NF-κB and AP-1 signaling. *Nutrition Journal*, *10*(1), 52. https://doi.org/10.1186/1475-2891-10-52

Ji, X., Peng, Q., & Wang, M. (2018). Anti-colon-cancer effects of polysaccharides: A mini-review of the mechanisms. *International Journal of Biological Macromolecules*, *114*, 1127–1133. https://doi.org/10.1016/j.ijbiomac.2018.03.186

Jiang, J., Grieb, B., Thyagarajan, A., & Sliva, D. (2008). Ganoderic acids suppress growth and invasive behavior of breast cancer cells by modulating AP-1 and NF-κB signaling. *International Journal of Molecular Medicine*, *21*(5), 577–584. https://doi.org/10.3892/ijmm.21.5.577

Jung, S., Lee, M.-S., Choi, A.-J., Kim, C.-T., & Kim, Y. (2019). Anti-Inflammatory Effects of High Hydrostatic Pressure Extract of Mulberry (Morus alba) Fruit on LPS-Stimulated RAW264.7 Cells. *Molecules*, *24*(7), 0. https://doi.org/10.3390/molecules24071425

Kaser, A., Lee, A.-H., Franke, A., Glickman, J. N., Zeissig, S., Tilg, H., Nieuwenhuis, E. E. S., Higgins, D. E., Schreiber, S., Glimcher, L. H., & Blumberg, R. S. (2008). XBP1 Links ER Stress to Intestinal Inflammation and Confers Genetic Risk for Human Inflammatory Bowel Disease. *Cell*, *134*(5), 743–756. https://doi.org/10.1016/j.cell.2008.07.021

Kawasaki, T., & Kawai, T. (2014). Toll-Like Receptor Signaling Pathways. *Frontiers in Immunology*, *5*, 461. https://doi.org/10.3389/fimmu.2014.00461

Khalifa, S. A. M., Farag, M. A., Yosri, N., Sabir, J. S. M., Saeed, A., Al-Mousawi, S. M., Taha, W., Musharraf, S. G., Patel, S., & El-Seedi, H. R. (2019). Truffles: From Islamic culture to chemistry, pharmacology, and food trends in recent times. *Trends in Food Science & Technology*, *91*, 193–218. https://doi.org/10.1016/j.tifs.2019.07.008

Khanapure, S. P., Garvey, D. S., Janero, D. R., & Gordon Letts, L. (2007). Eicosanoids in Inflammation: Biosynthesis, Pharmacology, and Therapeutic Frontiers. *Current Topics in Medicinal Chemistry*, *7*(3), 311–340.

Kim, D.-S., Lee, H.-J., Jeon, Y.-D., Han, Y.-H., Kee, J.-Y., Kim, H.-J., Shin, H.-J., Kang, J., Lee, B. S., Kim, S.-H., Kim, S.-J., Park, S.-H., Choi, B.-M., Park, S.-J., Um, J.-Y., & Hong, S.-H. (2015). Alpha-Pinene Exhibits Anti-Inflammatory Activity Through the Suppression of MAPKs and the NF-κB Pathway in Mouse Peritoneal Macrophages. *The American Journal of Chinese Medicine*, *43*(04), 731–742. https://doi.org/10.1142/S0192415X15500457

Kim, J., Cha, Y.-N., & Surh, Y.-J. (2010). A protective role of nuclear factor-erythroid 2-related factor-2 (Nrf2) in inflammatory disorders. *Mutation Research/Fundamental and Molecular Mechanisms of Mutagenesis*, *690*(1), 12–23. https://doi.org/10.1016/j.mrfmmm.2009.09.007

Kıvrak, İ. (2015). Analytical Methods Applied to Assess Chemical Composition, Nutritional Value and In Vitro Bioactivities of Terfezia olbiensis and Terfezia claveryi from Turkey. *Food Analytical Methods*, *8*(5), 1279–1293. https://doi.org/10.1007/s12161-014-0009-2

Kobayashi, E. H., Suzuki, T., Funayama, R., Nagashima, T., Hayashi, M., Sekine, H., Tanaka, N., Moriguchi, T., Motohashi, H., Nakayama, K., & Yamamoto, M. (2016). Nrf2 suppresses macrophage inflammatory response by blocking proinflammatory cytokine transcription. *Nature Communications*, *7*(1), 11624. https://doi.org/10.1038/ncomms11624

Lee, H., Nam, K., Zahra, Z., & Farooqi, M. Q. U. (2020). Potentials of truffles in nutritional and medicinal applications: A review. *Fungal Biology and Biotechnology*, *7*(1), 9. https://doi.org/10.1186/s40694-020-00097-x

Li, A., Dubey, S., Varney, M. L., Dave, B. J., & Singh, R. K. (2003). IL-8 Directly Enhanced Endothelial Cell Survival, Proliferation, and Matrix Metalloproteinases Production and Regulated Angiogenesis. *The Journal of Immunology*, *170*(6), 3369–3376. https://doi.org/10.4049/jimmunol.170.6.3369

Li, R., Chen, W., Yanes, R., Lee, S., & Berliner, J. A. (2007). OKL38 is an oxidative stress response gene stimulated by oxidized phospholipids. *Journal of Lipid Research*, *48*(3), 709–715. https://doi.org/10.1194/jlr.M600501-JLR200

Li, S., & Shah, N. P. (2016). Anti-inflammatory and anti-proliferative activities of natural and sulphonated polysaccharides from Pleurotus eryngii. *Journal of Functional Foods*, *23*, 80–86. https://doi.org/10.1016/j.jff.2016.02.003

Lin, S.-C., Lo, Y.-C., & Wu, H. (2010). Helical assembly in the MyD88:IRAK4:IRAK2 complex in TLR/IL-1R signaling. *Nature*, *465*(7300), 885–890. https://doi.org/10.1038/nature09121

Lin, W., Wu, R. T., Wu, T., Khor, T.-O., Wang, H., & Kong, A.-N. (2008). Sulforaphane suppressed LPS-induced inflammation in mouse peritoneal macrophages through Nrf2 dependent pathway. *Biochemical Pharmacology*, *76*(8), 967–973. https://doi.org/10.1016/j.bcp.2008.07.036

Lin, Z., Lu, J., Zhou, W., & Shen, Y. (2012). Structural Insights into TIR Domain Specificity of the Bridging Adaptor Mal in TLR4 Signaling. *PLOS ONE*, *7*(4), e34202. https://doi.org/10.1371/journal.pone.0034202

Ma, L., Chen, H., Dong, P., & Lu, X. (2013). Anti-inflammatory and anticancer activities of extracts and compounds from the mushroom Inonotus obliquus. *Food Chemistry*, *139*(1), 503–508. https://doi.org/10.1016/j.foodchem.2013.01.030

Marshall, J. S., Warrington, R., Watson, W., & Kim, H. L. (2018). An introduction to immunology and immunopathology. *Allergy, Asthma & Clinical Immunology*, *14*(2), 49. https://doi.org/10.1186/s13223-018-0278-1

Martín-de-Saavedra, M. D., Budni, J., Cunha, M. P., Gómez-Rangel, V., Lorrio, S., del Barrio, L., Lastres-Becker, I., Parada, E., Tordera, R. M., Rodrigues, A. L. S., Cuadrado, A., & López, M. G. (2013). Nrf2 participates in depressive disorders through an anti-inflammatory mechanism. *Psychoneuroendocrinology*, *38*(10), 2010–2022. https://doi.org/10.1016/j.psyneuen.2013.03.020

Martinez, F. O., & Gordon, S. (2014). The M1 and M2 paradigm of macrophage activation: Time for reassessment. *F1000Prime Reports*, *6*, 13. https://doi.org/10.12703/P6-13

Martinez-Pomares, L., & Gordon, S. (2007). Antigen Presentation the Macrophage Way. *Cell*, *131*(4), 641–643. https://doi.org/10.1016/j.cell.2007.10.046

Medina, K. L. (2016). Overview of the immune system. *Handbook of Clinical Neurology*, *133*, 61–76. https://doi.org/10.1016/B978-0-444-63432-0.00004-9

Medzhitov, R. (2008). Origin and physiological roles of inflammation. *Nature*, *454*(7203), 428–435. https://doi.org/10.1038/nature07201

Medzhitov, R. (2010). Inflammation 2010: New Adventures of an Old Flame. *Cell*, *140*(6), 771–776. https://doi.org/10.1016/j.cell.2010.03.006

Mehta, A., & Baltimore, D. (2016). MicroRNAs as regulatory elements in immune system logic. *Nature Reviews Immunology*, *16*(5), 279–294. https://doi.org/10.1038/nri.2016.40

Mello, A., Murat, C., & Bonfante, P. (2006). Truffles: Much more than a prized and local fungal delicacy. *FEMS Microbiology Letters*, *260*(1), 1–8. https://doi.org/10.1111/j.1574-6968.2006.00252.x

Meng, L.-Z., Feng, K., Wang, L.-Y., Cheong, K.-L., Nie, H., Zhao, J., & Li, S.-P. (2014). Activation of mouse macrophages and dendritic cells induced by polysaccharides from a novel Cordyceps sinensis fungus UM01. *Journal of Functional Foods*, *9*, 242–253. https://doi.org/10.1016/j.jff.2014.04.029

Meng, Y., Lyu, F., Xu, X., & Zhang, L. (2020). Recent Advances in Chain Conformation and Bioactivities of Triple-Helix Polysaccharides. *Biomacromolecules*. https://doi.org/10.1021/acs.biomac.9b01644

Mueller, A., Raptis, J., Rice, P. J., Kalbfleisch, J. H., Stout, R. D., Ensley, H. E., Browder, W., & Williams, D. L. (2000). The influence of glucan polymer structure and solution conformation on binding to (1→3)-β-d-glucan receptors in a human monocyte-like cell line. *Glycobiology*, *10*(4), 339–346. https://doi.org/10.1093/glycob/10.4.339

Nakasa, T., Miyaki, S., Okubo, A., Hashimoto, M., Nishida, K., Ochi, M., & Asahara, H. (2008). Expression of microRNA-146 in rheumatoid arthritis synovial tissue. *Arthritis & Rheumatism*, *58*(5), 1284–1292. https://doi.org/10.1002/art.23429

Newton, K., & Dixit, V. M. (2012). Signaling in Innate Immunity and Inflammation. *Cold Spring Harbor Perspectives in Biology*, *4*(3), a006049. https://doi.org/10.1101/cshperspect.a006049

Newton, R., Kuitert, L. M. E., Bergmann, M., Adcock, I. M., & Barnes, P. J. (1997). Evidence for Involvement of NF-κB in the Transcriptional Control of COX-2 Gene Expression by IL-1β.

Biochemical and Biophysical Research Communications, *237*(1), 28–32. https://doi.org/10.1006/bbrc.1997.7064

O'Connell, R. M., Taganov, K. D., Boldin, M. P., Cheng, G., & Baltimore, D. (2007). MicroRNA-155 is induced during the macrophage inflammatory response. *Proceedings of the National Academy of Sciences*, *104*(5), 1604–1609. https://doi.org/10.1073/pnas.0610731104

O'Neill, L. A. J., & Bowie, A. G. (2007). The family of five: TIR-domain-containing adaptors in Toll-like receptor signalling. *Nature Reviews Immunology*, *7*(5), 353–364. https://doi.org/10.1038/nri2079

Owaid, M. N. (2018). Bioecology and Uses of Desert Truffles (Pezizales) in the Middle East. *Walailak Journal of Science and Technology (WJST)*, *15*(3), 179–188. https://doi.org/10.48048/wjst.2018.3058

Özyürek, M., Bener, M., Güçlü, K., & Apak, R. (2014). Antioxidant/antiradical properties of microwave-assisted extracts of three wild edible mushrooms. *Food Chemistry*, *157*, 323–331. https://doi.org/10.1016/j.foodchem.2014.02.053

Palleschi, A., Bocchinfuso, G., Coviello, T., & Alhaique, F. (2005). Molecular dynamics investigations of the polysaccharide scleroglucan: First study on the triple helix structure. *Carbohydrate Research*, *340*(13), 2154–2162. https://doi.org/10.1016/j.carres.2005.06.026

Palombo, E. A. (2011). Traditional Medicinal Plant Extracts and Natural Products with Activity against Oral Bacteria: Potential Application in the Prevention and Treatment of Oral Diseases. *Evidence-Based Complementary and Alternative Medicine*, *2011*, enep067. https://doi.org/10.1093/ecam/nep067

Park, B. S., & Lee, J.-O. (2013). Recognition of lipopolysaccharide pattern by TLR4 complexes. *Experimental & Molecular Medicine*, *45*(12), e66–e66. https://doi.org/10.1038/emm.2013.97

Park, C., Cha, H.-J., Lee, H., Kim, G.-Y., & Choi, Y. H. (2021). The regulation of the TLR4/NF-κB and Nrf2/HO-1 signaling pathways is involved in the inhibition of lipopolysaccharide-induced inflammation and oxidative reactions by morroniside in RAW 264.7 macrophages. *Archives of Biochemistry and Biophysics*, *706*, 108926. https://doi.org/10.1016/j.abb.2021.108926

Parkin, J., & Cohen, B. (2001). An overview of the immune system. *The Lancet*, *357*(9270), 1777–1789. https://doi.org/10.1016/S0140-6736(00)04904-7

Patel, S., Rauf, A., Khan, H., Khalid, S., & Mubarak, M. S. (2017). Potential health benefits of natural products derived from truffles: A review. *Trends in Food Science & Technology*, *70*, 1–8. https://doi.org/10.1016/j.tifs.2017.09.009

Patil, K. R., Mahajan, U. B., Unger, B. S., Goyal, S. N., Belemkar, S., Surana, S. J., Ojha, S., & Patil, C. R. (2019). Animal Models of Inflammation for Screening of Anti-inflammatory Drugs: Implications for the Discovery and Development of Phytopharmaceuticals. *International Journal of Molecular Sciences*, *20*(18), 4367. https://doi.org/10.3390/ijms20184367

Porta, C., Riboldi, E., Ippolito, A., & Sica, A. (2015). Molecular and epigenetic basis of macrophage polarized activation. *Seminars in Immunology*, *27*(4), 237–248. https://doi.org/10.1016/j.smim.2015.10.003

Quinn, S. R., & O'Neill, L. A. (2011). A trio of microRNAs that control Toll-like receptor signalling. *International Immunology*, *23*(7), 421–425. https://doi.org/10.1093/intimm/dxr034

Raman, D., Sobolik-Delmaire, T., & Richmond, A. (2011). Chemokines in health and disease. *Experimental Cell Research*, *317*(5), 575–589. https://doi.org/10.1016/j.yexcr.2011.01.005

Rao, X., Huang, X., Zhou, Z., & Lin, X. (2013). An improvement of the 2ˆ(–delta delta CT) method for quantitative real-time polymerase chain reaction data analysis. *Biostatistics, Bioinformatics and Biomathematics*, *3*(3), 71–85.

Rao, Y. K., Fang, S.-H., & Tzeng, Y.-M. (2007). Evaluation of the anti-inflammatory and anti-proliferation tumoral cells activities of Antrodia camphorata, Cordyceps sinensis, and Cinnamomum osmophloeum bark extracts. *Journal of Ethnopharmacology*, *114*(1), 78–85. https://doi.org/10.1016/j.jep.2007.07.028

Ricciotti, E., & FitzGerald, G. A. (2011). Prostaglandins and Inflammation. *Arteriosclerosis, Thrombosis, and Vascular Biology*, *31*(5), 986–1000. https://doi.org/10.1161/ATVBAHA.110.207449

Riera Romo, M., Pérez-Martínez, D., & Castillo Ferrer, C. (2016). Innate immunity in vertebrates: An overview. *Immunology*, *148*(2), 125–139. https://doi.org/10.1111/imm.12597

Saha, S., Buttari, B., Panieri, E., Profumo, E., & Saso, L. (2020). An Overview of Nrf2 Signaling Pathway and Its Role in Inflammation. *Molecules*, *25*(22), 5474. https://doi.org/10.3390/molecules25225474

Şahin, A., Kaşık, G., Alkan, S., & Özcan, M. M. (2020). Total phenol, antioxidant activity, fatty acid composition and mineral contents of the species of fungi known as domalan. *Journal of Agroalimentary Processes and Technologies*, 6.

Saleh, H. A., Ramdan, E., Elmazar, M. M., Azzazy, H. M. E., & Abdelnaser, A. (2021). Comparing the protective effects of resveratrol, curcumin and sulforaphane against LPS/IFN-γ-mediated inflammation in doxorubicin-treated macrophages. *Scientific Reports*, *11*, 545. https://doi.org/10.1038/s41598-020-80804-1

Sánchez, C. (2017). Bioactives from Mushroom and Their Application. In M. Puri (Ed.), *Food Bioactives: Extraction and Biotechnology Applications* (pp. 23–57). Springer International Publishing. https://doi.org/10.1007/978-3-319-51639-4_2

Saxena, R. N., Pendse, V. K., & Khanna, N. K. (1984). Anti-inflammatory and analgesic properties of four amino-acids. *Indian Journal of Physiology and Pharmacology*, *28*(4), 299–305.

Schmittgen, T. D., & Livak, K. J. (2008). Analyzing real-time PCR data by the comparative CT method. *Nature Protocols*, *3*(6), 1101–1108. https://doi.org/10.1038/nprot.2008.73

Schoenborn, J. R., & Wilson, C. B. (2007). Regulation of Interferon-γ During Innate and Adaptive Immune Responses. In *Advances in Immunology* (Vol. 96, pp. 41–101). Academic Press. https://doi.org/10.1016/S0065-2776(07)96002-2

Sevindik, M., Pehlivan, M., Dogan, M., & Selamoglu, Z. (2018). *Phenolic Content and Antioxidant Potential of Terfezia boudieri*. 5.

Shapouri-Moghaddam, A., Mohammadian, S., Vazini, H., Taghadosi, M., Esmaeili, S.-A., Mardani, F., Seifi, B., Mohammadi, A., Afshari, J. T., & Sahebkar, A. (2018). Macrophage plasticity, polarization, and function in health and disease. *Journal of Cellular Physiology*, *233*(9), 6425–6440. https://doi.org/10.1002/jcp.26429

Sheedy, F. J., Palsson-McDermott, E., Hennessy, E. J., Martin, C., O'Leary, J. J., Ruan, Q., Johnson, D. S., Chen, Y., & O'Neill, L. A. J. (2010). Negative regulation of TLR4 via targeting of the proinflammatory tumor suppressor PDCD4 by the microRNA miR-21. *Nature Immunology*, *11*(2), 141–147. https://doi.org/10.1038/ni.1828

Shimazu, R., Akashi, S., Ogata, H., Nagai, Y., Fukudome, K., Miyake, K., & Kimoto, M. (1999). MD-2, a Molecule that Confers Lipopolysaccharide Responsiveness on Toll-like Receptor 4. *The Journal of Experimental Medicine*, *189*(11), 1777–1782.

Sica, A., Erreni, M., Allavena, P., & Porta, C. (2015). Macrophage polarization in pathology. *Cellular and Molecular Life Sciences*, *72*(21), 4111–4126. https://doi.org/10.1007/s00018-015-1995-y

Sinha, M., Gautam, L., Shukla, P. K., Kaur, P., Sharma, S., & Singh, T. P. (2013). Current Perspectives in NSAID-Induced Gastropathy. *Mediators of Inflammation*, *2013*, e258209. https://doi.org/10.1155/2013/258209

Song, H.-H., Chae, H.-S., Oh, S.-R., Lee, H.-K., & Chin, Y.-W. (2012). Anti-Inflammatory and Anti-Allergic Effect of Agaricus blazei Extract in Bone Marrow-Derived Mast Cells. *The American Journal of Chinese Medicine*, *40*(05), 1073–1084. https://doi.org/10.1142/S0192415X12500796

Sonkoly, E., Ståhle, M., & Pivarcsi, A. (2008). MicroRNAs and immunity: Novel players in the regulation of normal immune function and inflammation. *Seminars in Cancer Biology*, *18*(2), 131–140. https://doi.org/10.1016/j.semcancer.2008.01.005

Stanikunaite, R., Khan, S. I., Trappe, J. M., & Ross, S. A. (2009). Cyclooxygenase-2 inhibitory and antioxidant compounds from the truffle Elaphomyces granulatus. *Phytotherapy Research*, *23*(4), 575–578. https://doi.org/10.1002/ptr.2698

Sukkar, M. B., & Harris, J. (2017). Potential impact of oxidative stress induced growth inhibitor 1 (OSGIN1) on airway epithelial cell autophagy in chronic obstructive pulmonary disease (COPD). *Journal of Thoracic Disease*, *9*(12), 4825–4827. https://doi.org/10.21037/jtd.2017.10.153

Sun, J., Zhang, X., Broderick, M., & Fein, H. (2003). Measurement of Nitric Oxide Production in Biological Systems by Using Griess Reaction Assay. *Sensors*, *3*(8), 276–284. https://doi.org/10.3390/s30800276

Swanson, L., Katkar, G. D., Tam, J., Pranadinata, R. F., Chareddy, Y., Coates, J., Anandachar, M. S., Castillo, V., Olson, J., Nizet, V., Kufareva, I., Das, S., & Ghosh, P. (2020). TLR4 signaling and macrophage inflammatory responses are dampened by GIV/Girdin. *Proceedings of the National Academy of Sciences*, *117*(43), 26895–26906. https://doi.org/10.1073/pnas.2011667117

Taganov, K. D., Boldin, M. P., Chang, K.-J., & Baltimore, D. (2006). NF-κB-dependent induction of microRNA miR-146, an inhibitor targeted to signaling proteins of innate immune responses. *Proceedings of the National Academy of Sciences of the United States of America*, *103*(33), 12481–12486. https://doi.org/10.1073/pnas.0605298103

Taguchi, T., & Mukai, K. (2019). Innate immunity signalling and membrane trafficking. *Current Opinion in Cell Biology*, *59*, 1–7. https://doi.org/10.1016/j.ceb.2019.02.002

Takahama, Y. (2006). Journey through the thymus: Stromal guides for T-cell development and selection. *Nature Reviews Immunology*, *6*(2), 127–135. https://doi.org/10.1038/nri1781

Taofiq, O., Calhelha, R. C., Heleno, S., Barros, L., Martins, A., Santos-Buelga, C., Queiroz, M. J. R. P., & Ferreira, I. C. F. R. (2015). The contribution of phenolic acids to the anti-inflammatory activity of mushrooms: Screening in phenolic extracts, individual parent molecules and synthesized glucuronated and methylated derivatives. *Food Research International*, *76*, 821–827. https://doi.org/10.1016/j.foodres.2015.07.044

Tasneem, S., Liu, B., Li, B., Choudhary, M. I., & Wang, W. (2019). Molecular pharmacology of inflammation: Medicinal plants as anti-inflammatory agents. *Pharmacological Research*, *139*, 126–140. https://doi.org/10.1016/j.phrs.2018.11.001

Tian, Y., Zhou, S., Takeda, R., Okazaki, K., Sekita, M., & Sakamoto, K. (2021). Anti-inflammatory activities of amber extract in lipopolysaccharide-induced RAW 264.7 macrophages. *Biomedicine & Pharmacotherapy*, *141*, 111854. https://doi.org/10.1016/j.biopha.2021.111854

TNF: A master switch for inflammation to cancer. (2008, May 1). https://doi.org/10.2741/3066

Tornatore, L., Thotakura, A. K., Bennett, J., Moretti, M., & Franzoso, G. (2012). The nuclear factor kappa B signaling pathway: Integrating metabolism with inflammation. *Trends in Cell Biology*, *22*(11), 557–566. https://doi.org/10.1016/j.tcb.2012.08.001

Tu, W., Wang, H., Li, S., Liu, Q., & Sha, H. (2019). The Anti-Inflammatory and Anti-Oxidant Mechanisms of the Keap1/Nrf2/ARE Signaling Pathway in Chronic Diseases. *Aging and Disease*, *10*(3), 637–651. https://doi.org/10.14336/AD.2018.0513

Turner, M. D., Nedjai, B., Hurst, T., & Pennington, D. J. (2014). Cytokines and chemokines: At the crossroads of cell signalling and inflammatory disease. *Biochimica et Biophysica Acta (BBA) - Molecular Cell Research*, *1843*(11), 2563–2582. https://doi.org/10.1016/j.bbamcr.2014.05.014

Turvey, S. E., & Broide, D. H. (2010). Innate immunity. *Journal of Allergy and Clinical Immunology*, *125*(2, Supplement 2), S24–S32. https://doi.org/10.1016/j.jaci.2009.07.016

Valkov, E., Stamp, A., DiMaio, F., Baker, D., Verstak, B., Roversi, P., Kellie, S., Sweet, M. J., Mansell, A., Gay, N. J., Martin, J. L., & Kobe, B. (2011). Crystal structure of Toll-like receptor adaptor MAL/TIRAP reveals the molecular basis for signal transduction and disease protection. *Proceedings of the National Academy of Sciences of the United States of America*, *108*(36), 14879–14884. https://doi.org/10.1073/pnas.1104780108

Veeraraghavan, V. P., Hussain, S., Papayya Balakrishna, J., Dhawale, L., Kullappan, M., Mallavarapu Ambrose, J., & Krishna Mohan, S. (2021). A Comprehensive and Critical Review on Ethnopharmacological Importance of Desert Truffles: Terfezia claveryi, Terfezia boudieri, and Tirmania nivea. *Food Reviews International*, *0*(0), 1–20. https://doi.org/10.1080/87559129.2021.1889581

Vonkeman, H. E., & van de Laar, M. A. F. J. (2010). Nonsteroidal Anti-Inflammatory Drugs: Adverse Effects and Their Prevention. *Seminars in Arthritis and Rheumatism*, *39*(4), 294–312. https://doi.org/10.1016/j.semarthrit.2008.08.001

Wang, H., Li, X., Li, T., Wang, L., Wu, X., Liu, J., Xu, Y., & Wei, W. (2019). Multiple roles of microRNA-146a in immune responses and hepatocellular carcinoma. *Oncology Letters*, *18*(5), 5033–5042. https://doi.org/10.3892/ol.2019.10862

Wang, N., Liang, H., & Zen, K. (2014). Molecular Mechanisms That Influence the Macrophage M1–M2 Polarization Balance. *Frontiers in Immunology*, *5*, 614. https://doi.org/10.3389/fimmu.2014.00614

Wang, S., & Marcone, M. F. (2011). The biochemistry and biological properties of the world's most expensive underground edible mushroom: Truffles. *Food Research International*, *44*(9), 2567–2581. https://doi.org/10.1016/j.foodres.2011.06.008

Wang, Z., Luo, D., & Liang, Z. (2004). Structure of polysaccharides from the fruiting body of Hericium erinaceus Pers. *Carbohydrate Polymers*, *57*(3), 241–247. https://doi.org/10.1016/j.carbpol.2004.04.018

Watanabe, S., Alexander, M., Misharin, A. V., & Budinger, G. R. S. (2019). The role of macrophages in the resolution of inflammation. *The Journal of Clinical Investigation*, *129*(7), 2619–2628. https://doi.org/10.1172/JCI124615

Wu, G.-J., Shiu, S.-M., Hsieh, M.-C., & Tsai, G.-J. (2016). Anti-inflammatory activity of a sulfated polysaccharide from the brown alga Sargassum cristaefolium. *Food Hydrocolloids*, *53*, 16–23. https://doi.org/10.1016/j.foodhyd.2015.01.019

Wu, Y., Antony, S., Meitzler, J. L., & Doroshow, J. H. (2014). Molecular mechanisms underlying chronic inflammation-associated cancers. *Cancer Letters*, *345*(2), 164–173. https://doi.org/10.1016/j.canlet.2013.08.014

Wynn, T. A., Chawla, A., & Pollard, J. W. (2013). Macrophage biology in development, homeostasis and disease. *Nature*, *496*(7446), 445–455. https://doi.org/10.1038/nature12034

Xie, Q. W., Kashiwabara, Y., & Nathan, C. (1994). Role of transcription factor NF-kappa B/Rel in induction of nitric oxide synthase. *The Journal of Biological Chemistry*, *269*(7), 4705–4708.

Yan, X., Wang, Y., Sang, X., & Fan, L. (2017). Nutritional value, chemical composition and antioxidant activity of three Tuber species from China. *AMB Express*, *7*(1), 136. https://doi.org/10.1186/s13568-017-0431-0

Youn, H. S., Kim, Y. S., Park, Z. Y., Kim, S. Y., Choi, N. Y., Joung, S. M., Seo, J. A., Lim, K.-M., Kwak, M.-K., Hwang, D. H., & Lee, J. Y. (2010). Sulforaphane Suppresses Oligomerization of TLR4 in a Thiol-Dependent Manner. *The Journal of Immunology*, *184*(1), 411–419. https://doi.org/10.4049/jimmunol.0803988

Zelová, H., & Hošek, J. (2013). TNF-α signalling and inflammation: Interactions between old acquaintances. *Inflammation Research*, *62*(7), 641–651. https://doi.org/10.1007/s00011-013-0633-0

Zhang, X., Qi, C., Guo, Y., Zhou, W., & Zhang, Y. (2016). Toll-like receptor 4-related immunostimulatory polysaccharides: Primary structure, activity relationships, and possible interaction models. *Carbohydrate Polymers*, *149*, 186–206. https://doi.org/10.1016/j.carbpol.2016.04.097

Zimmerman, L. M., Vogel, L. A., & Bowden, R. M. (2010). Understanding the vertebrate immune system: Insights from the reptilian perspective. *Journal of Experimental Biology*, *213*(5), 661–671. https://doi.org/10.1242/jeb.038315